UC Irvine
UC Irvine Electronic Theses and Dissertations

Title
Development of Rapid and Portable Detection Methods for Antibiotics, Viruses, and Antibiotic-Resistant Bacteria in Wastewater

Permalink
https://escholarship.org/uc/item/7z22h6s5

Author
Huang, Yen Hsiang

Publication Date
2024

Peer reviewed|Thesis/dissertation

eScholarship.org Powered by the California Digital Library
University of California

UNIVERSITY OF CALIFORNIA,
IRVINE

Development of Rapid and Portable Detection Methods for Antibiotics, Viruses, and Antibiotic-Resistant Bacteria in Wastewater

DISSERTATION

submitted in partial satisfaction of the requirements
for the degree of

DOCTOR OF PHILOSOPHY

in Civil & Environmental Engineering

by

Yen-Hsiang Huang

Dissertation Committee:
Professor Sunny Jiang, Chair
Assistant Professor Adeyemi Adeleye
Assistant Professor Christopher Olivares Martinez

2024

Chapter 2 © 2023 Yen-Hsiang Huang
All other materials © 2024 Yen-Hsiang Huang

DEDICATION

To

my family and friends

Your support means the world to me. Thank you for always having my back.

TABLE OF CONTENTS

LIST OF FIGURES

LIST OF TABLES

ACKNOWLEDGEMENTS

I want to start by expressing my deepest appreciation to my Ph.D. advisor, Professor Sunny Jiang, for her consistent support, guidance, and understanding throughout my research journey. Her invaluable insights and expertise have been inspiring, and her kindness remained a consistent source of encouragement, motivating me through the most challenging moments. Many times when I was struggling to make things work, she always guided me in the correct direction and gave me all of her support. I am eternally grateful to be her student, and I sincerely hope that I met her expectations occasionally.

I would like to thank my committee members, Professor Adeyemi Adeleye and Professor Christopher Olivares Martinez, for their guidance and assistance throughout the past few years. They have inspired me to think about the big picture of my research as well as the detail that I should have considered. I would also like to thank Professor Regina Ragan, Professor Marc Madou, and Professor Lawrence Kulinsky, who have provided me with their expertise and lab recourses, allowing me to achieve my academic goals.

I would like to extend my thanks to my past and present lab mates: Dr. Marisa Nielsen, Dr. Srikiran Chandrasekaran, Dr. Hamsa Gowda, Dr. Zhiquan Song, Dr. Lixun Zhang, Dr. Shengyin Tang, Dr. Hunter Quon, Ashley Green, Alexis Guerra, Aiswarya Rani Pappu, Katherine Brenner and Jacquelynn Nguyen for their support and feedback over these years. It has been a great pleasure to work with them in the lab, realizing that I'm not alone on this journey.

I can never complete this journey without the support of my family and friends, including my fluffy sidekick, Benny. Their presence has made the tough times easier to bear. Their love and understanding have been my greatest motivation.

I would like to acknowledge the various sources of financial support I received to complete my dissertation which include U.S. Department of Interior, grant no. R21AC10079-00, the National Science Foundation (CBET-1926612), the National Science Foundation Materials Research Science and Engineering Center program through the UC Irvine Center for Complex and Active Materials (DMR-2011967), and USBR R21AC10079-00.

I would like to thank the American Chemical Society for permission to include Chapter 2 of this dissertation, which was originally published in ACS Environmental Science & Technology. Additionally, I would like to thank the co-authors listed in this publication: Hong Wei, Peter J. Santiago, William John Thrift, Professor Regina Ragan, and Professor Sunny Jiang for their support and guidance.

VITA

Yen-Hsiang Huang

EDUCATION

2024	Ph.D. in Civil and Environmental Engineering, University of California, Irvine
2018	M.S. in Civil and Environmental Engineering, University of California, Irvine
2016	B.S. in Environmental Engineering, National Cheng Kung University

TEACHING & RELATED EXPERIENCE

2020-2024	EH&S Representative for Environmental Microbiology BSL 2 Laboratory
2018-2024	Graduate Student Researcher, UC Irvine
2023	Teaching Assistant: Environmental Microbiology for Engineers (ENGRCEE 169)
2021	Teaching Assistant: Environmental Processes (ENGRCEE 160)
2020	National Science Foundation INTERN Program at Orange County Sanitation District
2019	Grader: Environmental Processes (ENGRCEE 160)

HONOR

2024	Most Innovative Research Award at the Microbes in Wastewater Symposium
2023	SCCAEPA Best Student Research Award
2020	UCI DTEI Summer Fellowship
2019	UCI EnE Summer Graduate Research Fellowship
2017	Rotary Global Grant Fellow

PUBLICATION

Yen-Hsiang Huang, Hong Wei, Peter Santiago, William John Thrift, Regina Ragan, Sunny Jiang. (2023) "Sensing Antibiotics in Wastewater using Surface-Enhanced Raman Scattering" Environmental Science & Technology

Hong Wei, Yixin Huang, Peter J. Santiago, Khachik E. Labachyan, Sasha Ronaghi, Martin Paul Banda Magana, **Yen-Hsiang Huang**, Sunny C. Jiang, Allon I. Hochbaum, and Regina Ragan. (2023) "Decoding the Metabolic Response of Escherichia Coli for Sensing Trace Heavy Metals in Water." Proceedings of the National Academy of Sciences 120, no. 7

Kuang-Wei Shi, **Yen-Hsiang Huang**, Hunter Quon, Zi-Lu Ou-Yang, Chengwen Wang, and Sunny C. Jiang. (2021) "Quantifying the Risk of Indoor Drainage System in Multi-Unit Apartment Building as a Transmission Route of SARS-CoV-2." Science of The Total Environment 762

CONFERENCES AND PRESENTATIONS

Research poster presentation: "Quantification of viruses in wastewater on a centrifugal microfluidic disc" Microbes in Wastewater 2024. Laguna Beach, CA. Jan 2024.

Research poster presentation: "Rapid Detection of PMMoV and SARS-CoV-2 in Wastewater by a Centrifugal Microfluidic Disc" ASM Microbe 2023. Houston, TX. June 2023.

AES Poster Spotlight: "Rapid Detection of PMMoV and SARS-CoV-2 in Wastewater by a Centrifugal Microfluidic Disc" ASM Microbe 2023. Houston, TX. June 2023.

Research poster presentation: "Development of Centrifugal Microfluidics for Pathogen Detection in Sewage" Center for Virus Research retreat, University of California, Irvine. February 2022.

Research poster presentation: "Rapid Detection of Residual Antibiotics in Wastewater Treatment Plants by Surface-Enhanced Raman Scattering (SERS) Analysis" ACS 2019 National Meeting and Exposition, San Diego, CA. August 2019.

ABSTRACT OF THE DISSERTATION

Development of Rapid and Portable Detection Methods for Antibiotics, Viruses, and Antibiotic-Resistant Bacteria in Wastewater

By

Yen-Hsiang Huang

Doctor of Philosophy in Civil & Environmental Engineering

University of California, Irvine, 2024

Professor Sunny Jiang, Chair

Antibiotic resistance has emerged as a critical global health threat in the 21st century, leading to untreatable infectious diseases and significantly increasing human morbidity and mortality. Rapid, portable, and user-friendly detection of antibiotics, microbial pathogens, and antibiotic-resistant organisms in aquatic environment plays a key role in controlling the spread of diseases and combating the emergence of antibiotic resistance. Unfortunately, current environmental monitoring practices are tedious, expensive and slow. These limitations impede timely detection and response to emerging threats, allowing the spread of diseases and antibiotic-resistant pathogens to human populations. This dissertation research aims to develop environmental monitoring strategies that streamline the current monitoring timeline and make it accessible to a wider range of users. This effort will contribute to more frequent and efficient monitoring of antibiotics, microbial pathogens, and antibiotic-resistant organisms in water matrices. Through this research, I first investigated the application of Surface Enhanced Raman Scattering (SERS) for label-free monitoring of antibiotics in wastewater. By utilizing carefully designed SERS substrates and artificial intelligence (AI) algorithms, I successfully quantified the target antibiotics even in the presence of other organic and inorganic molecules in wastewater. Next, I developed a portable and semi-automatic virus detection centrifugal microfluidic disc (CD) that integrates sample

concentration, purification, amplification, and quantification steps for environmental water monitoring. The on-CD assay is completed in less than 1.5 hours, and its performance is comparable to that of the benchtop in-tube assay. Lastly, building upon the foundation of the virus detection CD system, I further designed a microfluidic CD that integrates the phenotypic bacterial culture with genotypic pathogen identification for monitoring of antibiotic resistant bacteria. This CD system successfully detected indigenous antibiotic-resistant bacteria in raw wastewater in under 3 hours. This dissertation serves as an important foundation for developing more advanced, field-applicable techniques and methodologies in environmental monitoring.

CHAPTER 1
INTRODUCTION

Infectious diseases have posed a critical threat to human society throughout our history (Finlay et al., 2021). From the Black Plague and cholera to influenza and the ongoing COVID-19 crisis, they have caused significant economic losses and claimed countless lives. Even with the advanced science and technology of the 21st century, diseases such as cholera, typhoid, and diarrhea continue to affect population around the world, causing over 3.4 million death each year (Dufour et al., 2013). The issue became even more challenging with the emergence of antibiotic resistance, making these diseases tougher to treat and significantly impacting public health and the environment (Mancuso et al., 2021). According to a review on antimicrobial resistance (AMR) commissioned by the United Kingdom government, if the emerging trend of antibiotic resistance continues, diseases related to antibiotic resistance could claim nearly 10 million lives each year by 2050 (O'neill, 2014). Therefore, urgent attention is needed to mitigate this rising global concern.

Environmental monitoring and preventive measures remain critically important in controlling the spread of diseases and combating the emergence of antibiotic resistance. Exposure to contaminated water sources and recreational waters serves as a primary pathway for the transmission of waterborne diseases. While wastewater reuse has become an increasingly common practice to address water scarcity, it also shortens the natural water cycle, further exacerbating the risk of disease transmission through water environments (Lazarova et al., 2001). Additionally, aquatic environments, especially wastewater treatment plants (WWTPs), are considered hotspots for the emergence and spread of antibiotic resistance. WWTPs serve as collection points for antibiotics from sewer networks that gather wastewater from domestic, clinical, agricultural, and

pharmaceutical sources (Huang et al., 2023). Unfortunately, the presence of antibiotics in wastewater can foster antibiotic-resistant bacteria (ARB) and antibiotic-resistant genes (ARG) during the biological wastewater treatment process. However, several studies have indicated that removal efficiencies of antibiotics, ARB, and ARG in WWTPs are usually low, making WWTPs serve as both hotspots for horizontal gene transfer of ARG and ARB, and primary sources of antibiotics, ARB, and ARG entering the environment and potentially entering the water supply (Joss et al., 2006; Dong et al., 2016; Aydin et al., 2019). As a result, monitoring of antibiotics, pathogens, and antibiotic-resistant organisms in wastewater, aquatic environments, and through the wastewater treatment processes is an important first step to understand their occurrence in the environment, identify human exposure hotspots, and develop more effective strategies for their removal.

Currently, environmental monitoring relies on centralized laboratory-based methods that require well-trained laboratory personnel and costly equipment. Chemical analysis techniques such as liquid chromatography-mass spectrometry (LC-MS) and gas chromatography-mass spectrometry (GC-MS) are commonly applied for detection of antibiotics (Hernández et al., 2007; Lacey et al., 2008), while cultured-based methods and nucleic acid amplification techniques are often used for detecting microbial pathogens and antibiotic-resistant organisms (Jennings et al., 2018; Motlagh and Yang, 2019). Although these methods are well-established and accurate, they are tedious, expensive and slow. Furthermore, conducting the analysis in centralized laboratories leads to a significant delay in turnaround time, which includes sample collection, transportation, sample preparation, and detection. As a result, despite substantial resources and personnel allocated by regional health departments, water resources agencies, and wastewater dischargers, challenges persist in ensuring timely, comprehensive water quality monitoring. These limitations significantly

impede our ability to promptly identify potential public health risks, resulting in delays in implementing necessary interventions. Additionally, the current monitoring approach is insufficient in providing a thorough understanding of antibiotic resistance occurrence and fate, allowing resistant strains to continue emerging and spreading within water sources.

In recent years, numerous efforts have focused on developing rapid, portable, and user-friendly monitoring techniques for on-site detection (Roy et al., 2022; Srinivasan and Tung, 2015). These techniques eliminate the need for well-trained personnel, high-end equipment, and centralized laboratories, resulting in reduced sample-to-answer time and improved accessibility to water quality monitoring. For example, surface-enhanced Raman scattering (SERS) has attracted considerable attention for antibiotic detection (Han et al., 2014; Li et al., 2016; Halvorson and Vikesland, 2010; Wei et al., 2015; Li et al., 2014; Pinheiro et al., 2018). This technique has the potential for label-free, real-time detection, while maintaining high sensitivity without the need for intensive sample preparation. In addition, handheld SERS devices have been developed and applied, making them practical for field applications (Logan et al., 2022; Wei et al., 2023). On the other hand, centrifugal microfluidic platforms have been a research focus for their application in point-of-care detection of microbial pathogens and antibiotic-resistant organisms (Tang et al., 2016). These platforms have the potential to integrate multiple laboratory tasks, such as mixing, centrifuging, metering, etc., onto a miniature and portable system, enabling semi-automated and on-site processing of the entire workflow involved in sample preparation and nucleic acid amplification techniques.

Despite the widespread application of these innovative technologies in the medical field, challenges persist in adapting them for environmental monitoring. In comparison to clinical samples, environmental samples contain a wide range of organic and inorganic compounds,

making their composition complex and unpredictable (Huang et al., 2023.) The complexity of environmental samples may interfere with the detection target, leading to false detection results. Furthermore, the concentration of contaminants in environmental samples is usually lower than in clinical samples, requiring more sensitive detection methods to ensure accurate monitoring and assessment of environmental quality. Therefore, significant efforts are needed to adapt these emerging detection methods for use in environmental monitoring.

In this dissertation, I aim to develop rapid, portable, and user-friendly strategies for detecting antibiotics, microbial pathogens, and antibiotic-resistant organisms in water matrices to address the pressing need for efficient and accessible environmental monitoring solutions. By investigating how major steps needed to overcome the critical challenges, this work highlights the strong potential of using emerging technologies such as SERS and microfluidic CD to revolutionize environmental monitoring practices.

CHAPTER 2
SENSING ANTIBIOTICS IN WASTEWATER USING SURFACE-ENHANCED RAMAN SCATTERING

The contents of this chapter appear in the journal Environmental Science & Technology, Huang et al., 2023.

2.1 Introduction

Intensive uses of antibiotics in clinical and agricultural applications have led to discharges of large quantities of antibiotics into sewer systems (Pazda et al., 2019). Wastewater treatment plants (WWTPs) serve not only as collection points for antibiotics from sewer networks but also play an important role in degrading and removing them before the water is discharged to the environment or is supplied for various reuse applications. However, several studies have indicated that removal efficiencies of antibiotics in WWTPs are usually low (Joss et al., 2006; Dong et al., 2016; Aydin et al., 2019). The wastewater antibiotics may also amplify the antibiotic-resistant bacteria (ARB) and antibiotic-resistant genes (ARG) during biological wastewater treatment (Le et al., 2022). Such that, treated wastewater has become an important source of antibiotics, ARB, and ARG entering the environment and reused water. Antibiotics in an aquatic environment, even at low concentrations, can promote the breeding of ARB through mutation or horizontal gene transfer allowing microorganisms to survive in the presence of antibiotics (Von Wintersdorff et al., 2016). Therefore, residual antibiotics in treated wastewater for surface discharge have the potential to adversely affect ecosystems. Residual antibiotics in reused water may have a direct impact on human health by inducing antibiotic resistant infections (Ben et al., 2019). The World Health

Organization (WHO) has listed antibiotic resistance as one of the biggest threats to global health, food security, and development (World Health Organization, n.d.). Moreover, US Centers for Disease Control and Prevention (CDC) estimates that at least 2.8 million people get an antibiotic-resistant infection, and more than 35,000 people die from such infections annually in the United States (Centers for Disease Control and Prevention (U.S.), 2019).

Rapid and cost-effective detection of antibiotics in wastewater and through the wastewater treatment processes is an important first step in developing more effective strategies for their removal. Numerous efforts have been devoted in developing robust analytical techniques for antibiotics detection and quantification. Instrument-based methods such as capillary electrophoresis (CE), high-performance liquid chromatography (HPLC), liquid chromatography-mass spectrometry (LC-MS), and liquid chromatography-tandem mass spectrometry (LC-MS/MS) are the well-established analytical methods (Hernández et al., 2007; Lacey et al., 2008). However, the instrumentation cost is high, and the analytical procedures require intensive sample preparation steps by well-trained laboratory personnel (Chauhan et al., 2016). Particularly, the pre-treatment and pre-concentration processes during sample preparation are time-consuming. There is a significant time delay from sample collection to results. Detection by enzyme-linked immunosorbent assay (ELISA) relies on the highly specific antigen-antibody interaction to capture and detect target antibiotics in samples. However, ELISA suffers from cross-reaction with interferences in environmental sample matrices, significantly lessens the accuracy and selectivity of the test (Ahmed et al., 2020). More recently, new analytical methods such as electrochemical, colorimetric, and fluorescence sensors are being developed for antibiotic monitoring in the environment (Parthasarathy et al., 2018; Munteanu et al., 2018; Sun et al., 2021). These methods reported a relatively short response time, ease to use, portability and sufficient sensitivity and

accuracy (Sun et al., 2021) but their performances in the complex environmental matrix remain to be validated. Optical and electrochemical sensing platforms have also been coupled with aptamers in recent studies known as aptasensors (Akki and Werth, 2018), which use either RNA or DNA aptamers for specific binding of target antibiotics. Despite the promise of aptasensors in detecting specific antibiotics in a wide range of matrices with minimum sample preprocessing, aptasensors are challenged by the aptamer design process. In addition, because of nonspecific interactions with interferences in environmental matrix, the sensitivity of the aptasensors is relatively poor in natural water matrices (Zhang et al., 2018). Hence, the selectivity of the aptasensors in environmental matrices still needs to be further evaluated.

Vibrational spectroscopy techniques, specifically Surface-Enhanced Raman Scattering (SERS), have attracted considerable attention for antibiotics detection (Han et al., 2014; Li et al., 2016; Halvorson and Vikesland, 2010; Wei et al., 2015; Li et al., 2014; Pinheiro et al., 2018). SERS is a highly sensitive technique that provides information about the molecular structure via vibrational spectra of molecular bonds. Raman signals can be enhanced significantly when the molecules are attached to rough metal surfaces or nanostructures because of the electromagnetic enhancement and the chemical charge transfer effect (Han et al., 2022). SERS has been shown to identify chemical and biomedical species at parts per billion (ppb) level or even single molecules (Thrift et al., 2020). For example, Dhakal et al. reported a label-free SERS method for the screening of tetracycline in whole milk. Although several tetracycline peaks overlap with those of milk, they found a few tetracycline peaks were unique for tetracycline identification (Dhakal et al., 2018). Therefore, SERS has the potential to serve as a label-free online sensor to identify specific molecules, including antibiotics.

Despite promises, unlike the relatively simple composition of milk which is usually predominant by numbers of known proteins and lipids, the complexity of environmental samples may yield unpredictable overlapping spectra that can interfere with the Raman signals of the target chemicals. Moreover, the interference species in wastewater can hinder the target chemical from attachment to hotspots (regions of field enhancements) on metal surfaces or nanostructures (Mosier-Boss, 2017; Mariño-Lopez et al., 2019). One strategy to overcome the interference is to pre-tag SERS reporters that have a higher selectivity for target molecules. For instance, antibody-based SERS reporters can capture the target biomolecules through antibody-antigen interactions, while aptamer-based SERS reporters are focusing on the selective enhancement of targets including metal ions, proteins, nucleic acids, viruses, cells, and even bacteria (Wang et al., 2017). However, the analytical methods using SERS reporters are limited to pre-determined target species and require considerable modifications of SERS substrates (Wei and Cho, 2021). Developing SERS reporters for rapid, highly efficient, and specific capture of target molecules that also achieve high SERS is also no small feat. Thus, label-free SERS is a preferred option for target detection.

Previously, we reported the fabrication of SERS substrates using the chemical assembly of gold nanoparticles from colloids using electrohydrodynamic flow and the creation of 2-dimensional arrays of discrete nanoparticle clusters. Our design of driving chemical reactions between ligands on nanoparticles (self-assembly) allows for precise control of nanogap spacing. This is advantageous for controlling near field optical properties, exhibiting reproducible billion-fold signal enhancement in Raman measurements (Thrift et al., 2017).

Here, we report testing and comparing of two surfaces of gold nanostructures as SERS substrates for label-free capture and Raman signal enhancement of quinoline, a small molecular weight antibiotic that is commonly found in wastewater. Quinoline is selected as a model molecule

because of its molecular size and ring structure, which is favorable for SERS detection. The Self-Assembled SERS substrate, as previously reported, was fabricated using a hierarchical chemical assembly method to control sub-nano gap spacings (Thrift et al., 2017). The second SERS substrate was purchased from Silmeco (Denmark), a commercial product with gold nanofingers. The study tests the hypothesis that nanogaps on the Self-Assembled SERS substrate have specific selectivity based on molecular size, which excludes the interreference from large molecules that are commonly found in wastewater samples. The study showed the rapid detection of quinoline molecules in wastewater on the Self-Assembled SERS substrate in the concentration spanning 5 orders of magnitude from 50 ppm down to 5 ppb in the presence of diverse organic and inorganic contaminants. The results from this proof-of-concept study indicate the potential for real-time, label-free sensing of antibiotics in wastewater.

2.2 Materials and methods

2.2.1 Chemicals and wastewater samples

Quinoline was used as the target analyte to evaluate the capability of label-free signal quantification using SERS in wastewater. 98% reagent grade quinoline (C_9H_7N, 129.16 g/mol) was purchased from Sigma-Aldrich (St. Louis, MO). A 50 ppm quinoline stock solution was prepared by diluting quinoline in nanopore deionized water (Milli-Q Millipore System).

To test the selectivity of SERS on the substrate, glycine ($C_2H_5NO_2$, 75.07 g/mol), L-arginine ($C_6H_{14}N_4O_2$, 174.2 g/mol), erythromycin ($C_{37}H_{67}NO_{13}$, 733.93 g/mol), humic acid ($C_{187}H_{186}O_{89}N_9S_1$, 4015.55 g/mol), and microcystin-LR ($C_{49}H_{74}N_{10}O_{12}$, 995.19 g/mol) were included as the reference molecules. Erythromycin and glycine were purchased from Sigma-Aldrich (St. Louis, MO). Humic acid and microcystin-LR were purchased from Fisher Scientific

(Pittsburgh, PA). L-arginine was purchased from Alfa Aesar (Haverhill, MA). Each reference chemical was dissolved in nanopore deionized water to prepare a 5 ppm stock solution.

Wastewater samples collected from a local wastewater treatment plant were used as the background sample matrix to examine the SERS signal intensification and interreferences from organic and inorganic molecules in sewage. The wastewater was treated by advanced primary sedimentation followed by an activated sludge process with nitrification and denitrification. The secondary effluent used in this study meets the wastewater discharge requirement for biochemical oxygen demand (BOD), trace organics, and metal water quality parameters (United States Environmental Protection Agency, 2010) and is treated further for indirect potable water reuse (Orange County Sanitation District, n.d.). The range of water quality parameters in the secondary effluent is provided in the supplementary information (Table A.1). Although trace antibiotics had been reported in secondary wastewater effluents (Karthikeyan and Meyer, 2006; Vidal-Dorsch et al., 2012), the presence of quinoline in the secondary wastewater effluent from the specific plant has not been reported. The annual total organic carbon (TOC) and total dissolved solids (TDS) in the secondary effluent from this plant is 14 mg/L and 935mg/L, respectively, suggesting the presence of interference organic and inorganic molecules in the secondary effluent (Table A.1).

2.2.2 SERS Substrates

Self-Assembled SERS substrates were fabricated in microfluidic channels with a capacitor architecture. Briefly, silicon substrates (NOVA Electronic Materials) were spin coated with poly (styrene-b-methyl methacrylate) (PS-b-PMMA) thin films as described in previous work (Adams et al., 2012) to serve as the working electrode. Indium tin oxide (ITO) coated glass slides (Delta Technologies) were served as the counter electrode. Electrical contacts were made by platinum

wires and silver paste (Epoxy Technology). 20 µL 2.6 nM lipoic acid functionalized Au nanoparticles (NPs, 40 nm, Nanocomposix) along with freshly prepared N-hydroxysulfosuccinimide (s-NHS, Sigma Aldrich) and 1-Ethyl-3-(3-dimethyl aminopropyl) carbodiimide (EDC, Sigma Aldrich) solution were placed inside microfluidic channel for chemical cross-linking reactions as described in previous work (Thrift et al., 2017). An oscillation electric field with potential of 5 Vp and frequency of 100 Hz was applied to the microfluidic channel for 2 min to deposit an Au NP seed layer, then the second deposition step was conducted with the same potential but with frequency of 1000 Hz for 2 min. After each deposition step, the electrode cell was dismantled and the sensor surface was thoroughly rinsed with DI water and isopropyl alcohol (IPA, Sigma Aldrich) and then dried with N_2. Chemical cross-linking reactions between NP leads to Au NP clusters with reproducible SERS signal over a large area (Thrift et al., 2017). A scanning electron microscopy (SEM) image of a Self-Assembled SERS surface is depicted in Figure 2.1. The observed gap spacing is 0.9 nm with high uniformity. A normalized SERS intensity map of benzenethiol's vibrational band acquired over a 100 µm × 100 µm area was shown in our previous report (Nguyen et al., 2018). The SERS intensity has an RSD of 10.4% indicating the uniform SERS enhancements on the Self-Assemble SERS substrates. Detailed characterizations of the Self-Assembled SERS substrate including preparation repeatability and reproducibility of signal can be found in previous reports (Thrift et al., 2017; Nguyen et al., 2018).

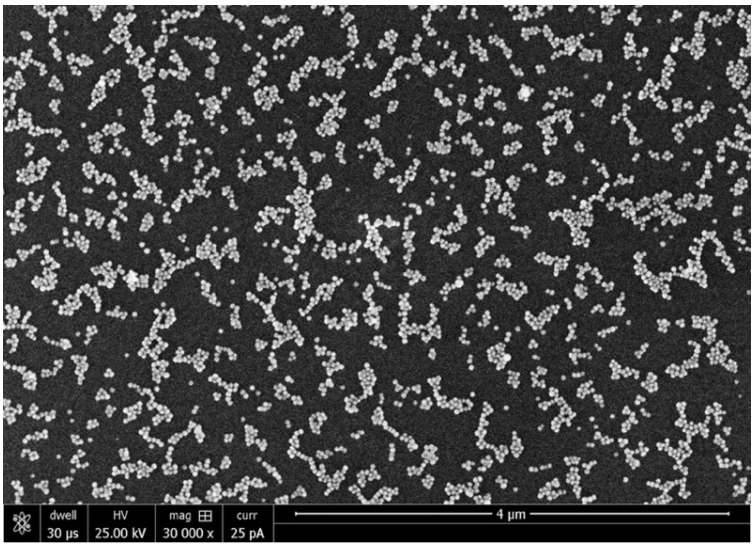

Figure 2.1. SEM image of Self-Assembled SERS substrate

SERStrates, the commercially available SERS substrates with gold nanopillar, were purchased from Silmeco (Denmark). According to Silmeco, SERStrate has the nanofinger design that is used to capture molecules and create hotspots via the leaning process happening with solvent evaporation. The structure of the SERStrate is available from the company's website (Silmeco, n.d.). SERStrate has been used for the detection of trace amounts of explosives as well as chemical warfare agents according to the manufacturer's website (Silmeco, n.d.).

2.2.3 Sample preparation

Before each experimental trial, quinoline working solutions in the concentration range from 5 ppm to 5 ppb were freshly prepared by diluting the stock solution with DI water. Wastewater samples were spiked with quinoline in the same concentration range to determine the sensitivity and interreference of chemical species in wastewater matrices for SERS.

For Raman spectral analysis on the Self-Assembled SERS substrate, 10 µl solution of the analyte was spotted directly onto the substrate for immediate Raman measurements without the need of

drying. After Raman measurements, the sample droplet was blown off from the substrate surface by pressured air, washed by DI water, and reused for the next sample to simulate the near real-time measurement of quinoline in wastewater stream. Quinoline spiked samples were tested from the low concentration to the high concentration in the serial diluted samples.

For Silmeco SERStrate, the same volume of the analyte solution was loaded onto the substrate. Since SERStrate relies on solvent evaporation to create leaning of gold fingers to shrink the nanogap space for SERS, the loaded samples were dried at room temperature for 40 minutes to evaporate water before Raman measurement following the manufacturer' protocols.

To test the selective intensification of target molecules on the Self-Assembled SERS substrate, 10 μl of 5 ppm quinoline, glycine, L-arginine, humic acid, microcystin-LR, and erythromycin solution were loaded onto the Self-Assembled SERS substrate, respectively, for Raman measurement following the same procedure as for quinoline.

2.2.4 Reusability of SERS substrate

The cleaning procedure for the Self-Assembled SERS substrate was carried out following the protocol described in the previous study (Nguyen et al., 2018). In brief, the used substrate was rinsed and soaked in 50 ml DI water for 20 mins, then air dried at the end of DI water soaking and re-examined for Ramen spectra to monitor the quinoline signal intensity. Quinoline Raman peaks collected using freshly made and DI water washed Self-Assembled SERS substrates were compared to evaluate the reusability of the Self-Assembled SERS substrate.

DI water washing as performed for the Self-Assembled SERS substrate could not remove the existing chemical signals from the SERStrate because of the trapping of dried chemicals within the nanofingers. A more aggressive procedure to removal organics was used to test the reusability

of SERStrate. Briefly, the used SERStrate was rinsed by DI water, then washed with 5N HCl for 10 mins to create an acidic environment for oxidizing carbonaceous molecules. Following the acid wash, the SERStrate was rinsed with 70% ethanol for 30 seconds, followed by 10 seconds of DI water rinse. The DI water was blown off by pressured air and dried. The cleaned SERStrate was examined for residual quinoline signal before being reused for the second round of quinoline testing.

2.2.5 Raman measurements on SERS substrate and UPLC-MS/MS analysis

Raman spectra were collected using a Renishaw InVia Raman Microscope (Renishaw, Wotton-under-Edge, UK) coupled with a 785 nm excitation wavelength laser. For droplet measurement using the Self-Assembled SERS substrate, a 60x water immersion objective lens with a 1.2 numerical aperture was used for Raman spectra collection. The measurements were taken with 7.3 μW laser power and 0.5 second exposure time, scanning a spectral region from 508 to 1640 cm^{-1}.

For Raman measurement using Silmeco SERStrate, a 50x objective lens was coupled with 7.3 μW laser power and 0.5 second exposure time to collect Raman spectra. Multiple Raman spectral measurements were collected from each sample using the simple mapping measurement method (Renishaw, UK). Pixels with 4 μm step size were generated within a 100 x 100 μm^2 area on the SERS substrate. A complete spectrum is acquired at each pixel. A total of 625 Raman spectra collected within 5 minutes were used in modeling and analysis. To validate the SERS assay, a Quattro Premier UPLC-MS/MS instrument coupled with an Acquity BEH C18 UPLC column (Waters Corp, Milford, MA) was applied to quantify the concentration of quinoline.

2.2.6 Spectral preprocessing

Raman spectra were preprocessed, analyzed, and visualized using Python 3.6.6. The details of the processing steps were presented in the previous studies (Thrift et al., 2019; Thrift et al., 2020). Briefly, the background subtraction was first carried out using the asymmetric least squares (AsLS) method (Eilers and Boelens, 2005) in NumPy with $\lambda = 10{,}000$, $p = 0.001$ to extract the true Raman peak intensities. Numerical processing was conducted using the Savitzky–Golay algorithm (Savitzky and Golay, 1964) with a third-order polynomial and window size of 11 for Raman spectra smoothing to increase the precision of the data without distorting the signal tendency. Outlier elimination was performed using the Isolation Forest algorithm in Scikit-Learn to isolate the misleading Raman data caused by background fluorescence, contamination, or poor focusing. Finally, Raman spectra were scaled to have a minimum value of 0 and a maximum value of 1 with MinMaxsScaler implemented in Scikit-Learn. The preprocessing allows for the comparison of measurements with slight intensity deviations due to the experimental setup.

2.2.7 Spectral analysis and modeling

According to a literature report, the Raman spectra of the quinoline within the region from 700 to 1640 cm^{-1} include several characteristic peaks locating at 760, 1014, 1034, 1372, 1392, 1433, and 1571 cm^{-1} (Fleischmann et al., 1983). The peaks at 760 cm^{-1} represents the ring deformation. The peaks at 1014 and 1034 cm^{-1} are attributed to the ring breathing. CCC stretching modes contribute to the peaks at 1372, 1392, and 1571 cm^{-1}. CH rocking modes give rise to the peaks at 1433 cm^{-1} (Bolboaca et al., 2002; Küçük et al., 2012; Fernandes et al., 2016). Two peaks at 760 and 1372 cm^{-1} are the most intense among all peaks. For quinoline quantification, the Raman peak at 770 cm^{-1} (a shift from 760 cm^{-1}) was first used for signal quantification. The relationship between this single

quinoline peak intensity from the averaged Raman spectra and the sample concentration was evaluated using the linear regression algorithm in Microsoft Excel. R^2 of the linear regression was calculated to present the sensitivity and accuracy of the detection method using the single peak intensity. Limit of detection (LOD) was calculated using the equation $LOD = 3S_a/b$ (Shrivastava and Gupta, 2011), where S_a is the standard deviation of the Raman peak intensities at 770 cm^{-1} in the measurements for the blank sample and b is the slope of the linear regression curves.

To further increase the detection sensitivity and minimize the background interference to the target Raman spectra, a predictive model was developed using non-negative matrix factorization (NMF) method (Cichocki and Phan, 2009) followed by the partial least squares (PLS) regression analysis (Geladi and Kowalski, 1986) as previous described (Nguyen et al., 2018; Thrift et al., 2019). Briefly, the model first applied NMF algorithm to differentiate the vibrational spectra of quinoline from interference species in wastewater, and the SERS substrate. NMF was implemented with Scikit-Learn using default settings to extract quinoline characteristic components that were decomposed from the complete Raman spectra. PLS regression, which combines characteristics of principal component analysis (PCA) with multiple linear regression to predict a set of dependent variables from a large set of independent variables, was also applied with Scikit-Learn. Consequently, PLS analyzed the full quinoline component extracted with NMF to build a predictive model of quinoline concentration in a complex matrix. The model was constructed using 80% of the spectral data and the remaining 20% of the spectra were used to evaluate the accuracy of the model. PCA (Minka, 2000) was performed on the SERS data collected from different samples using Scikit-Learn to visualize the difference of each sample by decreasing the dimensional variables. For each sample, 50 Raman spectra were randomly selected and displayed on a coordinate system.

2.3 Results

2.3.1 Detection of quinoline in pure water

Averaged Raman spectra of quinoline in DI water collected using the Self-Assembled SERS substrate at concentrations of 0, 5ppb, 50 ppb, 500 ppb, 5 ppm, and 50 ppm are shown in Figure 2.2a. The experimental spectra locating at 770, 1019, 1030, 1376, 1391, 1440, and 1579 cm^{-1} were in good agreement with the quinoline characteristic peaks shown in the literature report (Fleischmann et al., 1983), while the peaks locating at 1057, 1133, 1264, 1314 and 1463 cm^{-1} were not previously reported in the literature. The peaks at 1057, 1133, and 1314 cm^{-1} are attributed to the CH bending. The peak at 1264 cm^{-1} represents the CNC bending, and the peak at 1463 can be assigned to the CH rocking (Bolboaca et al., 2002; Küçük et al., 2012; Fernandes et al., 2016). The quinoline peak assignments are summarized in the supplementary information (Table A.2). Two non-quinoline peaks at 1002 and 1145 cm^{-1} found in the experimental spectra could be contributed to the residual of methanol used to clean the microscope objective lens as their peak intensity did not increase with the increase of quinoline concentration. Quinoline Raman peaks located at 770 and 1376 cm^{-1} are two most intense peaks, and the intensity increase with the increase of quinoline concentration from 5 ppb to 50 ppm. Figure 2.2c demonstrates the linear relationship between log10 transformed quinoline concentration and log10 Raman intensity at 770 cm^{-1}. The linear regression equation: $\text{Log } C = 0.209 \log I + 2.9994$, was established using the data from the quinoline samples of 5 ppb to 50 ppm with the R^2 of 0.97, where C and I represent quinoline concentration and Raman spectral intensity at 770 cm^{-1}, respectively. The results of quinoline detection using UPLC-MS/MS show the similar detection range of quinoline concentrations indicating the validate of SERS quantification (Figure A.1).

Similarly, quinoline in DI water was also captured by the SERStrate (Figure 2.2b). Similar to the spectra collected using the Self-Assembled substrate, characteristic quinoline peaks at 770 and 1376 cm^{-1} were clearly observed on SERStrate down to the concentration of 5 ppb (Figure 2.2b). The linear regression equation: Log $C = 0.2505 \log I + 3.1624$, calculated using log10 transformed quinoline concentration and Raman spectral intensity at 770 cm^{-1} showed a strong correlation with $R^2 = 0.97$ (Figure 2.2d). SERStrate and Self-Assembled SERS substrate had a similar sensitivity to effectively detect and quantify quinoline in pure water with the LOD of 1.15 and 2.57 ppb, respectively. The relative standard deviation (RSD) of peak intensities was larger in the measurements by the Self-Assembled SERS substrate, which is attributed to the molecular diffusion around the hotspots when collecting signals in the wet mode.

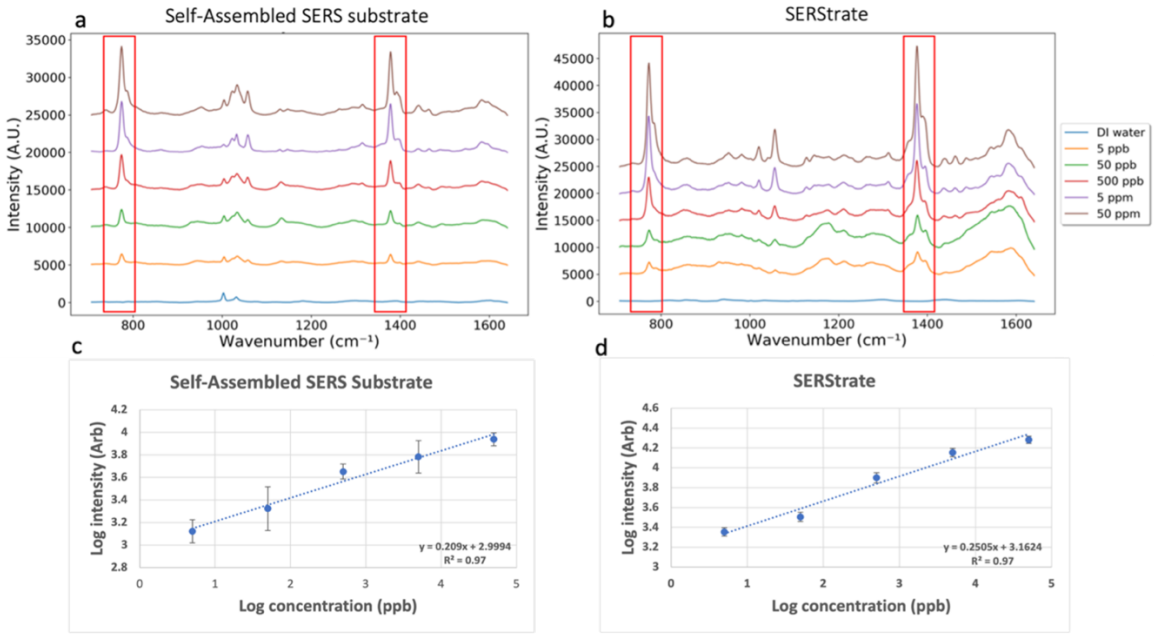

Figure 2.2. SERS spectra of DI water and quinoline spiked DI water in the concentration range between 5 ppb and 50 ppm collected using (a) Self-Assembled SERS substrate and (b) SERStrate. And the relationship between the log values of Raman intensity of the quinoline peak at 770 cm^{-1} and log10 values of quinoline concentration using (c) Self-Assembled SERS substrate and (d) SERStrate.

2.3.2 Detection of quinoline in wastewater

When the vibrational spectra of quinoline spiked wastewater was characterized on the two different SERS substrates, two very different outcomes were observed (Figure 2.3). Similar Raman spectra as seen for pure water samples were observed on the Self-Assembled substrate (Figure 2.3a). Characteristic quinoline peaks at 770 and 1376 cm^{-1} (shift from 760 and 1372 cm^{-1}) were clearly seen at seeding concentrations between 5 ppb and 50 ppm. When comparing the spectra of 5 ppb quinoline spiked DI water, the quinoline peak intensity of 5 ppb quinoline spiked wastewater was slightly lower. This might be a consequence of the adsorption of a small amount of quinoline to large organic molecules and debris in wastewater, which prevents quinoline access to the SERS hotspot. In addition, Raman spectra of quinoline spiked wastewater exhibited greater RSDs compared with the spectra of quinoline spiked DI water, suggesting some inferences of sewage molecules in the Raman spectra.

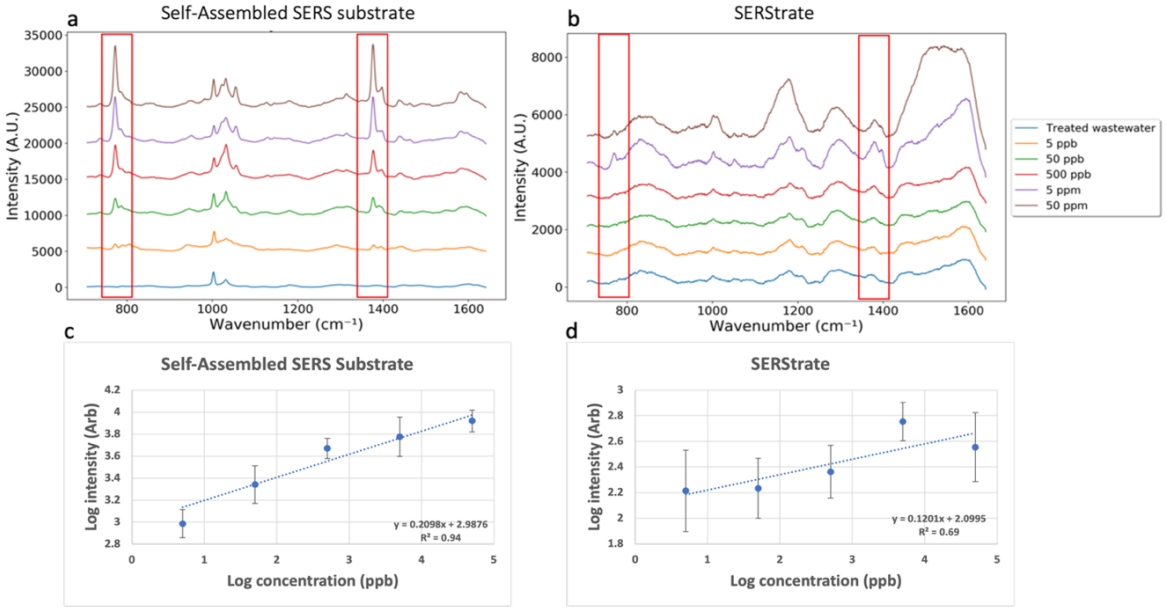

Figure 2.3. SERS spectra of treated wastewater and quinoline spiked wastewater in the concentration range between 5 ppb and 50 ppm collected using (a) Self-Assembled SERS substrate and (b) SERStrate. And the relationship between the log values of Raman intensity of the quinoline peak at 770 cm^{-1} and log values of quinoline concentration using (c) Self-Assembled SERS substrate and (d) SERStrate.

Examination of the wastewater only control sample revealed similar Raman spectra to pure water on the Self-Assembled substrate; no other visible peak was found in the Raman spectra other than the substrate background peaks. This result suggests that the wastewater organics and inorganics had a minimal impact on the Raman spectra in the region because sewage molecules were not intensified by the Self-Assembled SERS substrate (Figure 2.3a). The relationship between log10 quinoline concentration and log10 Raman intensity at 770 cm^{-1} collected from wastewater samples was plotted in Figure 2.3c. A linear relationship with the R^2 of 0.94 was identified. The linear regression curves were nearly identical for quinoline in wastewater and in DI water, while the actual peak intensity of 5 ppb quinoline in treated wastewater was slightly lower than the intensity estimated by the linear regression curves. Furthermore, the SERS measurement of this scenario yields a LOD of 5.01 ppb, which is slightly higher than the LOD of the pure water scenario. The results suggest that the complex matrix did not significantly interfere the Raman spectra of quinoline on the Self-Assembled SERS substrate at the high concentration range, but it had a slight effect on the quantification accuracy at the concentration of 5 ppb when using a single characteristic Raman peak to detect quinoline concentrations.

Raman spectra of quinoline spiked wastewater collected on SERStrate (Figure 2.3b) only showed discernable quinoline peaks at 770 and 1376 cm^{-1} in the two samples with the highest spiked concentrations of 5 ppm and 50 ppm. The characteristic Raman peaks were not observed at seeding concentrations below 500 ppb (Figure 2.3b). There were high background spectral noises detected on the control wastewater. The noise spectra were enhanced when the quinoline spiked wastewater samples were loaded on the SERStrate from the low to the high concentration, suggesting Raman signals of wastewater molecules were captured and intensified during the drying process. In comparison with results for quinoline spiked in pure water, the signal intensity of quinoline peaks

was significantly reduced (Figure 2.3d) due to the interference from wastewater molecules that likely blocked the SERS hotspots. There was no linear relationship between the log10 Raman intensity of the quinoline peak at 770 cm^{-1} and log10 quinoline concentration (Figure 2.3d). In fact, the Raman signal intensity for quinoline concentration of 50 ppm was lower than its intensity at 5 ppm (Figure 2.3d), suggesting interference of sewage molecules likely by occupying the nanogap space and blocking the access of quinoline to the hotspots. Moreover, the Raman spectral intensities collected from the randomly selected spots on the 100 x 100 μm^2 SERStrate were highly heterogeneous as shown by the large RSDs in the measurements for each sample (Figure 2.3d). The heterogeneity could be the result of "coffee ring effect" (Ambroziak et al., 2020) created during drying of samples on SERStrate. The poor sensitivity and high heterogeneity in this detection scenario led to a LOD of 97.5 ppm, around 10,000-fold higher compared to the LOD of the pure water setting (1.15 ppb) and even higher than the maximum spiked concentration.

When applying PCA to Raman spectral data in an attempt to further classify the spectra from the target and interferences, the results showed that Raman spectra of treated wastewater were very similar to pure water on the Self-Assembled substrate (Figure A.2a). The spectra observed from the quinoline negative control samples reflected the spectra of water and the Self-Assembled substrate. Specifically, the Raman spectra of the contaminants in treated wastewater were not observed due to the lack of Raman signal amplification of large molecules in small nanogaps. A few outliers of the wastewater control measurements were observed in the PCA plot, which may be due to variability of the substrate surface or detection of molecules in the background of the wastewater. The Raman spectra of the samples spiked with 50 ppm quinoline in either pure water or wastewater overlapped on the PCA plot, indicating similar Raman spectral profiles of the two samples on the Self-Assembled SERS substrate.

On the other hand, the PCA plot of the Raman spectra of quinoline in DI water and in wastewater on the SERStrate were very different (Figure A.2b). First, a separation between Raman spectra of wastewater and pure water was found, suggesting molecules in wastewater were intensified by SERStrate. The quinoline spectra of the samples spiked with 50 ppm quinoline in DI water and wastewater formed separate clusters on the PCA plot, indicating the drastically decreased intensity of quinoline signals and the high background signal from the molecules in wastewater.

SERStrate and the Self-Assembled substrate are designed differently in achieving SERS. SERStrate requires drying to trap molecules within the nanofingers. Therefore, there is no selectivity for the molecular size of the target. Wastewater molecules regardless of size can be trapped by the nanofingers and intensified. The Self-Assembled substrate enhances spectral signals from molecules within the designed nanogap space, therefore, small molecules on length scales of nanogap distance can enter the gap space and be disproportionally enhanced. Large molecules in wastewater, for example, humic acid (General molecular weight: 4015.55 g/mol), did not interfere with the signal from the Raman spectra of the small molecular weight quinoline (Figure A.3). In fact, insignificant Raman signal was observed for larger molecular weight chemicals such as erythromycin (733.93 g/mol), microcystin-LR (995.189 g/mol), and humic acid (4015.55 g/mol) according to our screening tests (Figure A.3), suggesting these large molecules may be excluded from approaching the nanogap space between gold nanoparticles. In addition to the large molecules, testing of the interferences from several small molecules that commonly found in wastewater such as glycine and L-arginine also showed negligible results (Figure A.3). This is likely because their molecular structures have very small Raman cross-section. Although these small molecules can enter the nanogap space between gold nanoparticles, they do not interfere

with the signal from the Raman spectra of quinoline, especially at the concentration of 5 ppm or less.

2.3.3 Quantitative detection of quinoline in wastewater using predictive model

Despite the reasonable quantification outcomes using a single characteristic Raman peak to detect quinoline concentrations in wastewater on the Self-Assembled substrate, the inclusion of multiple quinoline Raman scattered peaks in the analysis may further improve the performance for detecting target molecule as shown in previous studies (Nguyen et al., 2018; Thrift et al., 2019). The results shown in Figure 2.4 demonstrate the application of NMF filtering and PLS regression model to separate the quinoline spectra among interference signals.

As seen in Figure 2.4a, NMF extraction of quinoline Raman signals yielded four major NMF components that could be separated from the Raman spectra of wastewater on the Self-Assembled SERS substrate. The first NMF component represents the quinoline characteristic Raman signal including two quinoline peaks located at 770 and 1376 cm^{-1}, while the other three NMF components are attributed to the signals of SERS substrate, background fluorescence, and minor contribution from molecules in wastewater.

Figure 2.4b shows SERStrate Raman spectra separated by NMF. In the NMF component 1, two discernable quinoline Raman peaks were observed at 770 and 1376 cm^{-1}. However, the peak intensity was significantly lower compared to the quinoline NMF component 1 in Figure 2.4a. Moreover, there were other interference peaks coexisting with quinoline signals in a single component, indicating the NMF algorithm was limited due to the high background spectra noises detected in the wastewater and the weak intensification of quinoline signals. Although NMF filtered out most of the background spectral noise and enhanced the identification of quinoline

signals, NMF could not resolve the issue of background interference, suggesting the importance of selective intensification of target molecules.

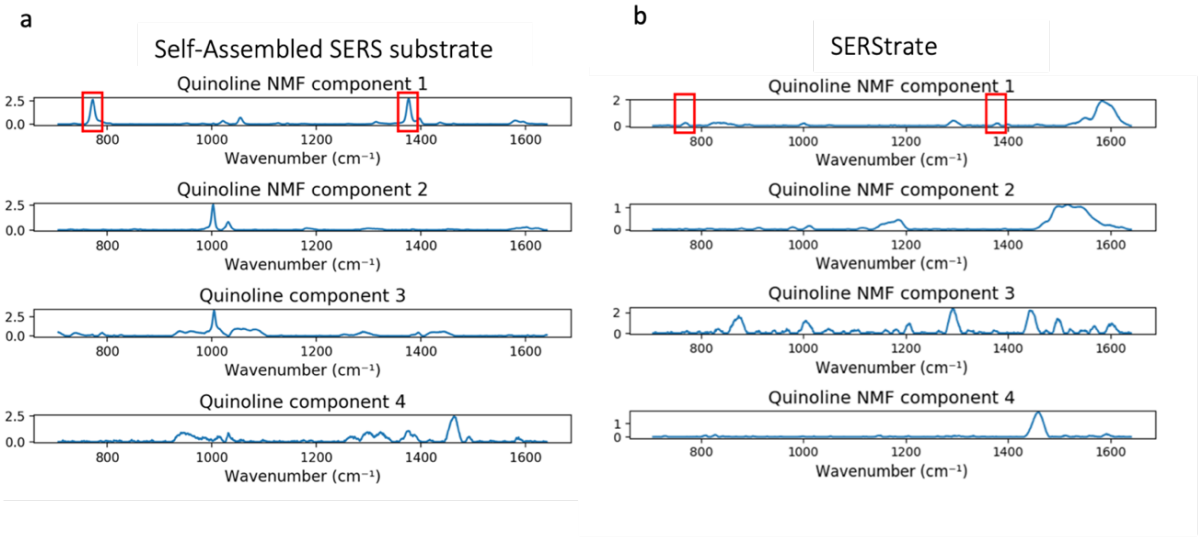

Figure 2.4. Four major non-negative matrix factorizations (NMF) components separated from a complete Raman spectrum of wastewater seeded with quinoline, collected using (a) Self-Assembled SERS substrate and (b) SERStrate.

Quinoline concentrations predicted by the PLS model for quinoline spiked wastewater collected using both Self-Assembled SERS substrate and SERStrate are presented in Figure 2.5. 80% of spectral data were used for model construction, and the remaining 20% of the spectral data were used as a holdout set to test the accuracy of the predictive model. Figure 2.5a shows the relationship between spiked quinoline concentrations in treated wastewater and their predicted concentrations based on spectra collected with the Self-Assembled SERS substrate. The horizontal line shown in Figure 2.5 is PLS model predicted quinoline concentration of un-spiked wastewater, which represents the background noise from the interference molecules in the wastewater.

A value of R^2=0.98 shows good performance of the predictive model when analyzing the holdout set. In comparison with the linear regression curve built with the same data set using a single

Raman peak (Figure 2.3c), there was a clear improvement in the predictive performance as indicated by an increase of R^2 value from 0.94 to 0.98. Moreover, unlike the linear regression curve that overestimated the concentration of 5 ppb quinoline spiked in wastewater, the predictive model achieved an accurate prediction between 5 ppb and 50 ppm of quinoline spiked in wastewater.

Figure 2.5b displays the predictive result based on spectra of quinoline spiked wastewater collected using SERStrate. Despite the overall underestimation of quinoline concentrations, which might be affected by the coexisting of the noise peaks in the NMF component, a substantial improvement was observed in comparison with the linear regression curve built with the same data set (Figure 2.3d). Overall, the predictive model improved the quantification of quinoline at 500 ppb, 5 ppm, and 50 ppm, while the concentrations at 5 and 50 ppb were below the background noise. These results suggest that the predictive modeling using NMF and PLS algorithm is useful for enhancing the sensitivity and accuracy of the detection method by analyte isolation followed by the multivariate analysis, even in a severe scenario with high background spectral noise.

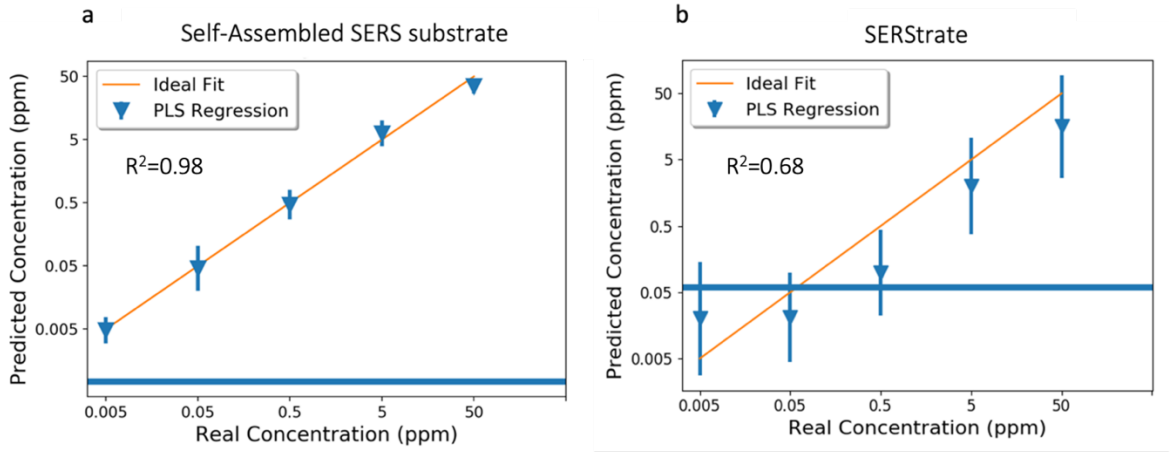

Figure 2.5. Quinoline concentration in spiked wastewater predicted by the PLS model. (a) Spectra collected using Self-Assembled SERS substrate. (b) Spectra collected using SERStrate. The blue line indicates PLS model predicted quinoline concentration in un-spiked wastewater, which represents the background noise from the interference molecules in the wastewater.

2.3.4 Reusability of SERS substrate

On the Self-Assembled substrate, SERS signal enhancement relies on target molecules entering the hotspot region near the nanogap space through molecular diffusions in liquid; measurements are performed in water. The analyte can be easily removed from substrate surface by DI water washing as shown Figure 2.6a. No quinoline peak was found on the Self-Assembled SERS substrate after 20 min DI water washing. The reusability was demonstrated by the similar signal intensity of quinoline peak when 50 ppm quinoline was loaded on virgin and washed Self-Assembled substrate, respectively (Figure 2.6a). The physical images of the Self-Assembled SERS substrate under the microscope before and after washes (Figure A.4) also indicated that the Self-Assembled gold nanoparticles were stable during reuse.

SERStrate requires evaporation of the carrying fluid and the clasping of the gold nanofingers to achieve Raman signal enhancements. The substrate reusability results showed that DI water washing only was ineffective at removal of the signal of dried analyte from the SERStrate surface. However, washing by acid followed by rinsing with ethanol was able to recovery SERStrate surface (Figure 2.6b). The second round of sample preparation and drying revealed the similar Raman spectra intensity of analyte (Figure 2.6b), suggesting recovery of gold nanofingers for recapturing the target molecules. However, the SERS capability degraded after the next round of the regeneration process, suggesting the deterioration of the performance, which is likely due to the deformation of the gold nanofingers on the substrate surface.

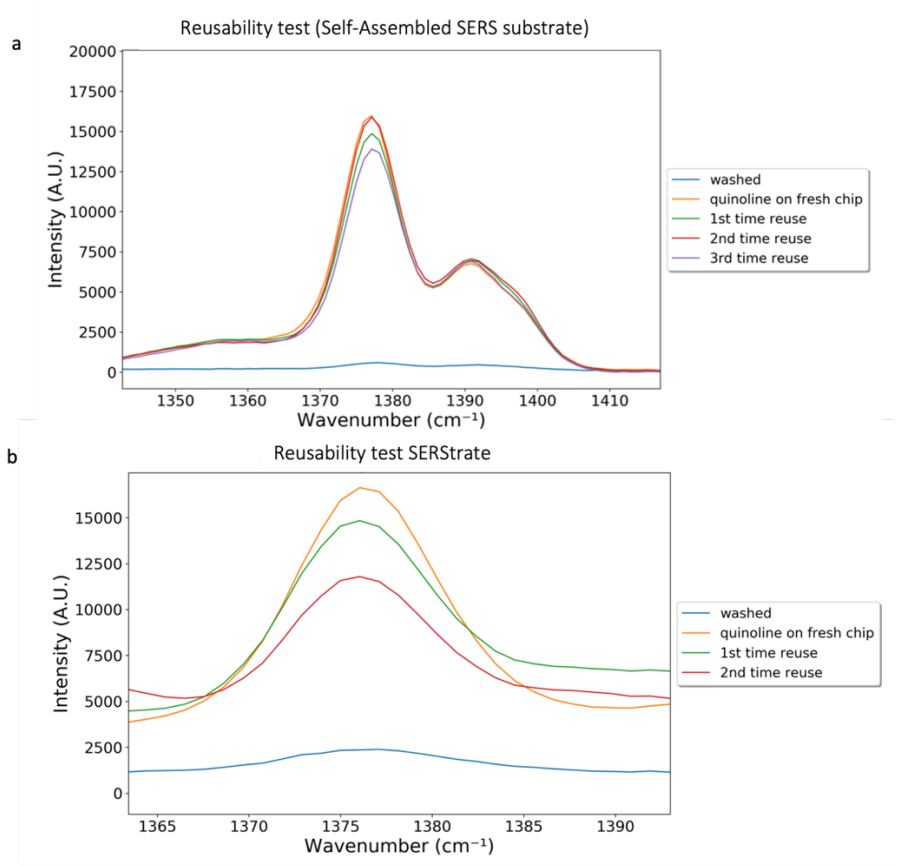

Figure 2.6. (a) SERS spectra of washed Self-Assembled substrate and comparison of 50 ppm quinoline collected using freshly-made and washed Self-Assembled SERS substrate at 1360 cm^{-1}. (b) SERS spectra of acid washed SERStrate and comparison of 50 ppm quinoline collected using fresh SERStrate and acid washed SERStrate at 1360 cm^{-1}.

2.4 Discussion

Real-time detection of antibiotics and other trace organic contaminants in wastewater is critical for human and environmental health protection. This research presents a proof-of-concept for the potential application of SERS as a label free, real-time sensor for monitoring of small molecular weight antibiotics in wastewater. Among various sensing techniques, Raman spectroscopy enables rapid, precise *in situ* molecular identification with the extremely low Raman activity of water molecules (Liang et al., 2021). SERS further expands the application scope of standard Raman spectroscopy and identifies molecules at the single-molecule scale (Kneipp and Kneipp, 2006).

Because of such promises, many forms of the SERS substrate have been developed thanks to the rapid advancement of material sciences (Mosier-Boss, 2017; Liu et al., 2020). However, different substrate designs affect the performance in different environments and for different targets.

Comparisons of results from the Self-Assembled substrate and SERStrate clearly show that SERStrate although can achieve great accuracy after capturing and immobilizing the target molecule within the nanogap space, the immobilization step limits the real-time potential of SERStrate. The evaporation of solvent to shrink the nanogap space of gold nanofingers is not only time consuming, but also the evaporation requirement limits the reusability of SERStrate due to the necessity of the more aggressive regeneration procedure to remove the dried chemicals trapped in the shrunken nanofingers. Aggressive cleaning caused the deformation of the gold nanofingers on the substrate surface. Therefore, SERStrate doesn't seem to have the potential to be incorporated into a real-time, reusable sensor design. On the contrary, the Self-Assembled substrate relies on molecular diffusion in the liquid around the gold nanoparticles on the surface with evenly distributed nanogap space to achieve SERS. Self-Assembled SERS substrate and SERStrate had a similar performance to effectively detect and quantify quinoline in pure water. The main advantage of Self-Assembled substrate is the ease of removal of analyte from the surface by a DI water washing for reuse in the next around of measurements. This allows a real-time sensor design by mounting a Self-Assembled SERS substrate in a testing chamber that is filled with a slow flowing side stream of the wastewater. The chamber is excited by a laser beam at pre-determined intervals and the signal is captured by a spectrophotometer. A clean water wash stream to the chamber can be incorporated by switching the valves between the sample stream and the wash stream. The reusability study showed that there was no signal degradation after washing away the analyte and re-exposure. Gold nanoparticles were stably maintained on the surface. The

proof-of-concept study presented here is to provoke thinking and future exploration of SERS application in real-time sensing of environmental contaminants.

Among various challenges facing SERS implementation as a label-free, real-time sensor for contaminants detection in the waste stream, interference from non-target molecules on the substrate surface is Achilles heel of the technology. The results of this research found that nanogap space between gold nanoparticles on the SERS substrate played an important role in selective intensification of target molecules. The SERS mainly depends on the electromagnetic effect, which is determined by the distance between metallic nanoparticles on the substrate, increasing with decreasing gap size. Single-molecule SERS intensity can be observed when nanogaps are on the order of 0.5-0.9 nm. In addition to the SERS enhancement factors, detection selectivity and reproducibility are also critical to ensure the performance of target detection in the wastewater environment. Self-Assembled SERS substrates have carefully designed gold-nanoparticle gap spacings of 0.9 nm with high uniformity, which form uniformly distributed electromagnetic hotspots over large areas, and thus have both uniform and large enhancement factors across SERS substrates to reproducibly achieve low detection limits. Moreover, the Self-Assembled SERS substrate relies on molecular diffusion in the liquid around the nano-spacings on the surface, which excludes the interreference from large molecules (size exclusion) that are commonly found in wastewater samples and selectively enhances signals from small molecules within the designed nanogap spaces. Previous studies (Nguyen et al., 2018; Thrift et al., 2019) showed that the Self-Assembled substrate can enhance Raman spectra of thiophenol (110.19 g/mol) and pyocyanin (210.236 g/mol) in addition to quinoline (129.16 g/mol) demonstrated in the current study. These chemicals have small molecular size and large Raman cross-section. They can diffuse into the nanogap space to achieve SERS. Raman signal enhancement was not observed for larger molecular

weight chemicals including humic acid, microcystin-LR, and erythromycin at concentration greater than environmental relevant concentrations. In addition to molecular sizes, Raman cross-section also played an important role of SERS. Experiments with amino acid including glycine (75.07 g/mol) and L-arginine (174.2 g/mol) showed minimal interference at the concentration below 5 ppm, which is the approximate concentration level of amnio acid in the wastewater (Caicedo et al., 2016). These molecules are small enough to fit in the hotspots, but they have low Raman cross-section. This explains our observation of selective intensification of quinoline in wastewater without the interferences of other wastewater molecules.

On the other hand, the commercial SERStrate platform requires drying to trap molecules within the nanofingers and to form the electromagnetic hotspots. Despite the promises of high enhancement factors and detection reproducibility, there is no selectivity for the molecular size of the target in the wastewater environment. Both large and small molecules can be trapped during the drying process, which resulting in high interreferences by wastewater molecules. Therefore, the ideal SERS substrate for real-time environmental sensing requires 1) uniformed sub-nanometer nanogap dimensions over a large area; 2) selective SERS enhancement based on molecular size or other structure; 3) SERS measurements in liquid environments to avoid side-effect of drying and to improve reusability of substrate.

The coffee ring effect has been used to increase the sensitivity of SERS (Hussain et al., 2019). However, the results using SERStrate suggest the coffee ring formation following the evaporation of solvent causes uneven distribution of Raman spectral intensity collected from randomly selected fields. The coffee ring formation depends on the time scale competition between the liquid evaporation and the movement of suspended particles, and hence the particle size plays an important role. The coffee ring forms successfully only when the movement of the particles is

faster than liquid evaporation. When the size of suspended particles is below 20 nm, the nanoparticles distribute uniformly onto the surface instead of forming a coffee ring structure after liquid evaporation (Shen et al., 2010). Therefore, the coffee ring was formed when the wastewater that contains many suspended particles > 20 nm was evaporated on the substrate but not in DI water that contains very low numbers of particles >20 nm. The coffee ring decreases the reproducibility and accuracy of Raman measurements due to the non-uniform distribution of the target molecules. The unevenness of Raman spectral intensity also creates additional noises in data analysis, which further challenges the separation of Raman spectra between the target and the noise. Therefore, the commercial SERStrate platform that relies on evaporation of solvent to create nanogaps has an unavoidable issue in signal uniformity. On the other hands, samples on the Self-Assembled SERS substrate do not form the coffee ring because the evaporation step is not required for Raman measurements. The Raman signal intensification is based on the molecular diffusion near the hotspots of the substrate, a key advantage for real-time measurement of target molecules.

Artificial intelligence (AI) was proposed as a potential solution to identify the target Raman signals among noises from interference molecules (Kim et al., 2020). Our previous work showed the successful separation of target Raman signals from background noises using a predictive model constructed with a machine learning algorithm for noise filtering (Nguyen et al., 2018). Here, we showed that NMF and PLS regression are powerful tools for analyzing the full Raman shift regime of the quinoline NMF component to keep the complete spectral information. We demonstrated the improvements in quinoline signal identification among high background noises in Raman spectra collected on SERStrate for quinoline spiked wastewater. However, the model is still limited by the signal to noise ratio. More importantly, the interference molecules in the complex matrix, such as wastewater, are not only generating overlapping Raman spectra with the analyte but also compete

for the binding site for hotspots. On the other hand, synergy between the mechanism of the selective intensification of target molecules in the Self-Assembled SERS substrate and artificial intelligence successfully identified the quinoline signal among complex matrices in the lowest spiked quinoline concentration. Therefore, the results of the comparative study indicate that the development of a real-time label-free sensor for residual antibiotic detection using SERS should start from the tunable design of the SERS substrate. The potential application of SERS in environmental sensing is exciting but significant research is needed to transform the concept into a field applicable technology.

CHAPTER 3
QUANTIFICATION OF VIRUSES IN WASTEWATER ON A CENTRIFUGAL MICROFLUIDIC DISC

This chapter has been submitted to the journal Water Research as Huang and Jiang, 2024.

3.1 Introduction

The COVID-19 pandemic has underscored the intricate relationship between microbes and human health, serving as a stark reminder of the historical impact infectious diseases have had on humanity (Finlay et al., 2021). From the black plague, cholera, to influenza and the ongoing COVID-19 crisis, infectious diseases have shaped history and disrupted societies. Detecting infectious pathogens in the environment is the first line of defense in safeguarding human health, preventing the spread of diseases before they reach the human population (Goddard et al., 2020).

However, despite the critical importance of environmental monitoring and preventive measures, our predominantly human-centric society and healthcare system remain entrenched in the age-old paradigm of reactive disease treatment. The vast disparity in funding between medical interventions and environmental monitoring is staggering. Much more research funding is allocated to medicine, while the budget for environmental monitoring and preventive environmental management lags far behind. Environmental monitoring for pathogen contamination still stuck on the half-century old methods using culture media to grow fecal indicator bacteria, such as *E. coli* and *Enterococcus*, to suggest the level of fecal contamination that is associated with human pathogens (Jennings et al., 2018; Motlagh and Yang, 2019). In the developed countries like the United States, the fecal indicator bacteria monitoring is carried out by

the coordinated effort of the regional health department, the water resources department and the wastewater dischargers (i.e., wastewater treatment plants) (Schiff et al., 2001). This practice has reduced the waterborne infectious disease outbreaks but leave gaps in knowledge of pathogen contamination in small pockets of communities, especially those under privileged.

The situation is even more dire in the developing regions. According to the UN World Water Development Report, 80% of human wastewater flows back into the ecosystem without adequate treatment, resulting in approximately 1.8 billion people relying on water sources contaminated with fecal matter as their primary drinking water supply (Bain et al., 2014). The World Health Organization (WHO) estimates that water-related diseases cause more than 3.4 million deaths each year, making them the leading cause of human morbidity and mortality worldwide (Dufour et al., 2013).

Significant research progresses have been made to improve the time-consuming culturing and isolation-based method for monitoring indicator organisms and pathogens in the water sample. Nucleic acid amplification techniques, such as polymerase chain reaction (PCR) and loop-mediated isothermal amplification (LAMP), are introduced to environmental testing, which offer faster detection time, increased sensitivity, and higher accuracy (Toze, 1999; Martzy et al., 2017). However, these techniques require intensive sample preparation steps carried out by well-trained laboratory personnel prior to downstream detection. The pre-concentration and nucleic acid extraction processes during sample preparation are laborious and time-consuming. Additionally, conducting the analysis in centralized laboratories leads to a significant delay in turnaround time, which includes sample collection, transportation, and detection (Nnachi et al., 2022). This delay impedes the ability to promptly assess the sanitary quality of water and take immediate action if necessary. Beyond pathogen monitoring for water quality assessment, the wastewater-based

surveillance of pathogens has gained momentum during the COVID-19 pandemic (Gonzalez et al., 2020; Green et al., 2024). Simple, distributed and affordable technologies for pathogen monitoring are needed to broader implementation of pathogen monitoring in wastewater.

In our previous work, we demonstrated the potential of a microfluidic centrifugal disc (CD) driven by a potable centrifuge CD driver for rapid molecular diagnosis of *E. coli* and *Enterococcus* by enabling the semi-automated processing of the entire workflow involved in monitoring pathogens, including sample extraction, nucleic acid amplification, detection and quantification (Gowda et al., 2022). This system utilizes the forces generated within a rotating platform, such as centrifugal force, Coriolis force, and Euler force, to manipulate the fluidic sequence on a centrifugal microfluidic disc (Kong et al., 2016). The integration of specifically designed chambers, microchannels, and valves with these forces has led to our proof-of-the-concept demonstration of bacterial quantification using *E. coli* and *Enterococcus* seeded in water sample.

Built upon the foundation of the bacterial pathogen CD system, we present the development of a CD for virus detection in wastewater matrices in response to COVID-19 pandemic and the need for virus monitoring in water quality assurance. The new CD integrates sample concentration and nucleic acid purification steps to address two key challenges of environmental viral detection – presence of inhibitor for nucleic acid amplification and low pathogen concentration (Julian and Schwab, 2012). Here we demonstrated, by coupling with pseudo and non-pseudo forces generated during the CD rotation or CD oscillation, the completion of sample purification, concentration and detection automatically in less than 1.5 hours after sample loading. We assessed the sensitivity of the on-CD assay in detecting seeded SARS-CoV-2 in raw sewage. Furthermore, we successfully detected and quantified indigenous pepper mild mottle virus (PMMoV) in sewage and other environmental water matrices, demonstrating the potential of this CD platform for real-world

applications. This technology has the potential to significantly reduce the sample-to-answer time of virus monitoring, as well as the reliance on well-trained laboratory personnel and costly equipment.

3.2 Materials and methods

3.2.1 Virus and water samples

Heat-inactivated SARS-CoV-2 (NR-52286), provided by the Centers for Disease Control and Prevention through BEI Resources, was used as the target virus to investigate the sensitivity of the quantification assays. A SARS-CoV-2 stock solution at a concentration of 10^7 copies/ml was prepared by diluting heat-inactivated SARS-CoV-2 in nuclease-free water (Fisher Scientific, Hampton, NH). The stock solution was then stored in a -80°C freezer for future use.

The 24-hour time-weighted composite wastewater samples were collected from the sewer manholes using autosamplers within University of California, Irvine (UCI) student housing area, and were preserved immediately upon collection by mixing with the 2x DNA/RNA Shield (Zymo Research, Irvine, CA) in a 1:1 ratio and stored at -80 °C for future analysis. Wastewaters were first used as the background sample matrix in SARS-CoV-2 spiked tests for assessing and troubleshooting interferences caused by organic and inorganic matters in the wastewater. Additionally, wastewater samples were used for the detection of indigenous pepper mild mottle virus (PMMoV) in non-spiked wastewater. PMMoV is commonly found in high concentrations in wastewater and is used as an indicator of viral fecal contamination (Rosario et al., 2009; Kitajima et al., 2018), making it an ideal choice for the testing.

To further explore the performance of the assays across diverse environmental sample matrices, stormwater collected from UCI campus, creek water from San Diego Creek, Irvine, California,

and seawater from Newport Bay, Newport Beach, California were also applied for the PMMoV detection.

3.2.2 In-tube virus detection assay

An in-tube detection assay was first developed to optimize assay chemistry and to troubleshoot procedural issues encountered on CD system, which then served as the template for developing the on-CD assay. The efficiency of in-tube assay was also used as a benchmark for evaluating assay performance on the CD. The assay comprised three main components: target concentration, nucleic acid purification, and RT-LAMP detection.

The Quick-DNA/RNA Viral MagBead kit from Zymo Research (Irvine, CA) was adapted for sample concentration and nucleic acid purification. The manufacturer's protocol was followed for the in-tube assay (Zymo research, 2022). The procedures started with mixing 100 μL of water sample with 5 μL of Proteinase K in a 0.6 ml PCR tube and incubating at room temperature for 15 minutes to degrade proteins present in the sample. Subsequently, 200 μL of Viral DNA/RNA Buffer and 5 μL of MagBinding Beads were added to the sample and mixed for 10 minutes to allow the lysis of viral particles and the binding of nucleic acids to the MagBinding beads. An external magnet was applied to pellet the MagBinding Beads to the side of the tube, and the supernatant was discarded. The nucleic acids bound to the MagBinding Beads were washed twice using 100 μL each of MagBead DNA/RNA Wash 1 and Wash 2, followed by two more washes using 99% ethanol (Fisher Scientific, Hampton, NH) to further remove impurities from the sample. After air drying the MagBinding beads in tube for 10 minutes, nucleic acids were eluted and resuspended in 15 μL of nuclease-free water, preparing them for LAMP detection. This process resulted in a 6.67-fold concentration of nucleic acids in water samples.

The nucleic acid extracts were analyzed immediately by one-step reverse transcription-LAMP (RT-LAMP). The RT-LAMP was carried out on a thermocycler (Applied Biosystems, Waltham, MA) at 65 °C for 30 min. The reaction mixture consists of the WarmStart 2× LAMP Master Mix with fluorescence dye (New England BioLabs, Ipswich, MA), nuclease free water, the nucleic acid extracts, and the primers targeting either the N gene of SARS-CoV-2 or the coat protein (CP) gene of PMMoV (Integrated DNA Technologies, Coralville, IA). The final volume of the mixture is 20 μL and specific volumes for each component are detailed in Table B.1. The LAMP primers for SARS-CoV-2 were reported by Ganguli et al. (Ganguli et al., 2020), while the primers for PMMoV were designed using PrimerExplorer V5 (Table B.2).

3.2.3 On-CD virus detection assay

To integrate the in-tube detection procedures onto the CD, several necessary modifications were made for on-CD assay requirements. Firstly, the Zymo wash buffers and 99% ethanol used for cleaning of MagBinding beads were replaced with 70% ethanol solutions. The modifications were necessary due to the reactions of washing buffers and pure ethanol with CD binding glue that release organics from glue to inhibit downstream nucleic acid amplification. Secondly, the use of an external magnet for MagBinding beads collection in-tube was replaced with pelleting the beads by centrifugation. Centrifugation is more efficient on the CD and eliminates the need for an external magnet. Finally, a reaction droplet generation step was included in the on-CD detection assay to convert the binary RT-LAMP results into the quantitative virus detection through droplet digital RT-LAMP (ddRT-LAMP) (Schuler et al., 2016). All other procedures remained the same as for the in-tube assay.

Two types of oil were tested for the on-CD droplet generation following recommendations from previous research (Schuler et al., 2016; Schlenker et al., 2021). The Novec HFE 7500 oil (3M, Saint Paul, MN) mixed with 5 wt% FluoroSurfactant (RAN Biotechnologies, Inc.) was used as the emulsification oil for homogeneous droplet generation. After the droplet generation, the FC-40 (3M, Saint Paul, MN) containing 2 wt% FluoroSurfactant (RAN Biotechnologies, Inc.) was mixed with the emulsification oil to enhance the stability of reaction-in-oil droplets during the heating procedure.

3.2.4 CD design

The CD design for integrated virus detection workflow was created using Solidworks. Taking advantage of the multiplexing capacity of the CD system, two identical microfluidic units were fabricated on a single CD. Each unit is capable of detecting different combinations of water samples and viruses. The design of the complete microfluidic unit is illustrated in Figure 3.1. An oval-shaped mixing chamber was strategically placed at the center of each microfluidic unit to mimic the functionality of a PCR tube, enabling sequential steps for nucleic acid concentration and purification. A sample loading chamber was positioned in the upper right area of the mixing chamber. The sample chamber was preloaded with proteinase K to facilitate protein digestion upon sample loading. Six reagent-holding chambers were located at the top and left areas of the mixing chamber. These chambers were preloaded with the Viral DNA/RNA Buffer, 70% ethanol, and nuclease-free water. These reagents were transferred to the mixing chamber sequentially for the steps of sample lysis, nucleic acid binding, washing, and elution. A waste chamber positioned at the lower right area of the mixing chamber was used to collect the waste reagents from the mixing chamber. The fluid flow sequences, the precision of the fluid volume transfer on CD were tested

on the CD driver equipped with a control software (Pacific scientific, Wilmington, MA) to precisely control the rotation speed and direction of the CD.

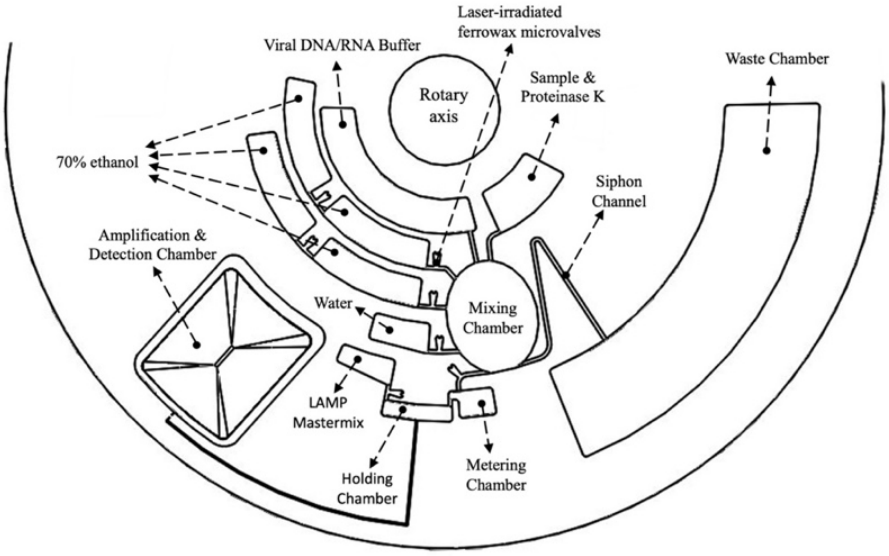

Figure 3.1. Microfluidic chambers and channel design on the half of the centrifugal disc (CD).

The ddRT-LAMP section was integrated into the lower left area of the mixing chamber. This section comprises a metering chamber, a LAMP reagent chamber, an intermediate reaction holding chamber, and an amplification and detection chamber. The metering chamber was linked to the mixing chamber and was used to meter and transfer the nucleic acid extract to the intermediate reaction holding chamber, where the Mastermix from LAMP reagent chamber also be transferred to at the opening of the ferrowax microvalve. The amplification and detection chamber, designed with a pyramid-like structure surrounded by deep trenches, was connected to the intermediate holding chamber through an L-shaped tapering microfluidic channel. This design facilitated the division of the LAMP reaction mixture into thousands of reaction-in-oil droplets that form a single layer above the pyramid structure prior to target amplification. The heating for LAMP reaction and to test the stability of the droplets in the reaction chamber was carried out on a heat block. The

details of the droplet generation microfluidic designs and LAMP heating control on the CD driver are found in our previous report (Gowda et al., 2022).

Two types of valves were applied in the CD design to control sequential fluid pumping and mixing for a fully automated on-CD virus detection assay. A series of laser-irradiated ferrowax microvalves (Peshin et al., 2022) were used as gates between different chambers, enabling precise control of fluid flow timing (Figure B.1). These valves were made of the mixture of paraffin wax (Sigma-Aldrich, St. Louis, MO) and ferric oxide (Ferrotec, Santa Clara, CA), which blocked the channels in their solid form at room temperature and restricted fluid flow between chambers. To open the valve, a laser was focused on the valve position, melting the ferrowax and allowing for the flow of fluids between chambers. In addition, a siphon channel valve was applied at the connection between the mixing chamber and the waste chamber where repeated transitioning between open and closed positions was required. The valve remained closed during the transfer of liquid from the reagent chambers to the mixing chamber and throughout the mixing processes. The valve was opened after the pelleting of MagBinding beads at the bottom of the mixing chamber, allowing the transfer of the supernatant into the waste chamber. Figure B.2 shows the switching of the siphon channel valve between open and close by simply controlling the spin speed of the CD.

3.2.5 CD fabrication

The CD prototype consists of four layers with an outer diameter of 120 mm (Figure 3.2a). The bottom layer is a polycarbonate disc (McMaster-Carr, Elmhurst, Illinois) containing the microfluidic chambers, channels, and ferrowax microvalve components. The third layer consists of a biocompatible single-sided microfluidic diagnostic tape (3M™ Microfluidic Diagnostic Tape

9795R, Saint Paul, MN) with cutouts for the chambers and ferrowax microvalve components. The second layer is a double-sided adhesive tape (FLEXMOUNT DFM 200 clear V-95 150 POLY H-9, Spencer, MA) that includes the chamber cutouts. The top layer is another polycarbonate disc featuring inlets for samples and reagents loading, as well as vent holes. The microfluidic components on the bottom polycarbonate disc were milled using a CNC machine (Tormach PCNC 440, Madison, WI). The cutouts on the two middle adhesive layers were created using a vinyl cutter (Silhouette CAMEO 2, Lindon, UT). The inlets and vent holes on the top layer were drilled using a drill press (Dremel, Mount Prospect, IL).

To assemble the four layers into a complete CD, the process began by affixing the single-sided adhesive tape (the third layer) to the bottom polycarbonate disc. Ferrowax was then loaded onto the CD through the cutouts for the ferrowax microvalve components on the single-sided adhesive tape. Following this, the double-sided adhesive tape (the second layer) was attached over this assembly. The microfluidic chambers were coated with UV-cured glue (Norland Products Inc, Jamesburg, NJ) and cured under UV light for 20 minutes. Finally, the top layer was attached to cover the entire assembly. A roller press was used to seal all the layers together. Image of actual fabricated and assembled CD are shown in Figure 3.2b.

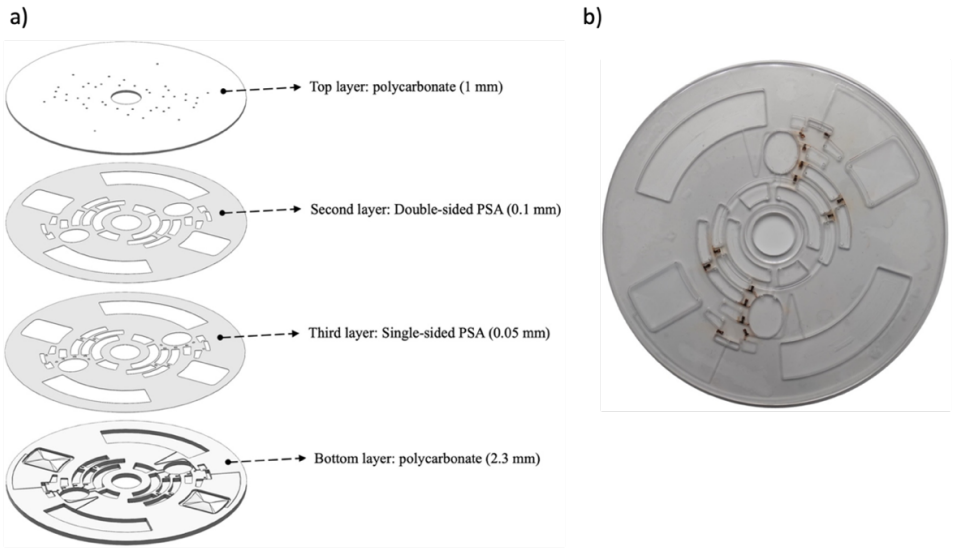

Figure 3.2. Centrifugal disc components. (a) Schematic illustrations of four main layers of CD assembly and (b) an image of actual fabricated and assembled CD.

3.2.6 Validation of the on-CD virus detection assay

While the on-CD virus detection assay was developed based on the protocols of benchtop in-tube assay, there was a concern of inefficient nucleic acid extraction as well as the sensitivity of detection when the on-CD assay was used for virus detection. This concern mainly arises from the differences in mixing, beads pelleting, washing and waste liquid disposal employed in the on-CD assay. Moreover, the potential presence of inhibitors in the CD setup such as ferrowax and adhesive tape might lead to detection failures.

To validate the on-CD virus detection assay, three major comparisons were performed. Firstly, the on-CD sample preparation procedures, which involved Proteinase K treatment, chemical lysis, nucleic acid binding, washing, elution, fluidic metering, and mixing the nucleic acid sample with the LAMP Master Mix, were evaluated by comparison with the in-tube sample preparation assay using serially diluted SARS-CoV-2 samples. SARS-CoV-2 working solutions in the concentration

range from 10^2 to 10^6 copies/ml were prepared by diluting the SARS-CoV-2 stock solution with nuclease-free water. Wastewater samples were spiked with SARS-CoV-2 in the same concentration range to assess the sensitivity and potential interference of inhibitors present in wastewater during the virus detection assay. In-tube RT-LAMP amplification was first applied to analyze the serially diluted SARS-CoV-2 spiked in both nuclease-free water and wastewater samples without sample concentration and purification procedures, serving as a benchmark for evaluating the virus recovery rate and purification efficiency of the in-tube and on-CD assay. Subsequently, the in-tube and on-CD assay were used to extract the nucleic acid from the serially diluted SARS-CoV-2 samples side-by-side. The bulk reaction mixtures of the nucleic acid extracts and LAMP Master Mix collected from either PCR tube or from the CD reaction holding chamber were then tested using the in-tube RT-LAMP assay for evaluation.

Next, the on-CD sample preparation procedures were evaluated for their efficacy to extract indigenous PMMoV in various environmental water matrices including wastewater, creek water, stormwater, and seawater. Wastewater samples were directly applied for the sample preparation procedures, while creek water, stormwater, and seawater were spiked with wastewater samples in a 1:1 ratio to simulate contamination scenarios while preserving the distinct characteristics of each environmental water source. These samples were extracted using on-CD procedures, followed by analysis using the in-tube RT-LAMP assay to assess the impact of different environmental water matrices on the virus detection assay.

Finally, the complete on-CD sample-to-answer procedures, including sample preparation and ddRT-LAMP were tested. Three wastewater samples collected from different manholes within the UCI student housing area were used to evaluate the accuracy of the on-CD assay for PMMoV quantification. Indigenous PMMoV in these samples were concentrated, purified, and quantified

all on the CD controlled by the programing of the CD driver. After the on-CD procedure, 3 microscope images were collected from each amplification chamber to obtain the droplet size and the number of positive droplets and negative droplets. The median of the droplet diameter was measured using the image quantification tool ImageJ and the number of positive and negative droplets in each image were counted. The concentration of PMMoV in the bulk RT-LAMP reaction mixture was calculated based on Poisson statistics shown in Eq. (1):

$$Concentration = \frac{-\ln\left(\frac{N_{neg}}{N}\right)}{V_{droplet}} \qquad (1)$$

Where N_{neg} is the number of the negative droplet, N is the total droplet number, and $V_{droplet}$ is the volume of each droplet. The original concentration of PMMoV in the wastewater samples was then calculated using the concentration of PMMoV in the bulk RT-LAMP reaction mixture including the estimated 10% nucleic acid recovery rate from the on-CD sample preparation procedure according to the recovery rate estimated from SARS-CoV-2 spiking study. The concentrations of wastewater PMMoV detected by on-CD assay were compared with those reported by UCI Genomics High Throughput Facility using PREvalence ddPCR PMMoV fecal indicator Assay (BioRad) on BioRad QX200 (ddPCR) system.

3.3 Results

3.3.1 Fluid control for on-CD virus detection assay

The integrated liquid handling for on-CD virus detection assay is demonstrated using colored liquids. Photo images after each processing step are shown in Figure 3.3, and their corresponding illustrations are found in Figure B.3. The CD rotation and oscillation protocols for each operational

step are summarized in Table 3.1. The results demonstrate precise control over valve operation, liquid flow, mixing, bead pelleting, metering, and droplet generation.

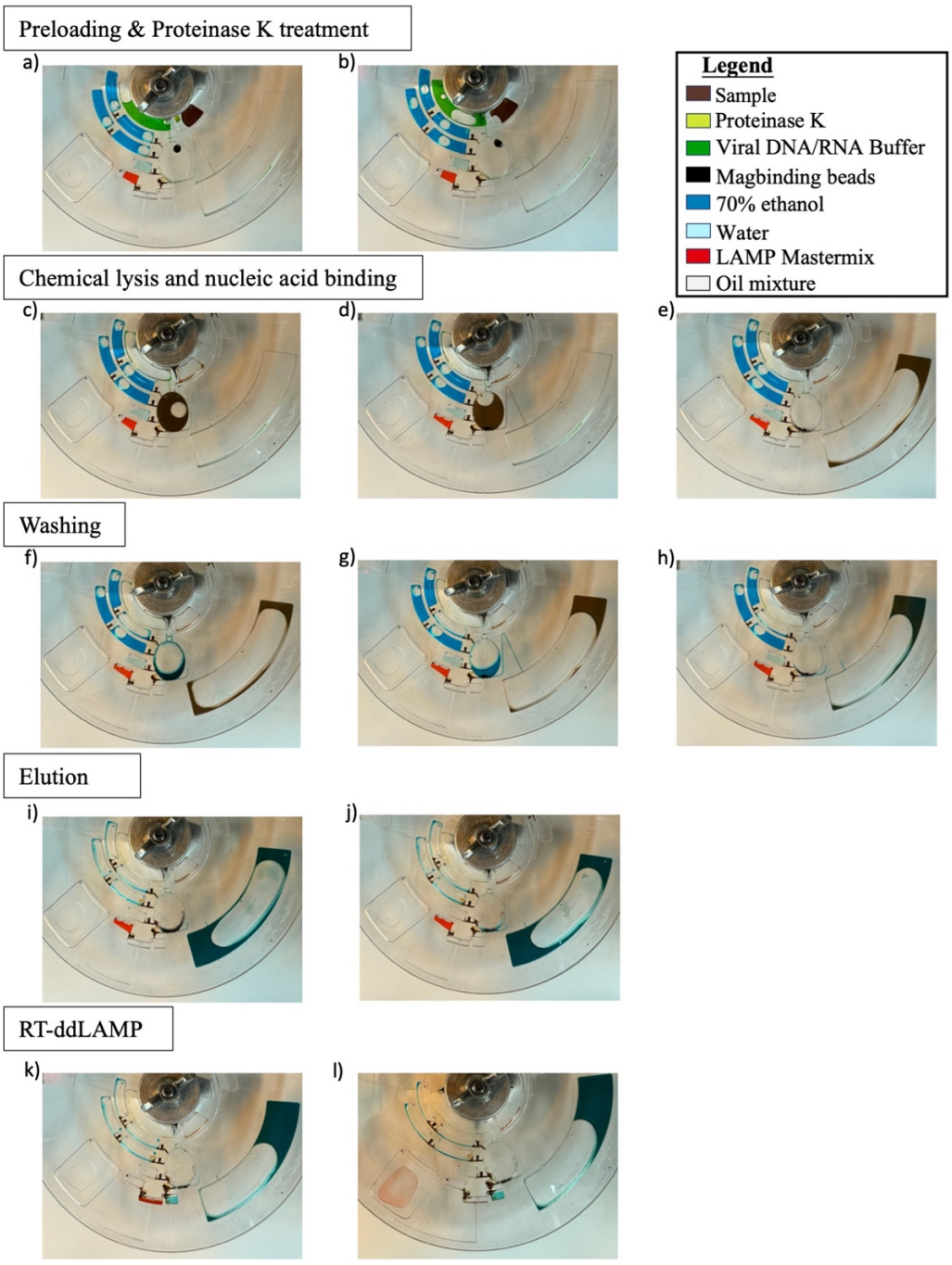

Figure 3.3. Photo images of the fluid handling process on CD. The main steps are captured at the pause of each procedure to demonstrate the operation. The color-dyes were added to the fluid for visualization.

Table 3.1. CD operational programing.

Steps	Protocol	Operation Details
CD preparation	Rotation (close the siphon)	800 RPM, 5 s
Proteinases K treatment	Oscillation (mixing) Pause (incubation)	48 rev/s², 0.1 rev, 30 s 0 RPM, 15 min
Chemical lysis & nucleic acid binding	Rotation (liquid transfer) Oscillation (mixing) Rotation (beads pelleting) Pause (open the siphon) Rotation (waste disposal + close the siphon)	800 RPM, 20 s 36 rev/s², 36°, 10 min 2500 RPM, 30 s 0 RPM, 10 s 800 RPM, 20 s
Nucleic acid washing (4 times)	Laser (open the ferrowax valve) Rotation (liquid transfer) Oscillation (mixing) Rotation (beads pelleting) Pause (open the siphon) Rotation (waste disposal + close the siphon)	N/A 1000 RPM, 20 s 36 rev/s², 0.1 rev, 30 s 2500 RPM, 30 s 0 RPM, 10 s 800 RPM, 20 s
Elution	Laser (open the ferrowax valve) Rotation (liquid transfer) Oscillation (mixing) Rotation (beads pelleting)	N/A 1000 RPM, 15 s 36 rev/s², 0.01 rev, 30 s 1500 RPM, 1 min
RT-ddLAMP	Laser (open the ferrowax valve) Rotation (liquid metering and transfer) Oscillation (mixing) Rotation (droplet generation) Heating (Amplification)	N/A 1000 RPM, 30 s 48 rev/s², 0.1 rev, 30 s 3500 RPM, 90 s 0 RPM, 35 min
Total time		~ 75 min

Figure 3.3a shows the pre-start condition of the CD, when the water sample and reagents were preloaded into their respective chambers, and the siphon channel valve was closed by a pre-spin of the CD for 5 seconds at 800 rpm to push 20 µL of Viral DNA/RNA buffer from the mixing chamber to the siphon channel to form an air lock. As shown in Figure 3.3a, sample chamber was

preloaded with 100 µL of water sample and 5 µL of Proteinase K; 200 µL of Viral DNA/RNA buffer was loaded into the buffer chamber; 100 µL of 70% ethanol was in each of the four washing reagent chambers; 5 µL of MagBinding beads was in the mixing chamber; 15 µL of nuclease-free water was in the water elution chamber; 16 µL of LAMP master mix was in the Mastermix chamber, and 40 µL of droplet generation oil was in the amplification chamber.

Figure 3.3b illustrates the Proteinase K treatment step, involving oscillation of the CD for 30 seconds followed by a 15-minute pause. The CD oscillation facilitated the mixing of the water sample and Proteinase K, while the subsequent 15-minute pause provided sufficient time for the reaction to occur. The colored image demonstrates thorough mixing of the water sample and Proteinase K, indicating that the oscillation protocol can create turbulence for sufficient mixing. Furthermore, the oscillation protocol was optimized to prevent the water sample and the Viral DNA/RNA buffer from holding cambers pre-maturely bursting into the mixing chamber during the oscillation period without the need of control valves between the water sample chamber and the mixing chamber, and between the Viral DNA/RNA buffer chamber and the mixing chamber, respectively.

The sample lysis and nucleic acid binding steps are shown in Figures 3c, 3d, and 3e. The procedure began by releasing the water sample and the Viral DNA/RNA buffer into the mixing chamber, where they were mixed with the MagBinding beads for the chemical lysis and nucleic acid binding (Figure 3.3c). To facilitate this process, the CD was rotated at 800 RPM for 20 seconds to transfer the liquid, followed by a 10-minute oscillation to ensure thorough mixing. The result indicates that the turbulence generated by the CD oscillation within the oval-shaped mixing chamber effectively dispersed the MagBinding beads throughout the mixture of water sample and Viral DNA/RNA buffer, as indicated by the homogeneous color observed in the mixing chamber. After mixing, the

CD was rotated at 2500 RPM for 30 seconds followed by a 10-second pause. The high-speed rotation pelleted the MagBinding beads to the bottom of the chamber and removed the air lock in the siphon channel, while the brief pause allowed the liquid to fill the siphon channel through capillary force, transitioning the valve to the open state (Figure 3.3d). Once the siphon channel valve was opened, the CD was rotated at 800 RPM for 20 seconds to transfer the waste liquid into the waste chamber and turn the siphon channel valve to the closed state by forming an air lock in the siphon (Figure 3.3e). According to the real-time image presented in Figure 3.3e, MagBinding beads were not observed in the waste chamber, suggesting that the beads were efficiently pelleted (Figure 3.3d) and only supernatant (brown colored liquid from mixing of maroon colored sample with green colored buffer) was transferred to the waste chamber. Effective beads recovery ensured effective nucleic acid recovery attached to the MagBinding beads.

After the nucleic acid binding, the MagBinding beads were washed four times using 70% ethanol sequentially release into the mixing chamber. Figures 3f to 3h demonstrate one complete round of the on-CD washing procedure. The ferrowax valve located at the connection between the ethanol chamber and the mixing chamber was first opened, allowing the release of ethanol into the mixing chamber by rotating the CD at 1000 RPM for 20 seconds. Subsequently, the MagBinding beads were resuspended in the ethanol by oscillating the CD for 30 seconds (Figure 3.3f). The result indicated sufficient mixing between the MagBinding beads and ethanol, suggesting that the oscillation protocol can provide adequate mixing for liquid volumes of 100 µl. Figure 3.3g and Figure 3.3h demonstrate re-pelleting of MagBinding beads and waste disposal step, respectively. Similarly, beads pelleting involved a CD rotation at 2500 RPM for 30 seconds, followed by a 10-second pause, while waste disposal was accomplished by a 20-second rotation at 800 RPM. This process was repeated four times to ensure sufficiency washing for nucleic acid purification.

The nucleic acid elution step is illustrated in Figure 3.3i and Figure 3.3j. As shown in Figure 3.3i, nuclease-free water was transferred to the mixing chamber by rotating the CD at 1000 RPM for 15 seconds after the ferrowax valve was opened. A modified oscillation protocol, which decreased the shaking angle while increasing the shaking frequency, was applied to effectively resuspend the MagBinding beads in the nuclease-free water. This oscillation protocol is essential for maintaining the nuclease-free water at the bottom of the mixing chamber during the mixing process, which is crucial to effectively resuspend the MagBinding beads in a small volume of liquid within a relatively larger chamber. Figure 3.3j shows the pelleting of the MagBinding beads from the nuclease-free nucleic acid elution water, using a modified spinning protocol. The CD was rotated at 1500 RPM for 1 minute to pellet the MagBinding beads while keeping the siphon valve closed.

Next, the eluted nucleic acid sample from the previous step was transferred for virus quantification using ddRT-LAMP reaction as demonstrated in Figure 3.3k & 3.3m. The CD was rotated at 1000 RPM for 30 seconds after opening the ferrowax valves connecting the mixing chamber to the metering chamber, and between the LAMP Mastermix chamber and the holding chamber. This process metered approximately 4 μL of nucleic acid extract and simultaneously transferred the LAMP Mastermix into the reaction holding chamber. The CD was oscillated for 30 seconds to mix the nucleic acid with LAMP Mastermix (Figure 3.3k), followed by a fast spin at 3500 RPM for 90 seconds to push the LAMP reaction mixture through the L-shaped droplet generation channel that steps down to the amplification and detection chamber filled with oil to create thousands of reaction-in-oil droplets. The design of the tapering L-shaped channel, the nozzle at the entry of the reaction chamber, and the chamber with a center pyramid structure was described in detail in our previous report (Gowda et al., 2022). After droplet generation, at the stop of centrifugal force, the narrow gap between the flat-top pyramid-like structure in the center of the amplification chamber

and the top of the chamber created a capillary force, pulling the droplets towards the center of the pyramid and collecting them in a single layer in the pyramid region, as shown in Figure 3.3l. This single-layer configuration minimized droplet loss during subsequent ddRT-LAMP amplification and allowed detection using a microscope. Microscopy images of reaction-in-oil droplets taken from four amplification chambers are displayed in the Supporting Information (Figure B.4). Slight variations in droplet size were observed among chambers, ranging from approximately 80 μm to 140 μm, while the size remained constant within the same chamber. These variations can be attributed to the precision limit of the CNC machine used in CD fabrication, which would not an issue should the CD be manufactured by mass production through injection molding.

3.3.2 Comparison of on-CD and in-tube sample preparation procedures

The comparison of RT-LAMP detection of serially diluted SARS-CoV-2 spiked in nuclease-free water and wastewater by different methods is shown in Table 3.2. When analyzing the SARS-CoV-2 spiked in the nuclease-free water with no sample pre-treatment, positive RT-LAMP results was observed at seeding concentrations between 10^3 and 10^6 copies/ml. The results indicate the detection sensitivity in the absence of external inhibition for unextracted viruses. When analyzing the SARS-CoV-2 spiked into the wastewater, a very different outcome was observed. Even at the highest spiked concentrations of 10^6 copies/ml, the signal for SARS-CoV-2 was not detected, suggesting that the organic and inorganic compounds presented in the wastewater can inhibit the RT-LAMP reaction and decrease the detection sensitivity of at least 1000 times.

Table 3.2. RT-LAMP detection of SARS-CoV-2 spiked in nuclease-free water and wastewater by different sample preparation procedures.

SARS-CoV-2 (copies/ml)	No sample preparation		In-tube procedures		On-CD procedures	
	NFW	WW	NFW	WW	NFW	WW
0	-	-	-	-	-	-
10^2	-	-	-	-	-	-
10^3	++	-	-	-	-	-
10^4	++	-	++	++	+	+
10^5	++	-	++	++	++	++
10^6	++	-	++	++	++	++

Abbreviations: NFW-nuclease-free water, WW-wastewater.
+ and - indicates positive and negative LAMP results, respectively. The ++ and + are based on the relative fluorescence intensity of LAMP reaction.

The traditional bench top in-tube sample preparation and nucleic acid purification for SARS-CoV-2-spiked samples yielded positive RT-LAMP results for both nuclease-free water and wastewater at concentrations ranging from 10^4 to 10^6 copies/ml (Table 3.2). However, SARS-CoV-2 was undetectable at the concentration of 10^3 copies/ml. These results suggested that the in-tube sample preparation procedures had effectively removed inhibitors present in the wastewater. However, a 10-fold decrease in the detection limit was observed in comparison with results from the virus spiked nuclease-free water without sample preparation. This reduction is likely due to the loss of nucleic acids during the sample preparation process, rather than the presence of residual inhibitors, as this reduction was also observed in the SARS-CoV-2-spiked nuclease-free water samples. In other words, the nucleic acid recovery rate of the in-tube sample preparation assay was approximately 10%.

The RT-LAMP detection of SARS-CoV-2 spiked samples, processed using the on-CD sample preparation procedures, are also presented in Table 3.2. Similar RT-LAMP outcomes were observed when comparing the on-CD sample preparation procedures with traditional in-tube

methods, revealing a detection range from 10^4 to 10^6 copies/ml for detecting SARS-CoV-2 in both nuclease-free water and wastewater samples. Despite the same detection range, slightly weaker SARS-CoV-2 signals were observed at the lowest spiked concentration of 10^4 copies/ml compared to the in-tube method. The photo images of positive, weak positive, and negative RT-LAMP results as indicated by the fluorescence intensity are shown in Figure B.5. The comparative results indicate that the on-CD sample preparation procedures have a similar but slightly lower nucleic acid recovery rate compared to the in-tube sample preparation procedures. The variance might be attributed to the use of 70% ethanol to replace the proprietary washing buffer during the on-CD washing steps. Furthermore, the on-CD assay demonstrated high purification efficiency, as the detection limit remained consistent when processing both the nuclease-free water sample and wastewater sample using the on-CD assay.

3.3.3 Detection of indigenous PMMoV in environmental samples

The on-CD RT-LAMP detection of indigenous PMMoV in various environmental water matrices are shown in Table 3.3. All tested water samples, including wastewater, wastewater contaminated stormwater, creek water, and seawater showed positive detection of PMMoV. A weaker positive result was observed in the seawater, possibly influenced by the salinity of the seawater that affecting nucleic acid binding efficiency on MagBinding beads (Lloyd et al., 2010; Corcoll et al., 2017). Overall, the results indicate that the on-CD sample preparation procedures are effective across diverse environmental water matrices for extracting viral RNA from non-spiked samples, suggesting its potential utility in monitoring and surveillance of viruses in the environment.

Table 3.3. RT-LAMP detection of indigenous PMMoV in various environmental water matrices.

PMMoV in environmental waters	RT-LAMP result (On-CD procedures)
Wastewater	++
Stormwater + wastewater (1:1 mixing ratio)	++
Creek water + wastewater (1:1 mixing ratio)	++
Seawater + wastewater (1:1 mixing ratio)	+

To demonstrate the performance of the complete sample-to-answer on-CD procedure, wastewater samples collected from three sewer manholes were analyzed for indigenous PMMoV on-CD. Starting from sample loading to quantitative results by on-CD ddRT-LAMP, the assay was completed in approximately 75 min (Table 3.1). Representative fluorescence microscopy images (grayscale) of reaction droplets at the end of reaction are shown in Figure 3.4. Droplets were uniform within each reaction chamber and the droplet numbers did not change significantly before and after LAMP reaction suggesting droplets were sufficiently stable at heating temperature of 65 °C for 30min. Variabilities of the droplet size were observed on three different microfluidic units produced by CNC, ranging from approximately 80 μm to 160 μm medium size in diameter. This variability was likely due to the CNC precision limit in producing the micrometer size of the droplet generation channel rather than the design flaw of the CD system (Gowda et al., 2022). The droplets in sample 3 were larger and less stable than in samples 1 and 2, and experienced some coalescence during heating, suggesting standardization of CD manufacture through injection molding is critical for reproducibility. Nevertheless, the remaining droplets in the prototype CD were sufficient to enable the calculation of the fraction of negative droplets for determining the original concentration of indigenous PMMoV in the wastewater samples. The concentrations of

PMMoV, ranging from 2.3 x10^5 to 1.09 x 10^6 copies /ml in three wastewater samples tested, were computed by counting of RT-LAMP positive droplets among total droplets and the medium droplet size (Table 3.4). These results matched well with the PMMoV concentrations determined by Nanotrap® KingFisher™ Concentration/Extraction protocol followed by ddRT-PCR using BioRad QX200 Droplet Digital PCR system. Thus, the results confirm that the PMMoV was successfully extracted and amplified within the on-CD detection assays. These observations suggest a satisfactory performance of the on-CD detection assays for the rapid quantification and detection of indigenous PMMoV in environmental samples, offering comparable results to the established benchtop virus detection assay without the need of expensive equipment.

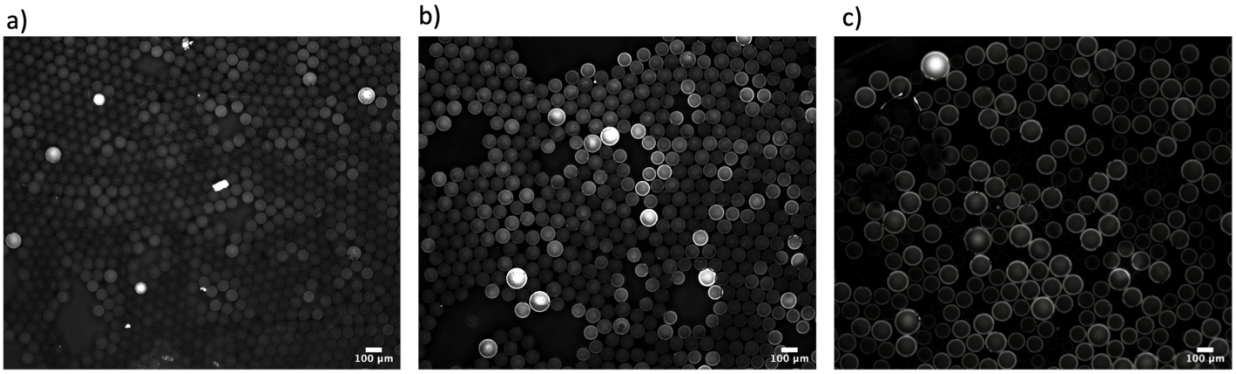

Figure 3.4. Fluorescence microscopy images of reaction droplets at the end of the ddRT-LAMP reaction for wastewater samples collected from three different manholes (3 samples are labeled as a, b, c). The positive reaction droplets are shown as the bright spots on the grayscale fluorescent images. The negative droplets are shown as the dark gray to black spots on the grayscale fluorescent images.

Table 3.4. Quantification results of indigenous PMMoV in three wastewater samples using benchtop in-tube virus detection assay and on-CD sample-to-answer virus detection assay.

	On-CD sample-to-answer virus detection assay by ddRT-LAMP			**Nanotrap KingFisher extraction and ddRT-PCR by BioRad QX200**
	Median size of the droplet	Fraction of the negative droplet	Measured concentration	Measured concentration
Sample #1	120 μm	98.8%	5.5×10^5 copies/ml	5.3×10^5 copies/ml
Sample #2	80 μm	99.5%	1.08×10^6 copies/ml	9.6×10^5 copies/ml
Sample #3	160 μm	99.6%	2.3×10^5 copies/ml	1.3×10^5 copies/ml

3.4 Discussion

The rapid and on-site detection of infectious pathogens or fecal indicator organisms in wastewater and wastewater contaminated environmental waters are crucial for protecting both human and environmental health. This research introduces a sample-to-answer microfluidic CD system for quantification of viruses in wastewater and other environmental water matrices. We demonstrated that the microfluidic CD could integrate the necessary steps for sample concentration and nucleic acid purification required for environmental viral detection. This next-generation virus detection

system offers rapid, portable, semi-automated, and user-friendly capabilities, having the potential to revolutionize current environmental monitoring practices.

The CD design plays an important role in facilitating a wide range of tasks that integrate sample concentration, purification, and ddRT-LAMP. It effectively utilizes the space on the disc, allowing for the processing of sample volumes up to 100 µl to achieve a 6.67-fold concentration factor without an external concentration requirement. The CD can accommodate multiple chambers necessary for preloading reagents for digestion and for multiple washing steps, ensuring sufficient purification when handling environmental samples. The oval-shaped mixing chamber, in cooperation with the optimized CD spinning protocols, provides sufficient mixing and bead pelleting efficiency across a wide range of operating volumes, from 15 µl to 300 µl. The droplet generation channel and amplification chamber used for the ddRT-LAMP reaction show comparable performance to state-of-the-art sample extraction and ddRT-PCR systems, successfully creating reaction-in-oil droplets and forming a single layer that ensures stability during the heating process. The ferrowax microvalves applied in this CD design have been widely adopted on the CD platform, primarily due to their biocompatibility and ease of operation (Kong et al., 2016). While the siphon channel is well-established for CD applications (Siegrist et al., 2010; Strohmeier et al., 2015), this is the first time of its use as a valve that capable of multiple open-close cycles. In earlier research, valves frequently rely on external tools like magnets for regulating their opening and closing (Peshin et al., 2022). In contrast, the siphon channel valve only requires CD rotation to control its open and close states, simplifying operations significantly. These combined advancements represent an innovation in microfluidic CD design, expanding its potential for application in environmental monitoring. Therefore, CD system has the capacity to

transform nearly all benchtop molecular diagnostic procedures into a semi-automatic assay with minimal hands-on operation.

The PMMoV validation results confirmed that the on-CD virus detection exhibits promising performances: a similar nucleic acid recovery rate to the traditional bench-top in-tube assay, high purification efficiency across various environmental water matrices, and precise quantification of indigenous viruses in wastewater, highlighting its values for practical application. However, it is noteworthy that while the nucleic acid recovery rates between the on-CD and in-tube assays were comparable, a slightly lower recovery rate was observed in the on-CD assay. This issue is attributed to the replacement of washing buffers with 70% ethanol during the beads washing steps to accommodate the hand-crafted prototype CD using adhesive tape (He et al., 2022). In our initial tests, we found the washing buffers provided by the manufacturer were not compatible with the adhesive tape, washing off the glue layer that interfered with downstream RT-LAMP reaction. Coating the chambers with UV-glue as a protective layer in the subsequent trials alleviated the major issue but it was challenging to seal the edges of the chamber tightly by hand-crafting. Using the lower concentration of ethanol reduced the wash-out inhibitors and allowed us to proof the concept of complete on-CD virus assay. Therefore, it is critical to advance materials and CD manufacture in order to transform this laboratory innovation to commercial products. Alternative CD bonding methods such as thermal bonding, solvent bonding, or ultrasonic bonding (Tsao and DeVoe, 2009; Giri and Tsao, 2022; Madadi et al., 2023) could eliminate the need for adhesive tape, enabling the utilization of higher concentrations of ethanol or optimized wash buffers. Nevertheless, hand-crafted CD on CNC machine will not be a solution for commercialization without bulk manufacture by injection molding.

Despite having demonstrated the on-CD PMMoV detection in environmental matrices, one of the primary challenges in implementing this assay is its limited detection sensitivity. Our CD design included an approximately 6.67-fold concentration factor, effectively quantified the indigenous PMMoV in the wastewater samples. However, it encountered difficulties in detecting lower concentrations of viruses, such as indigenous SARS-CoV-2 in wastewater, which typically exist at concentrations below 10^3 copies/ml (Medema et al., 2020; LaTurner et al., 2021; Wu et al., 2022). Employing thicker or larger polycarbonate materials for CD design could increase the CD capacity for water samples and reagents, thereby further enhancing the concentration factor from the single digit to double digits. Furthermore, it is important to mention that the detection sensitivity issue is not limited to the on-CD system. It is a challenge faced by all molecular biology-based methods for environmental monitoring (Bonadonna et al., 2019). Large-scale environmental water concentration systems, such as NanoCeram Viral Sampler (Argonide), were designed to concentrate tens to hundreds of liters of water for virus monitoring (Williams et al., 2001). CD system has the advantage to include a centrifugal-based add-on concentration system to integrate with the on-CD detection system. In our previous research, an add-on concentration cup was developed, utilizing SAP (superabsorbent polymer) beads capable of selectively absorbing water and salts while repelling microbial pathogens (Gowda et al., 2022). Future studies could explore the feasibility of utilizing the developed external concentration cup for virus concentration purposes and investigate its integration onto the current CD design.

Additionally, the droplet generation technology should be further improved to enhance the stability of reaction-in-oil droplets, subsequently increasing the accuracy in quantifying lower virus concentrations. Enhancing droplet generation technology could involve adopting a more precise fabrication technique such as injection molding (Lee et al., 2018; Scott and Ali, 2021), to replace

CNC machining in CD manufacturing. It could machine consistently finer channels, essential for generating smaller and more stable droplets, thereby enhancing the assay's performance.

The current research focused on CD design, fluidic handling and assay validation. The CD testing was carried out on a benchtop CD driver with programable rotation controls, a handheld laser to open ferrowax valves, and a CD heating block for LAMP reaction. The portable CD driver, consisting of programable disc rotation controls, heating and temperature controls, and digital image capture and processing, was described in our previous report (Gowda et al., 2022). This CD driver will require modification to include a laser light for control of ferrowax valves for the new CD operation. Several studies have integrated a laser into a portable CD driver for controlling active valves (Li et al., 2019; Perebikovsky et al., 2021). The laser was attached to either a stepper motor or an actuator, enabling precise targeting of the laser at specific valve positions. Moving forward, the development of an updated CD driver incorporating a laser control system is necessary for enabling fully automated CD operation. While significant research is required to translate this concept into a field-applicable technology, this work demonstrates the strong potential of using microfluidic CDs for environmental virus monitoring and serves as an important foundation for developing more advanced CD technologies. Its portability allows for on-site testing, eliminating the need for sample transportation to specialized laboratories and thereby further saving time and resources. Moreover, the user-friendly interface making it accessible for a wider range of users, contributing to more frequent and efficient monitoring of infectious pathogens in water sources.

CHAPTER 4

INTEGRATING PHENOTYPIC AND GENOTYPIC METHODS FOR THE RAPID DETECTION OF ANTIBIOTIC-RESISTANT E. COLI ON A CENTRIFUGAL MICROFLUIDIC DISC

4.1 Introduction

Antibiotic resistance has become one of the top global health threats in the 21st century. In the United States alone, more than 2.8 million people develop antibiotic-resistant infections, leading to over 35,000 deaths each year (Centers for Disease Control and Prevention (U.S.), 2019). Unfortunately, the burden of antibiotic resistance is anticipated to intensify in the coming decades if not addressed. According to a review on antimicrobial resistance (AMR) commissioned by the United Kingdom government, up to 10 million deaths may result from antibiotic-resistant diseases annually, surpassing cancer deaths to become the leading cause of mortality worldwide (O'neill, 2014).

While the primary focus on antibiotic resistance related issues has been on healthcare settings and clinical practices, there is growing concern that more effort should be focused on the water environment monitoring (Liguori et al., 2022). Wastewater treatment plants (WWTPs) have been considered primary sources for the transmission of antibiotic-resistant bacteria (ARB) and antibiotic-resistant genes (ARG) into the aquatic environment. This is because WWTPs serve as collection points for antibiotics from sewer networks that collect wastewater from domestic, clinical, agricultural, and pharmaceutical sources. However, the presence of these wastewater antibiotics may contribute to the amplification of ARB and ARG during biological wastewater

treatment through mutation or horizontal gene transfer. Ultimately, they are discharged into the environment without complete removal by treatment processes, posing a considerable risk to both ecological integrity and human health (Huang et al., 2023). Aquatic environments not only serve as ideal hotspots for the further evolution and proliferation of ARB and ARG due to increased selective pressure but also facilitate the acquisition of new ARG by pathogens. Recent studies indicate an increasing trend in the abundance of environmental ARB and ARG (Zhuang et al., 2021; Larsson and Flach, 2022), raising concerns about their potential transmission to human populations through recreational activities and contaminated food or drinking water. To mitigate the increasing threat of antibiotic-resistant infections and diseases, it is necessary to understand their occurrence in the environment, identify human exposure hotspots, and develop more effective strategies for their removal. A critical first step in achieving these goals is monitoring ARB and ARG in the environment, as well as throughout wastewater treatment processes.

Currently, monitoring antibiotic-resistant organisms relies on traditional laboratory methods that are laborious and time-consuming. Phenotypic methods, such as agar disc diffusion and broth dilution, are most commonly used in current practices involving the observation of real-time growth and metabolic responses of bacterial populations to antibiotics (Sahoo et al., 2023). Despite being well-established and considered the gold standard for providing information on antibiotic-resistant organisms, lengthy incubation times of up to several days are required for these culture-based methods. Significant research progresses have been made to improve the time-consuming culturing-based methods for monitoring antibiotic-resistant organisms in the environment. Genotypic methods, including nucleic acid amplification techniques and metagenomic-based approaches, have been introduced to antibiotic-resistant organisms monitoring (Pillay et al., 2022; Yamin et al., 2023). These methods rely on identifying specific resistance genes, providing faster

detection times, and increased sensitivity. Despite the promises, these methods require a thorough understanding of antibiotic resistance mechanisms. Consequently, occurrences of false negatives and positives are common, with false negatives attributed to new or unknown resistance mechanisms and false positives arising from database inaccuracies or misinterpretation of sequencing data. Moreover, these techniques require intensive sample preparation steps prior to downstream detection. As a result, challenges such as the need for highly trained lab personnel and a centralized lab remain, leading to a significant turnaround time. The development of rapid and cost-effective methods that can overcome these challenges is crucial for advancing antibiotic-resistant organisms monitoring, making approaches more accessible and practical for routine use, and facilitating broader implementation.

The microfluidic centrifugal disc (CD) system has been a research focus (Tang et al., 2016). This innovative system has the potential to integrate multiple laboratory functions onto a single disc, enabling the semi-automated processing of the entire workflow involved in nucleic acid amplification techniques, including sample preparation, nucleic acid amplification, detection, and quantification (Gowda et al., 2022; Huang and Jiang, 2024). It can significantly reduce the time required to obtain results from several days to a matter of hours, while also eliminating the need for highly skilled personnel and advanced equipment. Despite primarily being utilized in clinical settings due to the relatively simple composition and higher concentration of microorganisms in clinical samples, we have successfully employed it for the quantification of indigenous viruses in wastewater and other water environments in our previous work (Huang and Jiang, 2024).

In this work, we presented a detection assay for ARB that takes advantages of both phenotypic and genotypic methods. Unlike conventional phenotypic methods, which involve culturing bacteria in the sample for days until growth or a metabolic response can be visually observed, we cultured the

bacteria in the samples for a short period (~2 hours) in the presence of antibiotics. We then applied the nucleic acid amplification technique to visualize the ARB detection results. This benchtop assay is designed to determine the presence of ARB in wastewater in a shorter detection time while retaining the characteristics of phenotypic methods. Furthermore, we developed a portable sample-to-answer microfluidic CD that integrates the entire process required by our benchtop ARB detection assay. By combining pseudo and non-pseudo forces generated through CD rotation and oscillation, the entire on-CD assay can be completed automatically in less than 3 hours after sample loading. We first assessed the performance of the on-CD assay in detecting seeded antibiotic-resistant E. coli in raw wastewater. Additionally, we successfully detected indigenous antibiotic-resistant E. coli in wastewater using the on-CD assay, demonstrating its potential for real-world applications.

4.2 Materials and methods

4.2.1 Bacteria, culture media, and wastewater samples

E. coli CN13 (ATCC 700609) and *E. coli Famp* (ATCC 700891) were used as the target bacteria to demonstrate the assay performance. Before each experimental trial, *E. coli* was cultured in Luria Bertani (LB) broth (Thermo Fisher Scientific, Waltham, MA) at 37°C for 8 hours and used as the stock solution. The concentration of the *E. coli* stock solution was estimated using the standard plate count method with LB agar plates (Neogen, Lansing, MI). Raw wastewater samples collected from WWTP served as both the background sample matrix in the *E. coli* spiked tests and for the detection of indigenous antibiotic-resistant *E. coli*. Wastewater samples were stored at 4°C after collection, and the experiments were conducted within three days of sample collection.

4.2.2 Benchtop assay for rapid ARB detection

A benchtop ARB detection assay that leverages both phenotypic and genotypic methods was first developed and tested. It served as the template for developing the on-CD assay, and its efficiency was used as a benchmark for evaluating the assay performance on the CD. This assay comprises four main steps: bacteria incubation, cell pelleting and resuspension, cell lysis, and LAMP detection.

The assay procedures started with the mixing of 100 μL of a water sample and 100 μL of LB broth in a 1.5 mL microcentrifuge tube. Ampicillin (Thermo Fisher Scientific, Waltham, MA) was added to the tube to achieve a final concentration of 15 ppm, followed by incubation at 37°C for 2 hours to selectively enrich ampicillin-resistant bacteria. After the incubation, the bacterial cells were pelleted by centrifuging at 5,000 RPM for 6 minutes using a microcentrifuge, and the supernatant was discarded. 100 μL of nuclease-free water was then added to the cell pellets and vortexed for 20 seconds for cell resuspension. The cell pelleting and resuspension procedure was applied to remove impurities present in the water sample and culture medium that could inhibit nucleic acid amplification. Subsequently, 0.1 gram of silica–zirconia beads with a 100 μm diameter (BioSpec, Bartlesville, OK) were added to the purified bacterial sample. The mixture was vortexed for 6 minutes, followed by centrifugation at 10,000 RPM for 1 minute to facilitate cell lysis and pellet the cell debris, respectively. 4 μL of DNA extracts was mixed with 10 μL of WarmStart 2× LAMP Master Mix (New England BioLabs, Ipswich, MA), 0.4 μL of fluorescence dye (New England BioLabs, Ipswich, MA), 3.6 μL of nuclease-free water, and 2 μL of a 10× concentrated primer mix targeting the E. coli malB gene (Integrated DNA Technologies, Coralville, IA). Finally, the reaction mixture was heated at 65 °C for 30 minutes using a thermocycler (Applied Biosystems,

Waltham, MA) for the LAMP reaction. The LAMP primers for E. coli were reported by Hill et al. (Hill et al., 2008) and shown in Table C.1.

4.2.3 Validation of the benchtop ARB detection assay

Before integrating into the on-CD assay, the benchtop assay was tested to address specific knowledge gaps and ensure its sensitivity and reliability in detecting ARB in environmental waters. Two crucial aspects were targeted for investigation: (1) The efficiency of the pelleting and resuspension procedure in removing inhibitors from water samples and culture medium; and (2) the performance of a 2-hour incubation period followed by the LAMP amplification in differentiating resistant and non-resistant bacteria.

To assess the effectiveness of the pelleting and resuspension procedure, *E. coli Famp* samples were prepared in the concentration range of 10^4 to 10^7 CFU/ml by diluting the *E. coli Famp* stock solution with both nuclease-free water and wastewater samples, which were filtered using a 0.45 μm MCE Membrane (MF-Millipore). The filtration step was implemented to eliminate indigenous bacteria from the wastewater samples while retaining impurities that could potentially inhibit the LAMP reaction for testing. Serially diluted *E. coli* samples were first lysed and detected using the LAMP reaction without the pelleting and resuspension procedure, establishing as the standard for comparison. In parallel, the pelleting and resuspension procedure was applied to the same serially diluted *E. coli* samples followed by cell lysis and LAMP detection. The LAMP results of both scenarios were then compared to assess the efficacy of the pelleting and resuspension procedure.

To further understand the performance of the proposed benchtop assay in differentiating between antibiotic-resistant bacteria and non-antibiotic-resistant bacteria in water samples, two strains of *E. coli*, one was resistant to ampicillin (*E. coli Famp*), while the other was not (*E. coli CN13*),

were separately spiked into the filtered wastewater at concentrations ranging from 10^3 to 10^5 CFU/ml. The complete benchtop assay procedures which involved incubation with the presence of ampicillin for two hours, impurities removal, cell lysis, and LAMP detection were applied to analyze the serially diluted *E. coli* spiked samples. The LAMP results of the two *E. coli* strains were compared to determine the accuracy and sensitivity of the proposed assay in differentiating between antibiotic-resistant and non-antibiotic-resistant bacteria in the water samples.

Finally, the assay was applied to detect indigenous ampicillin-resistant *E. coli* in wastewater samples. Given that the number of indigenous *E. coli* in wastewater is typically higher than the detection limit (Raboni et al., 2016), a parallel set of assay procedures without the incubation step was implemented to establish a baseline signal. LAMP signals obtaining by the assay procedures with and without the incubation steps were compared for the discernment of ARB in the wastewater samples. Increased LAMP signals indicate the presence of ampicillin-resistant *E. coli* in the water samples, as they can flourish in the presence of ampicillin. Conversely, the absence of significant signal enhancement suggests the absence of antibiotic-resistant strains.

4.2.4 CD design

The CD design for an integrated ARB detection workflow was created using Solidworks. Three identical microfluidic units were fabricated on a single CD, and each unit can detect different combinations of water samples and ARB. Figure 4.1 illustrates the design of a complete functional microfluidic unit. An oval-shaped mixing chamber was placed at the top center of each microfluidic unit. This chamber was designed for incubating bacteria and for pelleting and resuspending cells after incubation. A waste chamber located at the bottom right area of the mixing chamber was designed to collect the supernatant from the mixing chamber after cell pelleting. A

holding chamber was positioned in the upper left area of the mixing chamber, designed to preload nuclease-free water used for resuspending the pelleted bacteria cells. A lysis chamber was integrated into the lower right area of the mixing chamber. This chamber is designed to be preloaded with silica–zirconia beads and a metal disc to mimic benchtop bead beating for cell lysis. A metering chamber was linked to the bottom of the mixing chamber and used to separate, meter, and transfer the DNA supernatant. An overflow waste chamber was placed to the right of the metering chamber to collect any excess sample. Finally, an amplification and detection chamber was integrated into the bottom right area of the metering chamber to collect both the DNA supernatant and the LAMP reaction mixture from the reagent holding chamber located at the top of the amplification and detection chamber.

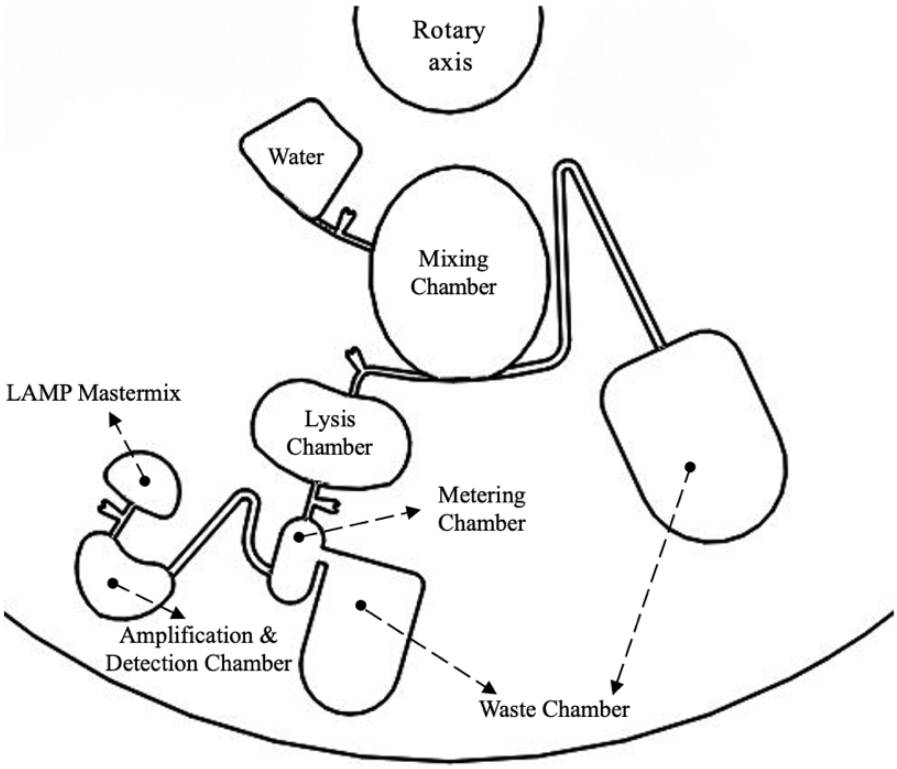

Figure 4.1. Microfluidic chambers and channel design of one functional microfluidic unit.

To enable a fully automated on-CD ARB detection assay, laser-irradiated ferrowax microvalves (Peshin et al., 2022) and siphon channel valves were applied to control sequential fluid pumping and mixing (Huang and Jiang, 2024). Laser-irradiated ferrowax microvalves are utilized as gates, blocking the channels in their solid form to restrict fluid flow between chambers, and they can be opened with a laser spot at a desired time. Siphon channel valves were employed at locations where repeated transitioning between open and closed positions was required. These siphon channel valves can be controlled between open and closed positions by simply adjusting the spin speed of the CD.

The fluid flow sequences and the precision of fluid volume transfer on the CD were tested using a CD driver equipped with control software (Pacific scientific, Wilmington, MA) to precisely control the rotation speed and direction of the CD. The heating for bacteria incubation and the LAMP reaction was carried out on a heat block and a shaking incubator, respectively. Details on the on-CD heating control and the valves operation are described in our previous report (Gowda et al., 2022; Huang and Jiang, 2024).

4.2.5 CD fabrication

The CD prototype consists of four layers with an outer diameter of 120 mm (Figure 4.2a). The top layer is a 1 mm polycarbonate disc featuring liquid inlets and vent holes drilled using a drill press (Dremel, Mount Prospect, IL). The second layer is a 0.1 mm double-sided adhesive tape (FLEXMOUNT DFM 200 clear V-95 150 POLY H-9, Spencer, MA) that includes cutouts for the chambers. The third layer is a 0.05 mm biocompatible single-sided microfluidic diagnostic tape (3M™ Microfluidic Diagnostic Tape 9795R, Saint Paul, MN) with cutouts for the chambers and ferrowax microvalve components. The fourth layer is a 2.3 mm polycarbonate disc containing the

microfluidic chambers, channels, and ferrowax microvalve components milled using a CNC machine (Tormach PCNC 440, Madison, WI). The cutouts on the adhesive tapes were created using a vinyl cutter (Silhouette CAMEO 2, Lindon, UT). A roller press was used to seal all the layers together after siphon channels were coated with Casein (ThermoFisher Scientific, Waltham, MA) and 0.1 gram of lysis beads and a metal disc (K&J Magnetics, Pipersville, PA) were placed into the lysis chamber. Image of actual fabricated and assembled CD are shown in Figure 4.2b. The details of the assembly steps are described in our previous report (Gowda et al., 2022; Huang and Jiang, 2024).

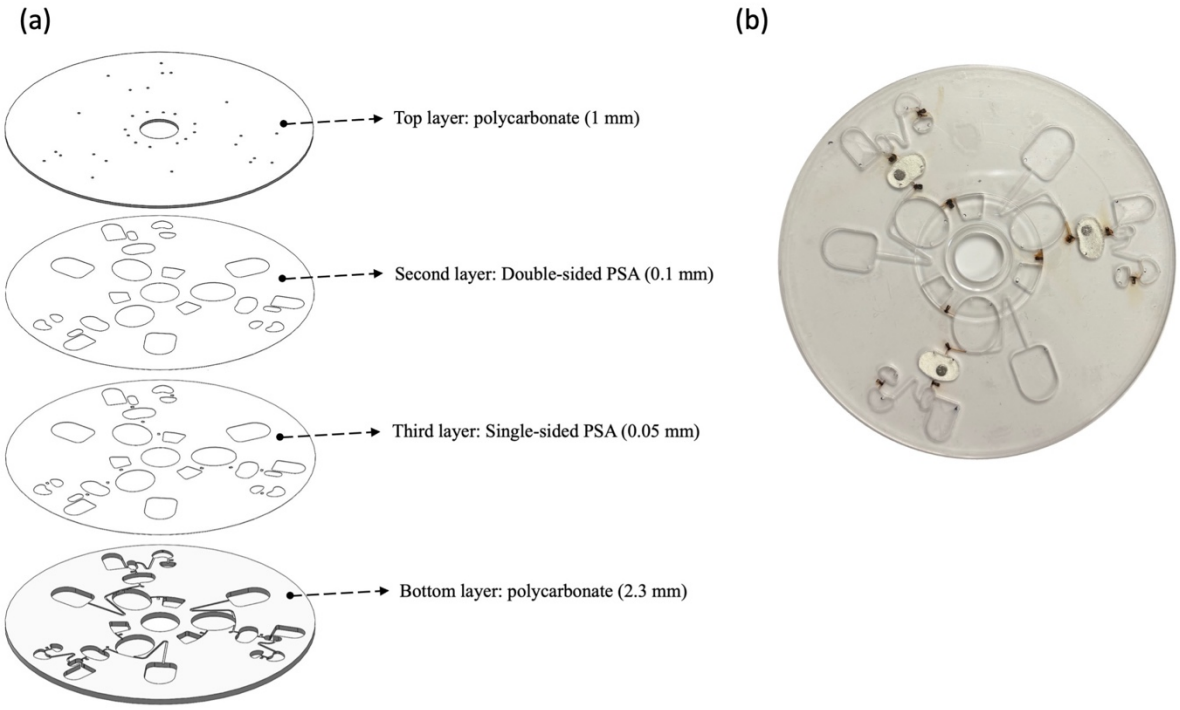

Figure 4.2. Centrifugal disc components. (a) Schematic illustrations of four main layers of CD assembly and (b) an image of actual fabricated and assembled CD.

4.2.6 Validation of the on-CD ARB detection assay

While the procedures for detecting ARB on-CD closely mirrors that of the benchtop procedure, certain variations exist between the benchtop and on-CD operation that may potentially decrease the sensitivity and accuracy of the on-CD assay. These variations include bacteria incubation conditions, parameters for cell pelleting and resuspension, and the mechanisms used for cell lysis. To ensure a comparable performance of the on-CD ARB detection assay to the benchtop assay, on-CD bacteria incubation, on-CD cell pelleting and resuspension, and on-CD cell lysis, were first tested and optimized individually by comparing with the benchtop procedures. The complete on-CD procedures, which include these optimized steps, were then evaluated to ensure the reliability in achieving ARB detection results.

Firstly, comparative experiments were conducted to evaluate the growth dynamics and antibiotic response of *E. coli Famp* and E. *coli CN13* within the CD chamber. Approximately 10^4 CFU/ml of each strain was prepared by diluting the *E. coli* stock solution with LB broth, and ampicillin was added to achieve a concentration of 15 ppm. 200 µL of bacteria solutions were cultured at 37°C in both CD chambers and 1.5 ml microcentrifuge tubes. The standard plate count method was applied to calculate the viable bacteria at 0, 1, and 2 hours. Subsequently, the growth dynamics of the bacteria in both microfluidic chambers and microcentrifuge tubes were compared to assess the suitability of the microfluidic environment for supporting bacterial growth and to identify differences in growth behavior between the strains in the presence of antibiotics when cultured in the microfluidic chamber.

Subsequently, the efficacy of on-CD pelleting and resuspension procedures was tested. Approximately 10^5 CFU/ml of *E. coli Famp* solutions were prepared by diluting the *E. coli* stock

solution with filtered wastewater. Both the benchtop and on-CD procedures were applied to process the 200 μL prepared samples and resuspend the pelleted cell in 100 μL of nuclease-free water, with the benchtop method serving as the benchmark to evaluate and optimize the on-CD procedure. The standard plate count method was employed to determine the bacteria concentration at various stages of the procedures, including the original bacteria samples, supernatant after pelleting, and resuspension samples. The bacteria concentrations were compared to assess the pelleting and resuspension efficiency.

Next, the comparison of the on-CD cell lysis and a traditional benchtop bead-beating cell lysis technique using *E. coli Famp* samples was performed to evaluate the performance of the on-CD cell lysis. *E. coli Famp* working solutions in the concentration range of 10^4 to 10^6 CFU/ml were prepared by diluting the *E. coli Famp* solution with nuclease-free water. On-CD cell lysis and a traditional benchtop bead-beating cell lysis technique were applied to lysis the bacteria cell among the prepared samples. The LAMP assay was employed to detect the extracted DNA using both cell lysis methods, and the results were analyzed to assess the efficiency and reliability of on-CD cell lysis method.

Finally, the complete on-CD sample-to-answer procedures, including bacteria incubation, impurity removal, cell lysis, and LAMP detection, were tested. Wastewater samples were used to evaluate the performance of the on-CD assay for ampicillin-resistant *E. coli* detection. Similar to the benchtop procedures, another CD was used without the incubation steps to determine the baseline signal of the *E. coli* in the wastewater. LAMP signals obtained from on-CD assays, both with and without the incubation step, were compared to determine the presence of ARB in the wastewater samples.

4.3 Results

4.3.1 Validation of the benchtop ARB detection assay

The LAMP detection results of *E. coli Famp* spiked in nuclease-free water and filtered wastewater, with and without the pelleting and resuspension procedure, are shown in Table 4.1. When analyzing the *E. coli* spiked in the nuclease-free water without the pelleting and resuspension procedure, seeding concentrations between 10^5 and 10^7 CFU/ml displayed positive LAMP signals, which increased with the increase of *E. coli* concentration, while seeding concentrations at 10^4 CFU/ml and non-spiked samples showed negative LAMP results. The photo images of three levels of positive signals, as indicated by the turbidity of reaction mixtures, are shown in Figure C.1. The results demonstrate the LAMP detection sensitivity for *E. coli* under ideal conditions, where external inhibition was absent and there was no loss of bacteria due to the pelleting and resuspension procedure. When analyzing the *E. coli* spiked in the filtered wastewater without the pelleting and resuspension procedure, no LAMP signal was displayed even at the highest spiked concentration of 10^7 CFU/ml. The results indicate that the impurities in the filtered wastewater can significantly inhibit the LAMP amplification if not removed.

When comparing the LAMP detection results of *E. coli* spiked in nuclease-free water that were processed with and without the pelleting and resuspension procedures (Table 4.1), similar detection sensitivity and LAMP signals intensity for each spiked concentration were observed. The results suggest that the majority of the bacterial cells can be retained in the microcentrifuge tubes after the pelleting and resuspension procedure. Additionally, the LAMP detection results of *E. coli* in filtered wastewater and nuclease-free water that were processed with the pelleting and resuspension procedures are also comparable (Table 4.1), suggesting that impurities in the filtered

wastewater can be sufficiently removed by the procedure. These comparative results demonstrate the reliability and efficacy of the pelleting and resuspension procedure as a DNA purification method for wastewater samples prior to downstream detection.

Table 4.1. LAMP detection results of *E. coli* spiked in nuclease-free water and filtered wastewater with and without pelleting and resuspension procedure.

E. coli Famp (CFU/ml)	**Without pelleting and resuspension procedure**		**With pelleting and resuspension procedure**	
	Pure water	Filtered wastewater	Pure water	Filtered wastewater
0	-	-	-	-
10^4	-	-	-	-
10^5	+	-	+	+
10^6	++	-	++	++
10^7	+++	-	+++	+++

The LAMP results for two strains of *E. coli* spiked in filtered wastewater, processed using the proposed benchtop ARB detection assay, are shown in Table 4.2. At initial spiked concentrations of 10^4 and 10^5 CFU/ml, the ARB detection assay successfully differentiated between ampicillin-resistant *E. coli (Famp)* and non-ampicillin-resistant *E. coli (CN13)*, with ampicillin-resistant *E. coli* displaying higher LAMP signals than non-ampicillin-resistant *E. coli*. However, at the lowest spiked concentration of 10^3 CFU/ml, the ARB detection assay failed to differentiate between the two strains of *E. coli*, as no LAMP signals were observed for either strain. Additionally, it is noteworthy that at the initial spiked concentration of 10^5 CFU/ml, while the difference in LAMP signal intensity was found between ampicillin-resistant *E. coli* and non-ampicillin-resistant *E. coli*, both strains displayed positive signals, indicating the presence of *E. coli* DNA at the end of the detection assay. This is because the initial spiked concentration was already higher than the LAMP detection sensitivity. Even though the non-ampicillin-resistant *E. coli* did not grow during the short-term incubation period, the assay still detected its DNA due to the high initial concentration.

Overall, the results suggest that a 2-hour incubation period followed by the LAMP amplification can differentiate antibiotic-resistant and non-resistant *E. coli* at concentrations above 10^4 CFU/ml but may be limited in sensitivity of the LAMP amplification at lower concentrations.

Table 4.2. LAMP results of *E. coli Famp* and *E. coli CN13* spiked in filtered wastewater using the benchtop detection assay.

Spiked concentration (CFU/ml)	**E. coli Famp**	**E. coli CN13**
10^3	-	-
10^4	+	-
10^5	++	+

Table 4.3a shows the results of indigenous ampicillin-resistant *E. coli* detection in wastewater using the benchtop ARB detection assay. Despite the concentration of *E. coli* in the wastewater sample already being above the LAMP detection limit, as indicated by the benchtop detection assay without the incubation step, an increased LAMP signal intensity was observed after incubating the wastewater sample with ampicillin for 2 hours, indicating the presence of ampicillin-resistant *E. coli* in the wastewater samples. The result suggests that the benchtop detection assay has the potential to be applied in monitoring ARB in the environment.

Table 4.3. LAMP results of indigenous ampicillin-resistant *E. coli* in wastewater using the (a) benchtop procedure and (b) On-CD procedure.

	(a)Benchtop detection		(a)On-CD detection	
	Without incubation	With incubation	Without incubation	With incubation
Indigenous E. coli in wastewater	+	++	+	++

4.3.2 Fluid control for on-CD ARB detection assay

Colored liquids were utilized to demonstrate integrated liquid handling for the on-CD ARB detection assay, with photo images of each processing step depicted in Figure 4.3. Table 4.4 summarizes the protocols employed for CD rotation and oscillation to accomplish each operational step. The on-CD assay was completed in approximately 3 hours with minimal hands-on tasks.

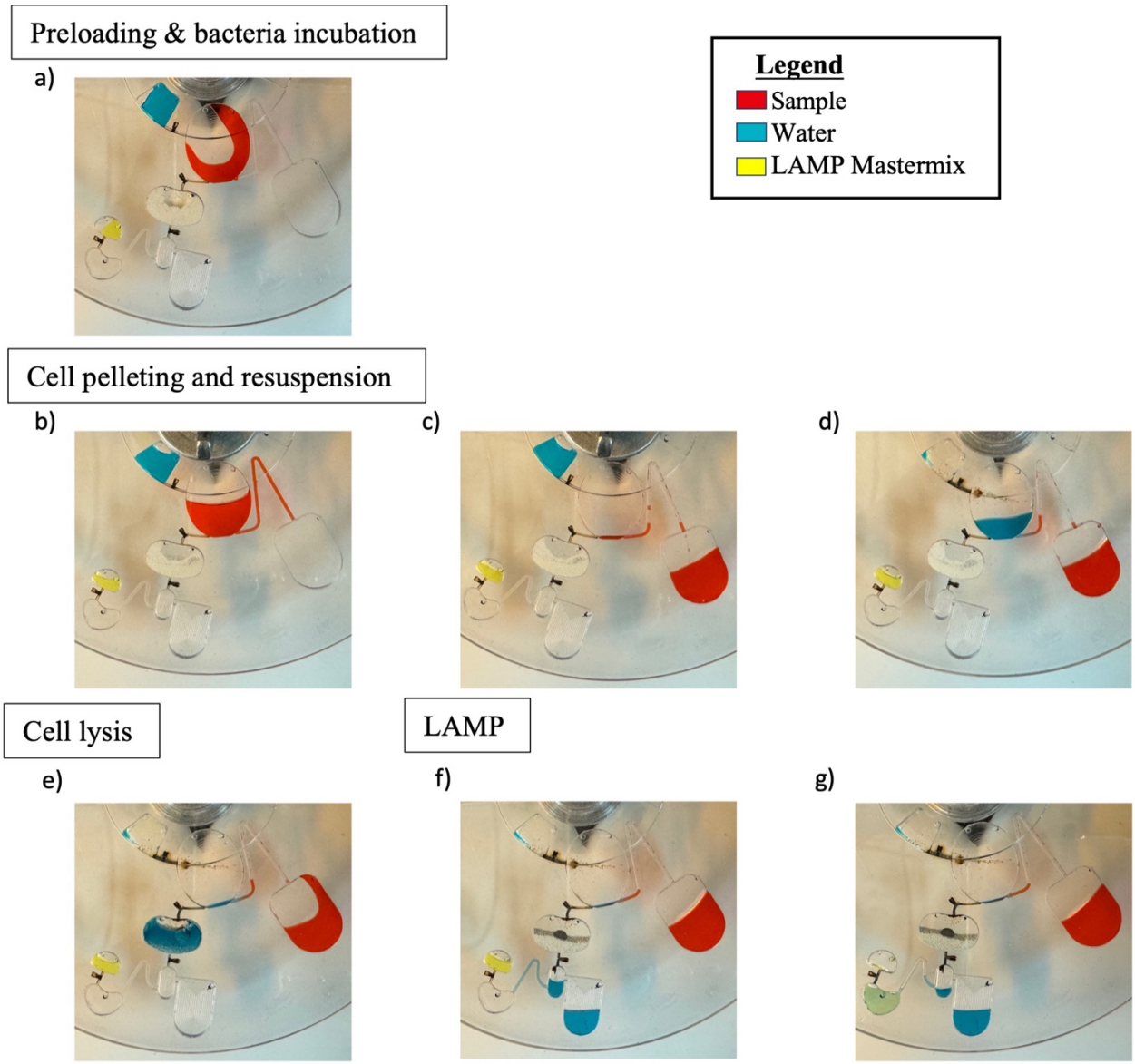

Figure 4.3. Photo images of the fluid handling process on CD. The color-dyes were added to the fluid for visualization.

Table 4.4. CD operational programing.

Steps	Protocol	Operation Details
Bacteria incubation	Oscillation (incubation)	12 rev/s², 0.1 rev, 2 hours
Cell pelleting	Rotation (cell pelleting) Pause (open the siphon) Rotation (waste disposal + close the siphon)	5000 RPM, 6 min 0 RPM, 10 s 800 RPM, 30 s
Cell resuspension	Laser (open the ferrowax valve) Rotation (liquid transfer) Oscillation (cell resuspension)	N/A 1000 RPM, 20 s 500 rev/s², 0.05 rev, 1 min
Cell lysis	Laser (open the ferrowax valve) Rotation (liquid transfer) Oscillation (beads beating) Laser (open the ferrowax valve) Rotation (cell debris pelleting)	N/A 1000 RPM, 20 s 128 rev/s², 0.3 rev, 6 min N/A 5000 RPM, 30 s
LAMP	Pause (open the siphon) Laser (open the ferrowax valve) Rotation (liquid transfer) Oscillation (Mixing) Heating (Amplification)	0 RPM, 10 s N/A 1000 RPM, 20 s 48 rev/s², 0.1 rev, 30 s 0 RPM, 35 min
Total time		~ 3 hours

Figure 4.3a illustrates the liquid preloading and bacteria incubation steps. The oval-shaped mixing chamber was preloaded with 100 µL of water sample and 100 µL of LB broth. Additionally, 100 µL of nuclease-free water was loaded into the holding chamber located at the top left area of the mixing chamber, while 16 µL of LAMP master mix was loaded into the holding chamber positioned at the top of the amplification and detection chamber. After liquid preloading, the CD was oscillated at 37 °C for 2 hours to create the ideal incubation condition.

The cell pelleting and resuspension steps are shown in Figure 4.3b, 4.3c, and 4.3d. The procedure began with the CD rotating at 5,000 RPM for 6 minutes followed by a 10-second pause. The high-

speed rotation pelleted the bacterial cells to the bottom of the chamber and pushed the supernatant into the siphon channel, while the brief pause allowed the supernatant to fill the siphon channel through capillary force, transitioning the valve to the open state (Figure 4.3b). The CD was then rotated at 800 RPM for 30 seconds to transfer the supernatant from the mixing chamber to the waste chamber and form an air lock in the siphon channel, switching the siphon channel valve back to the closed state (Figure 4.3c). Subsequently, the ferrowax valve located at the connection between the nuclease-free water holding chamber and the mixing chamber was opened, and the CD was rotated at 1000 RPM for 20 seconds to transfer the water into the mixing chamber. Following this, the CD was then oscillated for 1 minute to resuspend the pelleted bacterial cells into the nuclease-free water (Figure 4.3d).

The CD was rotated at 1000 RPM for 20 seconds after the ferrowax valve was opened to transfer the prepared bacterial sample to the lysis chamber. Subsequently, it was oscillated for 6 minutes, driving the metal disc to move back and forth within the lysis chamber to generate the bead-beating action of silica beads (Figure 4.3e). This action provides shear forces to physically disrupt the cells, releasing genomic sequences for further analysis (Perebikovsky et al., 2021).

After the cell lysis, the ferrowax valve between the lysis chamber and the metering chamber was opened and the CD was rotated at 5,000 RPM for 30 seconds followed by a 10-seconds pause (Figure 4.3f). The lysed sample was transferred from the lysis chamber to the metering chamber. Due to the high-speed rotation, cell debris were pelleted to the bottom of the metering chamber, and the overflow liquid was pushed to the waste chamber next to the metering chamber. Additionally, the siphon channel was filled by the extracted DNA sample during the brief pause. The CD was then rotated at 1000 RPM for 20 seconds to transfer the LAMP master mix and approximately 4 μL of extracted DNA together into the amplification and detection chamber

(Figure 4.3g) at the opening of the ferrowax microvalve. Finally, the CD was oscillated for 30 seconds to mix the extracted DNA with the LAMP Mastermix, followed by heating for 35 minutes for the LAMP amplification.

4.3.3 Validation of on-CD assay for ARB detection

Figure 4.4a illustrates the comparison results of on-CD and benchtop incubation for ampicillin-resistant *E. coli* at a concentration of 15 ppm ampicillin. The growth dynamics of both incubation scenarios are similar, with a lag phase observed during the first hour followed by growth occurring in the second hour. After the 2-hour growing period, both conditions show an approximately 10-fold increase in bacteria concentration, with on-CD incubation demonstrating slightly higher growth rates compared to benchtop incubation. The results suggest that ampicillin-resistant *E. coli* can proliferate effectively at a concentration of 15 ppm ampicillin using either incubation method. Additionally, it indicates that the on-CD incubation method may provide a more favorable environment for bacterial growth, possibly due to increased turbulence and advection within the CD mixing chamber. Non-ampicillin-resistant *E. coli* was also incubated with 15 ppm ampicillin using both incubation methods. However, no bacterial colonies were observed when applying the standard plate count method to measure the *E. coli* concentration at both the 1-hour and 2-hour time points, indicating that the non-resistant strain did not grow under these conditions. Overall, the results suggest a comparable performance between on-CD and benchtop incubation assays in facilitating the growth of bacteria, as well as differentiating the antibiotic-resistant strains under short-term incubation.

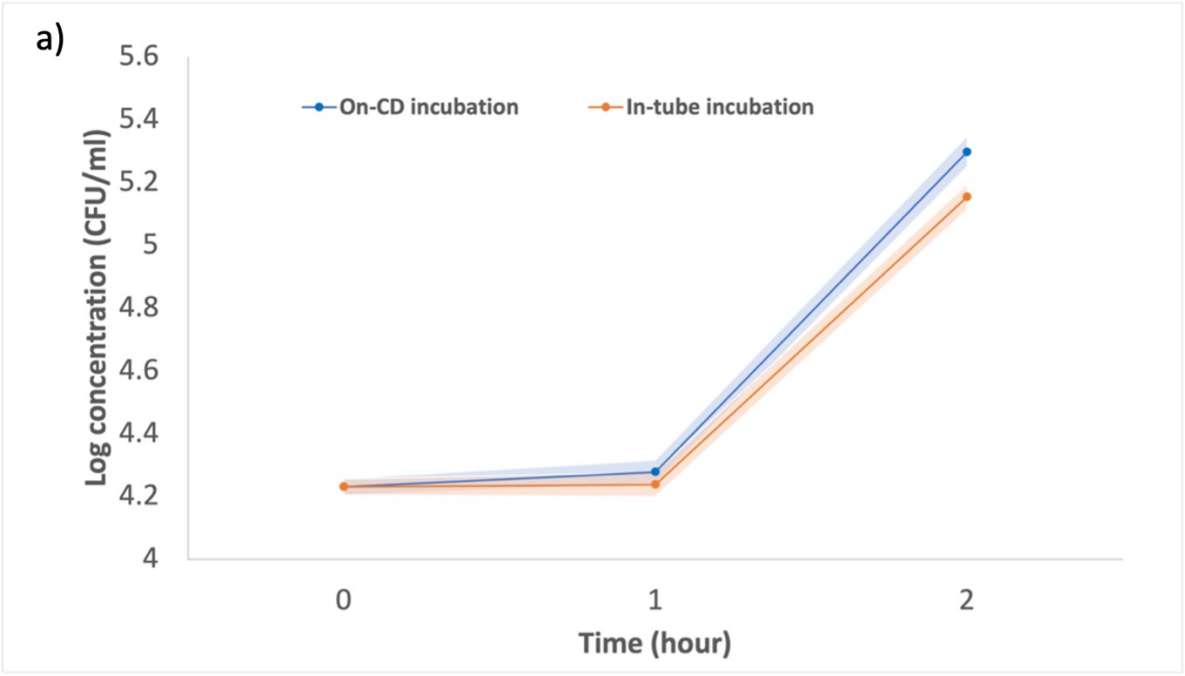

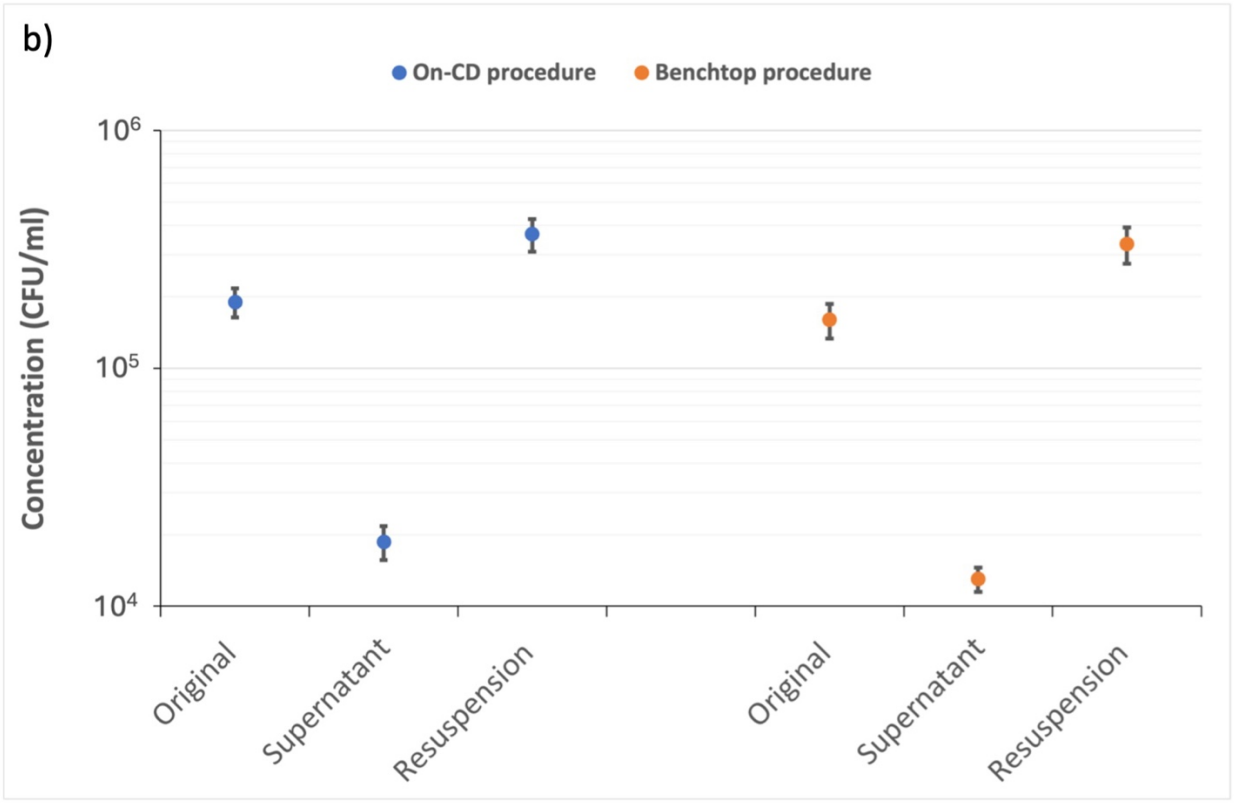

Figure 4.4. (a) *E. coli* growth dynamics of on-CD and in-tube incubation. Shading represents the standard deviations. (b) The comparison results of cell pelleting and resuspension procedures using on-CD and benchtop methods. The standard deviations are plotted as error bars.

The comparison results of cell pelleting and resuspension procedures using on-CD and benchtop methods are illustrated in Figure 4.4b. Both methods exhibit similar recovery rates of bacterial cells after the procedures. Following the cell pelleting step, the bacteria concentration in the supernatant is approximately 10% of the concentration in the original sample for both on-CD and benchtop methods, indicating that approximately 90% of the bacterial cells were pelleted using both methods. Moreover, an approximately 2-fold increase in bacterial concentration was observed in the resuspension sample compared to the original sample, suggesting that the oscillation protocol employed for both benchtop and on-CD methods efficiently resuspends the pelleted cells. It is noteworthy that the increase in concentration before and after the procedures is likely attributed to the concentration factor applied during the procedure, where cells are pelleted in 200 µl of bacterial sample and then resuspended in 100 µl of water. Additionally, bacterial growth may occur during the procedure period, contributing to the observed increase in concentration.

The comparison between on-CD cell lysis and a traditional benchtop bead-beating cell lysis technique using *E. coli* samples is shown in Table 4.5. When analyzing the *E. coli* samples lysed using the benchtop method, seeding concentrations at 10^5 and 10^6 CFU/ml exhibited positive LAMP signals, while no LAMP signals were found for the seeding concentration at 10^4 CFU/ml. When analyzing the *E. coli* samples lysed using the on-CD method, the same detection sensitivity was observed, suggesting a comparable performance between the two lysis techniques.

Table 4.5. LAMP results of *E. coli* spiked in nuclease-free water and extracted using different cell lysis methods.

Spiked E. coli concentration (CFU/ml)	On-CD cell lysis	Benchtop cell lysis
0	-	-
10^4	-	-
10^5	+	+
10^6	++	++

Finally, the complete on-CD ARB detection assay, including on-CD bacteria incubation, on-CD purification, on-CD cell lysis, and on-CD LAMP reaction, was tested in real-world conditions to further evaluate its overall effectiveness and performance. Table 4.3b shows the detection results of indigenous ampicillin-resistant *E. coli* in wastewater using the on-CD assay. Similar to the detection results using the benchtop assay (Table 4.3a), the LAMP signals of *E. coli* increased with 2 hours incubation with ampicillin, indicating the presence of ampicillin-resistant *E. coli* in the wastewater. The result demonstrates that the on-CD assay effectively identifies ARB in complex environmental samples, validating its utility for practical application in environmental monitoring and public health surveillance.

4.4 Discussion

With the antibiotic resistance threat to humans and the environment rapidly escalating, there is an urgent need to develop rapid and effective detection methods for antibiotic-resistant organisms in aquatic environments to safeguard human and environmental health. This research introduces an ARB detection assay with significantly reduced assay processing time, while still maintaining the characteristics of phenotypic methods. In addition, a microfluidic CD was developed to integrate all assay steps, eliminating the need for a centralized laboratory and well-trained personnel to perform the assays, thereby facilitating broader accessibility and faster responses to emerging threats.

The validation results of the benchtop ARB detection assay confirmed that a short-term bacteria incubation with antibiotics followed by LAMP detection is sufficient to determine ARB in water. The concentration of antibiotic-resistant *E. coli* increased approximately 10-fold, while non-antibiotic-resistant *E. coli* were not viable after the 2-hour incubation period exposed to the

antibiotic. Despite the potential presence of DNA even after the bacteria were killed by the antibiotic (Fang et al., 2018), no significant increase in DNA of non-antibiotic-resistant *E. coli* was observed during incubating with the antibiotic. Although the difference in bacteria concentration cannot be visually observed after short-term incubation, LAMP detection can efficiently differentiate this 10-fold increase in DNA concentration and determine if water samples present ARB. In addition, we have shown that incorporating cell pelleting and resuspension procedures effectively eliminates potential LAMP inhibitors found in culture media and water samples. While commercial nucleic acid extraction products may offer superior purification efficacy, cell pelleting and resuspension procedures are more straightforward for on-CD application and can also provide purification efficiency that is sufficient for LAMP reaction.

We have further demonstrated that the microfluidic CD can integrate the benchtop ARB detection procedures, including short-term bacteria incubation, impurities removal, cell lysis, and LAMP reaction. The microfluidic CD was carefully designed and optimized to accommodate multiple chambers, channels, and valves, facilitating precise control of samples and reagents. To provide a healthy growth condition for the bacteria, which requires sufficient aeration and turbulence, we employed an oval-shaped chamber that has been demonstrated to provide sufficient mixing across a wide range of operating volumes for bacteria incubation (Huang and Jiang, 2024). Additionally, the volume of the incubation chamber was designed to be approximately five times that of the bacterial sample, ensuring access to fresh oxygen for growth. The incubation chamber was also utilized for the cell pelleting and resuspension procedures, serving as a critical step to remove potential LAMP inhibitors. By optimizing the rotation speed and duration, the efficiency of on-CD cell pelleting demonstrates comparable performance to that of the benchtop microcentrifuge. Similarly, the optimized oscillation protocol coupled with the oval-shaped chamber serves as an

effective alternative to using a vortex mixer for liquid mixing in a PCR-tube, ensuring thorough resuspension of the pelleted cells in the microfluidic chamber. On-CD cell lysis has been reported in several studies (Perebikovsky et al., 2021; Gowda et al., 2022), and the chamber shape, amount of silica beads, and process time have been optimized. However, most of the design relied on an external magnet array to drive the metal disc in the chamber in order to grind the silica beads for bead beating. In this study, we developed an oscillation protocol to drive the metal disc to move back and forth within the chamber, eliminating the need for an external magnet array, while adhering to the recommendations of previous research for other design and operating parameters. The modified approach was confirmed to be effective in achieving efficient cell lysis directly on the microfluidic CD platform. These optimized CD design and operating parameters play an important role in transforming the traditional laboratory-based procedures into a rapid, portable, semi-automated, and user-friendly ARB detection method for water environments.

Despite having demonstrated the performance of the on-CD detection assay in detecting ampicillin-resistant *E. coli* in environmental matrices, further research is needed to translate this proof-of-concept into practical solutions. One of the primary challenges is its limited detection sensitivity. The assay can detect ampicillin-resistant *E. coli* above a concentration of 10^4 CFU/ml. However, it struggled to differentiate between ampicillin-resistant and non-ampicillin-resistant strains at lower concentrations, as both strains exhibit negative LAMP results. It is important to mention that the detection sensitivity of the ARB detection assay is mainly limited by the LAMP amplification efficiency. Designing a different set of LAMP primers for *E. coli* that have better detection sensitivity may improve the assay's performance. Increasing the assay's concentration factor or extending the bacteria incubation duration could also enhance the sensitivity in detecting ARB in water. Another improvement direction is to convert the binary detection assay into a

quantitative ARB detection method through droplet digital LAMP (dd-LAMP) (Schuler et al., 2016), which has been successfully integrated into the CD platform in our previous research (Gowda et al., 2022; Huang and Jiang, 2024). The assay developed in this study determines ARB based on comparing the LAMP intensities of water samples with and without incubation process. Implementing dd-LAMP would allow for more precise quantification of ARB levels, providing clearer and more accurate results. Finally, to enable mass production, it is necessary to explore more advanced CD manufacturing methods, such as injection molding combined with ultrasonic bonding (Lee et al., 2018; Scott and Ali, 2021; Giri and Tsao, 2022). Additionally, utilizing valves that are easier to manufacture rather than manually loading the ferrowax into the CD will streamline the production process.

In this research, the primary focus was on CD design and assay validation. We tested and validated the on-CD assay using a benchtop CD driver for rotation controls, a handheld laser for opening ferrowax valves, an incubating shaker for bacteria incubation, and a CD heating block for LAMP reaction. A portable CD driver that integrates all the necessary functions for on-CD assay operation has not yet been fully developed. In our previous research, we reported a portable CD driver consisting of programmable disc rotation controls, heating and temperature controls, and digital image capture and processing (Gowda et al., 2022). Further modifications are needed to optimize this CD driver for the operation of the on-CD ARB detection assay. This includes adding a laser control system, utilizing either a stepper motor or an actuator, to open the active valves at specific positions, as described in previous studies (Li et al., 2019; Perebikovsky et al., 2021; Gowda et al., 2022). Additionally, the heating and temperature control system requires further optimization, such as rearranging the number and location of the infrared heaters, to accurately control the chamber's temperature for bacteria incubation and the LAMP reaction. While the microfluidic CD

system remains an emerging research area, with limited exploration of its application in environmental detection, our study demonstrates the significant potential of microfluidic CDs as a next-generation method for detecting ARB in water environments. The portability, rapidity, and user-friendly characteristics of this detection platform can facilitate more frequent and widespread monitoring of ARB. This capability enhances our ability to safeguard public health and the environment, as well as to understand the occurrence and fate of antibiotic resistance, thereby enabling the development of more effective mitigation strategies. With the rapid advancement of microfluidic CD technology, our proof-of-concept study serves as a foundational step towards the development of more advanced CD technologies for environmental applications.

CHAPTER 5
CONCLUSIONS

In this dissertation, I investigated the feasibility of using two emerging technologies: surface enhanced Raman scattering (SERS) and centrifugal microfluidic disc (CD) as rapid, portable, and user-friendly methods for the detection of antibiotics, microbial pathogens, and antibiotic-resistant organisms in environmental water matrices.

One of the main challenges in implementing Surface Enhanced Raman Scattering (SERS) as a label-free, real-time sensor for antibiotic detection in environmental water matrices is the interference from non-target molecules. These molecules can generate overlapping SERS signals and prevent the target chemical from attaching to the hotspots for signal enhancement. In Chapter 2, I investigate the effectiveness of two gold nanostructures as SERS substrates for detecting quinoline, a common antibiotic found in wastewater. The results show that the carefully designed SERS substrates with uniformed sub-nanometer nanogap can excludes the interference from large molecules (size exclusion) that are commonly found in wastewater samples, and selectively enhances signals from small molecules within the designed nanogap spaces. On the other hands, the commercial SERS substrates, while having high enhancement factors and detection reproducibility when detecting antibiotic in pure water, there is no selectivity for the molecular size of the target in the wastewater environment. Additionally, I demonstrated that the synergy between the mechanism of the selective intensification of target molecules of the SERS substrate and AI algorisms can further increase the selectivity of the label-free SERS methods.

The centrifugal microfluidic disc (CD) has emerged as a popular platform for integrating sample preparation and nucleic acid amplification technologies into a lab-on-a-CD system. However, two

key challenges for environmental microbe detection – the presence of inhibitors for nucleic acid amplification and low pathogen concentrations – make it difficult to integrate the entire procedure required for environmental monitoring onto a single CD. In Chapter 3, I presented a CD design that effectively utilizes the space on the disc, facilitating a wide range of tasks including sample concentration, purification, and ddRT-LAMP for virus quantification in the environmental water matrices. The CD design included an approximately 6.67-fold concentration factor and multiple washing procedures to address the challenges of inhibitory substances and low pathogen concentrations. The chambers, valves, and operating protocol were carefully optimized, ensuring comparable sample extraction and nucleic acid purification efficiency with in-tube sample preparation procedures. Moreover, this assay can accurately quantify indigenous PMMoV in wastewater in less than 1.5 hours.

In chapter 4, I further explored the feasibility of using the CD system to detect antibiotic-resistant bacteria (ARB) in wastewater. I started by proposing an innovative benchtop ARB detection assay designed to determine the presence of ARB in wastewater in a shorter detection time while retaining the characteristics of phenotypic methods. According to the assay validation results, I demonstrated that a short-term incubation period with the presence of antibiotics followed by LAMP amplification can differentiate between antibiotic-resistant bacteria and non-antibiotic-resistant bacteria. Additionally, I confirmed that cell pelleting and resuspension procedures are sufficient to remove potential LAMP inhibitors in the wastewater. Built upon the foundation of the virus detection CD system developed in chapter 3, I integrated the entire process of the benchtop ARB detection procedure, including short-term bacteria incubation, cell pelleting and resuspension procedures, cell lysis, and amplification steps onto a CD system. The performance

of the on-CD assay is comparable to the benchtop assay. Indigenous ampicillin-resistant *E. coli* in raw wastewater has been successfully detected in less than 3 hours using the on-CD assay.

Overall, this dissertation highlights the strong potential of applying SERS and microfluidic CD technologies as rapid, portable, and user-friendly methods for the detection of antibiotics, microbial pathogens, and antibiotic-resistant organisms in environmental water matrices. The innovative strategies reported in this research offer promising solutions to overcome key challenges in environmental monitoring. Despite the necessity for future development to enhance their detection performance and scalability, this dissertation serves as an important first step towards advancing the field of environmental monitoring and revolutionizing current environmental monitoring practices.

BIBLIOGRAPHY

Adams, S.M., Campione, S., Caldwell, J.D., Bezares, F.J., Culbertson, J.C., Capolino, F., Ragan, R., 2012. Non-lithographic SERS Substrates: Tailoring Surface Chemistry for Au Nanoparticle Cluster Assembly. Small 8, 2239–2249. https://doi.org/10.1002/smll.201102708

Ahmed, S., Ning, J., Peng, D., Chen, T., Ahmad, I., Ali, A., Lei, Z., Abu Bakr Shabbir, M., Cheng, G., Yuan, Z., 2020. Current advances in immunoassays for the detection of antibiotics residues: a review. Food and Agricultural Immunology 31, 268–290. https://doi.org/10.1080/09540105.2019.1707171

Akki, S.U., Werth, C.J., 2018. Critical Review: DNA Aptasensors, Are They Ready for Monitoring Organic Pollutants in Natural and Treated Water Sources? Environ. Sci. Technol. 52, 8989–9007. https://doi.org/10.1021/acs.est.8b00558

Ambroziak, R., Krajczewski, J., Pisarek, M., Kudelski, A., 2020. Immobilization of Cubic Silver Plasmonic Nanoparticles on TiO_2 Nanotubes, Reducing the Coffee Ring Effect in Surface-Enhanced Raman Spectroscopy Applications. ACS Omega 5, 13963–13972. https://doi.org/10.1021/acsomega.0c01356

Aydin, S., Aydin, M.E., Ulvi, A., Kilic, H., 2019. Antibiotics in hospital effluents: occurrence, contribution to urban wastewater, removal in a wastewater treatment plant, and environmental risk assessment. Environ Sci Pollut Res 26, 544–558. https://doi.org/10.1007/s11356-018-3563-0

Bain, R., Cronk, R., Hossain, R., Bonjour, S., Onda, K., Wright, J., Yang, H., Slaymaker, T., Hunter, P., Prüss-Ustün, A., Bartram, J., 2014. Global assessment of exposure to faecal contamination through drinking water based on a systematic review. Tropical Med Int Health 19, 917–927. https://doi.org/10.1111/tmi.12334

Bonadonna, L., Briancesco, R., La Rosa, G., 2019. Innovative analytical methods for monitoring microbiological and virological water quality. Microchemical Journal 150, 104160. https://doi.org/10.1016/j.microc.2019.104160

Ben, Y., Fu, C., Hu, M., Liu, L., Wong, M.H., Zheng, C., 2019. Human health risk assessment of antibiotic resistance associated with antibiotic residues in the environment: A review. Environmental Research 169, 483–493. https://doi.org/10.1016/j.envres.2018.11.040

Bolboaca, M., Kiefer, W., Popp, J., 2002. Fourier transform Raman and surface-enhanced Raman spectroscopy of some quinoline derivatives. J Raman Spectroscopy 33, 207–212. https://doi.org/10.1002/jrs.816

Caicedo, C., Beutel, S., Scheper, T., Rosenwinkel, K.H., Nogueira, R., 2016. Occurrence of Legionella in wastewater treatment plants linked to wastewater characteristics. Environ Sci Pollut Res 23, 16873–16881. https://doi.org/10.1007/s11356-016-7090-6

Chauhan, R., Singh, J., Sachdev, T., Basu, T., Malhotra, B.D., 2016. Recent advances in mycotoxins detection. Biosensors and Bioelectronics 81, 532–545. https://doi.org/10.1016/j.bios.2016.03.004

Cichocki, A., Phan, A.-H., 2009. Fast Local Algorithms for Large Scale Nonnegative Matrix and Tensor Factorizations. IEICE Trans. Fundamentals E92-A, 708–721. https://doi.org/10.1587/transfun.E92.A.708

Corcoll, N., Österlund, T., Sinclair, L., Eiler, A., Kristiansson, E., Backhaus, T., Eriksson, K.M., 2017. Comparison of four DNA extraction methods for comprehensive assessment of 16S rRNA bacterial diversity in marine biofilms using high-throughput sequencing. FEMS Microbiology Letters 364. https://doi.org/10.1093/femsle/fnx139

Centers for Disease Control and Prevention (U.S.), 2019. Antibiotic resistance threats in the United States, 2019. Centers for Disease Control and Prevention (U.S.). https://doi.org/10.15620/cdc:82532

Dufour, A., Snozzi, M., Koster, W., Bartram, J., Ronchi, E., Fewtrell, L., 2013. Assessing Microbial Safety of Drinking Water: Improving Approaches and Methods. IWA Publishing. https://doi.org/10.2166/9781780405872

Dhakal, S., Chao, K., Huang, Q., Kim, M., Schmidt, W., Qin, J., Broadhurst, C., 2018. A Simple Surface-Enhanced Raman Spectroscopic Method for on-Site Screening of Tetracycline Residue in Whole Milk. Sensors 18, 424. https://doi.org/10.3390/s18020424

Dong, H., Yuan, X., Wang, W., Qiang, Z., 2016. Occurrence and removal of antibiotics in ecological and conventional wastewater treatment processes: A field study. Journal of Environmental Management 178, 11–19. https://doi.org/10.1016/j.jenvman.2016.04.037

Eilers, P.H.C., Boelens, H.F.M., 2005. Baseline Correction with Asymmetric Least Squares Smoothing.

Fang, X., Li, W., Zhang, C., Huang, Z., Zeng, H., Dong, Z., Zhang, W., 2018. Detecting the Presence of Bacterial DNA and RNA by Polymerase Chain Reaction to Diagnose Suspected Periprosthetic Joint Infection after Antibiotic Therapy. Orthopaedic Surgery 10, 40–46. https://doi.org/10.1111/os.12359

Fleischmann, M.; Hill, I. R.; Sundholm, G., 1983. A Raman spectroscopic study of quinoline and isoquinoline adsorbed on copper and silver electrodes. J. Electroanal. Chem. Interfacial Electrochem, 158, 153– 164. https://doi.org/10.1016/S0022-0728(83)80345-3

Finlay, B.B., Amato, K.R., Azad, M., Blaser, M.J., Bosch, T.C.G., Chu, H., Dominguez-Bello, M.G., Ehrlich, S.D., Elinav, E., Geva-Zatorsky, N., Gros, P., Guillemin, K., Keck, F., Korem, T., McFall-Ngai, M.J., Melby, M.K., Nichter, M., Pettersson, S., Poinar, H., Rees, T., Tropini, C., Zhao, L., Giles-Vernick, T., 2021. The hygiene hypothesis, the COVID pandemic, and consequences for the human microbiome. Proc. Natl. Acad. Sci. U.S.A. 118, e2010217118. https://doi.org/10.1073/pnas.2010217118

Fernandes, R.F., Stroppa, P.H.F., Ferreira, G.R., Da Silva, A.D., Edwards, H.G.M., De Oliveira, L.F.C., 2016. Vibrational spectroscopic study of some quinoline derivatives. Vibrational Spectroscopy 86, 128–133. https://doi.org/10.1016/j.vibspec.2016.06.005

Geladi, P., Kowalski, B.R., 1986. Partial least-squares regression: a tutorial. Analytica Chimica Acta 185, 1–17. https://doi.org/10.1016/0003-2670(86)80028-9

Ganguli, A., Mostafa, A., Berger, J., Aydin, M.Y., Sun, F., Ramirez, S.A.S.D., Valera, E., Cunningham, B.T., King, W.P., Bashir, R., 2020. Rapid isothermal amplification and portable detection system for SARS-CoV-2. Proc. Natl. Acad. Sci. U.S.A. 117, 22727–22735. https://doi.org/10.1073/pnas.2014739117

Goddard, F.G.B., Ban, R., Barr, D.B., Brown, J., Cannon, J., Colford, J.M., Eisenberg, J.N.S., Ercumen, A., Petach, H., Freeman, M.C., Levy, K., Luby, S.P., Moe, C., Pickering, A.J., Sarnat, J.A., Stewart, J., Thomas, E., Taniuchi, M., Clasen, T., 2020. Measuring Environmental Exposure to Enteric Pathogens in Low-Income Settings: Review and Recommendations of an Interdisciplinary Working Group. Environ. Sci. Technol. 54, 11673–11691. https://doi.org/10.1021/acs.est.0c02421

Gonzalez, R., Curtis, K., Bivins, A., Bibby, K., Weir, M.H., Yetka, K., Thompson, H., Keeling, D., Mitchell, J., Gonzalez, D., 2020. COVID-19 surveillance in Southeastern Virginia using wastewater-based epidemiology. Water Research 186, 116296. https://doi.org/10.1016/j.watres.2020.116296

Gowda, H.N., Kido, H., Wu, X., Shoval, O., Lee, A., Lorenzana, A., Madou, M., Hoffmann, M., Jiang, S.C., 2022. Development of a proof-of-concept microfluidic portable pathogen analysis system for water quality monitoring. Science of The Total Environment 813, 152556. https://doi.org/10.1016/j.scitotenv.2021.152556

Giri, K., Tsao, C.-W., 2022. Recent Advances in Thermoplastic Microfluidic Bonding. Micromachines 13, 486. https://doi.org/10.3390/mi13030486

Green, A., Song, Z., Tran, C., Reifsnyder, S., Rosso, D., Hsia, P., Melitas, N., Holden, P.A., Jiang, S., 2024. Community-Scale Surveillance of SARS-CoV-2: Optimizing Sampling Strategies for Centralized Wastewater Treatment Plants. Environmental Engineering Science 41, 7–17. https://doi.org/10.1089/ees.2023.0142

Huang, Y.-H., Wei, H., Santiago, P.J., Thrift, W.J., Ragan, R., Jiang, S., 2023. Sensing Antibiotics in Wastewater Using Surface-Enhanced Raman Scattering. Environ. Sci. Technol. 57, 4880–4891. https://doi.org/10.1021/acs.est.3c00027

Huang, Y.-H., Jiang, S., 2024. Quantification of viruses in wastewater on a centrifugal microfluidic disc. (manuscript submitted for publication)

He, S., Cao, B., Yi, Y., Huang, S., Chen, X., Luo, S., Mou, X., Guo, T., Wang, Yujie, Wang, Yanwei, Yang, G., 2022. DNA precipitation revisited: A quantitative analysis. Nano Select 3, 617–626. https://doi.org/10.1002/nano.202100152

Halvorson, R.A., Vikesland, P.J., 2010. Surface-Enhanced Raman Spectroscopy (SERS) for Environmental Analyses. Environ. Sci. Technol. 44, 7749–7755. https://doi.org/10.1021/es101228z

Han, C., Chen, J., Wu, X., Huang, Y., Zhao, Y., 2014. Detection of metronidazole and ronidazole from environmental Samples by surface enhanced Raman spectroscopy. Talanta 128, 293–298. https://doi.org/10.1016/j.talanta.2014.04.083

Han, X.X., Rodriguez, R.S., Haynes, C.L., Ozaki, Y., Zhao, B., 2022. Surface-enhanced Raman spectroscopy. Nat Rev Methods Primers 1, 87. https://doi.org/10.1038/s43586-021-00083-6

Hernández, F., Sancho, J.V., Ibáñez, M., Guerrero, C., 2007. Antibiotic residue determination in environmental waters by LC-MS. TrAC Trends in Analytical Chemistry 26, 466–485. https://doi.org/10.1016/j.trac.2007.01.012

Hussain, A., Sun, D.-W., Pu, H., 2019. SERS detection of urea and ammonium sulfate adulterants in milk with coffee ring effect. Food Additives & Contaminants: Part A 36, 851–862. https://doi.org/10.1080/19440049.2019.1591643

Hill, J., Beriwal, S., Chandra, I., Paul, V.K., Kapil, A., Singh, T., Wadowsky, R.M., Singh, V., Goyal, A., Jahnukainen, T., Johnson, J.R., Tarr, P.I., Vats, A., 2008. Loop-Mediated Isothermal Amplification Assay for Rapid Detection of Common Strains of Escherichia coli. J Clin Microbiol 46, 2800–2804. https://doi.org/10.1128/JCM.00152-08

Julian, T.R., Schwab, K.J., 2012. Challenges in environmental detection of human viral pathogens. Current Opinion in Virology 2, 78–83. https://doi.org/10.1016/j.coviro.2011.10.027

Jennings, W.C., Chern, E.C., O'Donohue, D., Kellogg, M.G., Boehm, A.B., 2018. Frequent detection of a human fecal indicator in the urban ocean: environmental drivers and covariation with enterococci. Environ. Sci.: Processes Impacts 20, 480–492. https://doi.org/10.1039/C7EM00594F

Joss, A., Zabczynski, S., Göbel, A., Hoffmann, B., Löffler, D., McArdell, C.S., Ternes, T.A., Thomsen, A., Siegrist, H., 2006. Biological degradation of pharmaceuticals in municipal wastewater treatment: Proposing a classification scheme. Water Research 40, 1686–1696. https://doi.org/10.1016/j.watres.2006.02.014

Karthikeyan, K.G., Meyer, M.T., 2006. Occurrence of antibiotics in wastewater treatment facilities in Wisconsin, USA. Science of The Total Environment 361, 196–207. https://doi.org/10.1016/j.scitotenv.2005.06.030

Kim, N., Thomas, M.R., Bergholt, M.S., Pence, I.J., Seong, H., Charchar, P., Todorova, N., Nagelkerke, A., Belessiotis-Richards, A., Payne, D.J., Gelmi, A., Yarovsky, I., Stevens, M.M., 2020. Surface enhanced Raman scattering artificial nose for high dimensionality fingerprinting. Nat Commun 11, 207. https://doi.org/10.1038/s41467-019-13615-2

Kneipp, K., Kneipp, H., 2006. Single Molecule Raman Scattering. Appl Spectrosc 60, 322A-334A. https://doi.org/10.1366/000370206779321418

Küçük, V., Altun, A., Kumru, M., 2012. Combined experimental and theoretical studies on the vibrational spectra of 2-quinolinecarboxaldehyde. Spectrochimica Acta Part A: Molecular and Biomolecular Spectroscopy 85, 92–98. https://doi.org/10.1016/j.saa.2011.09.026

Kong, L.X., Perebikovsky, A., Moebius, J., Kulinsky, L., Madou, M., 2016. Lab-on-a-CD: A Fully Integrated Molecular Diagnostic System. SLAS Technology 21, 323–355. https://doi.org/10.1177/2211068215588456

Kitajima, M., Sassi, H.P., Torrey, J.R., 2018. Pepper mild mottle virus as a water quality indicator. npj Clean Water 1, 19. https://doi.org/10.1038/s41545-018-0019-5

Larsson, D.G.J., Flach, C.-F., 2022. Antibiotic resistance in the environment. Nat Rev Microbiol 20, 257–269. https://doi.org/10.1038/s41579-021-00649-x

Liguori, K., Keenum, I., Davis, B.C., Calarco, J., Milligan, E., Harwood, V.J., Pruden, A., 2022. Antimicrobial Resistance Monitoring of Water Environments: A Framework for Standardized Methods and Quality Control. Environ. Sci. Technol. 56, 9149–9160. https://doi.org/10.1021/acs.est.1c08918

Lloyd, K.G., MacGregor, B.J., Teske, A., 2010. Quantitative PCR methods for RNA and DNA in marine sediments: maximizing yield while overcoming inhibition. FEMS Microbiology Ecology 72, 143–151. https://doi.org/10.1111/j.1574-6941.2009.00827.x

Lee, U.N., Su, X., Guckenberger, D.J., Dostie, A.M., Zhang, T., Berthier, E., Theberge, A.B., 2018. Fundamentals of rapid injection molding for microfluidic cell-based assays. Lab Chip 18, 496–504. https://doi.org/10.1039/C7LC01052D

Li, L., Miao, B., Li, Z., Sun, Z., Peng, N., 2019. Sample-to-Answer Hepatitis B Virus DNA Detection from Whole Blood on a Centrifugal Microfluidic Platform with Double Rotation Axes. ACS Sens. 4, 2738–2745. https://doi.org/10.1021/acssensors.9b01270

LaTurner, Z.W., Zong, D.M., Kalvapalle, P., Gamas, K.R., Terwilliger, A., Crosby, T., Ali, P., Avadhanula, V., Santos, H.H., Weesner, K., Hopkins, L., Piedra, P.A., Maresso, A.W., Stadler, L.B., 2021. Evaluating recovery, cost, and throughput of different concentration methods for SARS-CoV-2 wastewater-based epidemiology. Water Research 197, 117043. https://doi.org/10.1016/j.watres.2021.117043

Lacey, C., McMahon, G., Bones, J., Barron, L., Morrissey, A., Tobin, J.M., 2008. An LC–MS method for the determination of pharmaceutical compounds in wastewater treatment plant influent and effluent samples. Talanta 75, 1089–1097. https://doi.org/10.1016/j.talanta.2008.01.011

Le, L.T., Huang, Z., Whiteson, K., Jiang, S., 2022. The occurrence and diversity of antibiotic resistance and virulence factor genes in wastewater from four North American treatment

plants. Environ. Sci.: Water Res. Technol. 10.1039.D1EW00820J. https://doi.org/10.1039/D1EW00820J

Li, D.-W., Zhai, W.-L., Li, Y.-T., Long, Y.-T., 2014. Recent progress in surface enhanced Raman spectroscopy for the detection of environmental pollutants. Microchim Acta 181, 23–43. https://doi.org/10.1007/s00604-013-1115-3

Li, Z., Wang, J., Li, D., 2016. Applications of Raman spectroscopy in detection of water quality. Applied Spectroscopy Reviews 51, 333–357. https://doi.org/10.1080/05704928.2015.1131711

Liang, X., Li, N., Zhang, R., Yin, P., Zhang, C., Yang, N., Liang, K., Kong, B., 2021. Carbon-based SERS biosensor: from substrate design to sensing and bioapplication. NPG Asia Mater 13, 8. https://doi.org/10.1038/s41427-020-00278-5

Liu, Y., Zhang, Y., Tardivel, M., Lequeux, M., Chen, X., Liu, W., Huang, J., Tian, H., Liu, Q., Huang, G., Gillibert, R., De La Chapelle, M.L., Fu, W., 2020. Evaluation of the Reliability of Six Commercial SERS Substrates. Plasmonics 15, 743–752. https://doi.org/10.1007/s11468-019-01084-8

Lazarova, V., Levine, B., Sack, J., Cirelli, G., Jeffrey, P., Muntau, H., Salgot, M., Brissaud, F., 2001. Role of water reuse for enhancing integrated water management in Europe and Mediterranean countries. Water Science and Technology 43, 25–33. https://doi.org/10.2166/wst.2001.0571

Logan, N., Haughey, S.A., Liu, L., Burns, D.T., Quinn, B., Cao, C., Elliott, C.T., 2022. Handheld SERS coupled with QuEChERs for the sensitive analysis of multiple pesticides in basmati rice. npj Sci Food 6, 3. https://doi.org/10.1038/s41538-021-00117-z

Mancuso, G., Midiri, A., Gerace, E., Biondo, C., 2021. Bacterial Antibiotic Resistance: The Most Critical Pathogens. Pathogens 10, 1310. https://doi.org/10.3390/pathogens10101310

Mariño-Lopez, A., Sousa-Castillo, A., Blanco-Formoso, M., Furini, L.N., Rodríguez-Lorenzo, L., Pazos-Perez, N., Guerrini, L., Pérez-Lorenzo, M., Correa-Duarte, M.A., Alvarez-Puebla, R.A., 2019. Microporous Plasmonic Capsules as Stable Molecular Sieves for Direct SERS Quantification of Small Pollutants in Natural Waters. ChemNanoMat 5, 46–50. https://doi.org/10.1002/cnma.201800355

Mosier-Boss, P., 2017. Review of SERS Substrates for Chemical Sensing. Nanomaterials 7, 142. https://doi.org/10.3390/nano7060142

Munteanu, F.-D., Titoiu, A., Marty, J.-L., Vasilescu, A., 2018. Detection of Antibiotics and Evaluation of Antibacterial Activity with Screen-Printed Electrodes. Sensors 18, 901. https://doi.org/10.3390/s18030901

Martzy, R., Kolm, C., Brunner, K., Mach, R.L., Krska, R., Šinkovec, H., Sommer, R., Farnleitner, A.H., Reischer, G.H., 2017. A loop-mediated isothermal amplification (LAMP)

assay for the rapid detection of Enterococcus spp. in water. Water Research 122, 62–69. https://doi.org/10.1016/j.watres.2017.05.023

Motlagh, A.M., Yang, Z., 2019. Detection and occurrence of indicator organisms and pathogens. Water Environment Research 91, 1402–1408. https://doi.org/10.1002/wer.1238

Medema, G., Heijnen, L., Elsinga, G., Italiaander, R., Brouwer, A., 2020. Presence of SARS-Coronavirus-2 RNA in Sewage and Correlation with Reported COVID-19 Prevalence in the Early Stage of the Epidemic in The Netherlands. Environ. Sci. Technol. Lett. 7, 511–516. https://doi.org/10.1021/acs.estlett.0c00357

Madadi, M., Madadi, A., Zareifar, R., Nikfarjam, A., 2023. A simple solvent-assisted method for thermal bonding of large-surface, multilayer PMMA microfluidic devices. Sensors and Actuators A: Physical 349, 114077. https://doi.org/10.1016/j.sna.2022.114077

Minka, T. P., 2000. Automatic choice of dimensionality for PCA. In Advances in Neural Information Processing Systems 12: Proceedings of the 1999 Conference; MIT Press, Vol. 13, pp 598– 604.

Nguyen, C.Q., Thrift, W.J., Bhattacharjee, A., Ranjbar, S., Gallagher, T., Darvishzadeh-Varcheie, M., Sanderson, R.N., Capolino, F., Whiteson, K., Baldi, P., Hochbaum, A.I., Ragan, R., 2018. Longitudinal Monitoring of Biofilm Formation via Robust Surface-Enhanced Raman Scattering Quantification of *Pseudomonas aeruginosa* -Produced Metabolites. ACS Appl. Mater. Interfaces 10, 12364–12373. https://doi.org/10.1021/acsami.7b18592

Nnachi, R.C., Sui, N., Ke, B., Luo, Z., Bhalla, N., He, D., Yang, Z., 2022. Biosensors for rapid detection of bacterial pathogens in water, food and environment. Environment International 166, 107357. https://doi.org/10.1016/j.envint.2022.107357

O'neill, J.I.M., 2014. Antimicrobial resistance: tackling a crisis for the health and wealth of nations. Rev. Antimicrob. Resist.

Orange County Sanitation District, n.d. https://www.ocsan.gov/ (accessed Feb 16, 2022).

Pillay, S., Calderón-Franco, D., Urhan, A., Abeel, T., 2022. Metagenomic-based surveillance systems for antibiotic resistance in non-clinical settings. Front. Microbiol. 13, 1066995. https://doi.org/10.3389/fmicb.2022.1066995

Perebikovsky, A., Liu, Y., Hwu, A., Kido, H., Shamloo, E., Song, D., Monti, G., Shoval, O., Gussin, D., Madou, M., 2021. Rapid sample preparation for detection of antibiotic resistance on a microfluidic disc platform. Lab Chip 21, 534–545. https://doi.org/10.1039/D0LC00838A

Peshin, S., George, D., Shiri, R., Kulinsky, L., Madou, M., 2022. Capillary Flow-Driven and Magnetically Actuated Multi-Use Wax Valves for Controlled Sealing and Releasing of Fluids on Centrifugal Microfluidic Platforms. Micromachines 13, 303. https://doi.org/10.3390/mi13020303

Peshin, S., Madou, M., Kulinsky, L., 2022. Microvalves for Applications in Centrifugal Microfluidics. Sensors 22, 8955. https://doi.org/10.3390/s22228955

Parthasarathy, R., Monette, C.E., Bracero, S., S. Saha, M., 2018. Methods for field measurement of antibiotic concentrations: limitations and outlook. FEMS Microbiology Ecology 94. https://doi.org/10.1093/femsec/fiy105

Pazda, M., Kumirska, J., Stepnowski, P., Mulkiewicz, E., 2019. Antibiotic resistance genes identified in wastewater treatment plant systems – A review. Science of The Total Environment 697, 134023. https://doi.org/10.1016/j.scitotenv.2019.134023

Pinheiro, P.C., Daniel-da-Silva, A.L., Nogueira, H.I.S., Trindade, T., 2018. Functionalized Inorganic Nanoparticles for Magnetic Separation and SERS Detection of Water Pollutants. Eur J Inorg Chem 2018, 3443–3461. https://doi.org/10.1002/ejic.201800132

Raboni, M., Gavasci, R., Torretta, V., 2016. Assessment of the Fate of Escherichia coli in Different Stages of Wastewater Treatment Plants. Water Air Soil Pollut 227, 455. https://doi.org/10.1007/s11270-016-3157-8

Rosario, K., Symonds, E.M., Sinigalliano, C., Stewart, J., Breitbart, M., 2009. *Pepper Mild Mottle Virus* as an Indicator of Fecal Pollution. Appl Environ Microbiol 75, 7261–7267. https://doi.org/10.1128/AEM.00410-09

Roy, S., Arshad, F., Eissa, S., Safavieh, M., Alattas, S.G., Ahmed, M.U., Zourob, M., 2022. Recent developments towards portable point-of-care diagnostic devices for pathogen detection. Sens. Diagn. 1, 87–105. https://doi.org/10.1039/D1SD00017A

Srinivasan, B., Tung, S., 2015. Development and Applications of Portable Biosensors. SLAS Technology 20, 365–389. https://doi.org/10.1177/2211068215581349

Silmeco, n.d. https://www.silmeco.com/products/sers-substrate-serstrate/ (accessed Feb 15, 2022).

Schiff, K.C., Weisberg, S.B., Dorsey, J.H., 2001. Microbiological Monitoring of Marine Recreational Waters in Southern California. Environmental Management 27, 149–157. https://doi.org/10.1007/s002670010140

Siegrist, J., Gorkin, R., Clime, L., Roy, E., Peytavi, R., Kido, H., Bergeron, M., Veres, T., Madou, M., 2010. Serial siphon valving for centrifugal microfluidic platforms. Microfluid Nanofluid 9, 55–63. https://doi.org/10.1007/s10404-009-0523-5

Strohmeier, O., Keller, M., Schwemmer, F., Zehnle, S., Mark, D., Von Stetten, F., Zengerle, R., Paust, N., 2015. Centrifugal microfluidic platforms: advanced unit operations and applications. Chem. Soc. Rev. 44, 6187–6229. https://doi.org/10.1039/C4CS00371C

Schuler, F., Siber, C., Hin, S., Wadle, S., Paust, N., Zengerle, R., Von Stetten, F., 2016. Digital droplet LAMP as a microfluidic app on standard laboratory devices. Anal. Methods 8, 2750–2755. https://doi.org/10.1039/C6AY00600K

Schuler, F., Trotter, M., Geltman, M., Schwemmer, F., Wadle, S., Domínguez-Garrido, E., López, M., Cervera-Acedo, C., Santibáñez, P., Von Stetten, F., Zengerle, R., Paust, N., 2016. Digital droplet PCR on disk. Lab Chip 16, 208–216. https://doi.org/10.1039/C5LC01068C

Schlenker, F., Kipf, E., Borst, N., Paust, N., Zengerle, R., Von Stetten, F., Juelg, P., Hutzenlaub, T., 2021. Centrifugal Microfluidic Integration of 4-Plex ddPCR Demonstrated by the Quantification of Cancer-Associated Point Mutations. Processes 9, 97. https://doi.org/10.3390/pr9010097

Scott, S., Ali, Z., 2021. Fabrication Methods for Microfluidic Devices: An Overview. Micromachines 12, 319. https://doi.org/10.3390/mi12030319

Savitzky, Abraham., Golay, M.J.E., 1964. Smoothing and Differentiation of Data by Simplified Least Squares Procedures. Anal. Chem. 36, 1627–1639. https://doi.org/10.1021/ac60214a047

Shen, X., Ho, C.-M., Wong, T.-S., 2010. Minimal Size of Coffee Ring Structure. J. Phys. Chem. B 114, 5269–5274. https://doi.org/10.1021/jp912190v

Shrivastava, A., Gupta, V., 2011. Methods for the determination of limit of detection and limit of quantitation of the analytical methods. Chron Young Sci 2, 21. https://doi.org/10.4103/2229-5186.79345

Sun, Y., Zhao, J., Liang, L., 2021. Recent development of antibiotic detection in food and environment: the combination of sensors and nanomaterials. Microchim Acta 188, 21. https://doi.org/10.1007/s00604-020-04671-3

Sahoo, R., Jadhav, S., Nema, V., 2023. Journey of technological advancements in the detection of antimicrobial resistance. Journal of the Formosan Medical Association S0929664623003224. https://doi.org/10.1016/j.jfma.2023.08.008

Tang, M., Wang, G., Kong, S.-K., Ho, H.-P., 2016. A Review of Biomedical Centrifugal Microfluidic Platforms. Micromachines 7, 26. https://doi.org/10.3390/mi7020026

Thrift, W.J., Cabuslay, A., Laird, A.B., Ranjbar, S., Hochbaum, A.I., Ragan, R., 2019. Surface-Enhanced Raman Scattering-Based Odor Compass: Locating Multiple Chemical Sources and Pathogens. ACS Sens. 4, 2311–2319. https://doi.org/10.1021/acssensors.9b00809

Thrift, W.J., Nguyen, C.Q., Darvishzadeh-Varcheie, M., Zare, S., Sharac, N., Sanderson, R.N., Dupper, T.J., Hochbaum, A.I., Capolino, F., Abdolhosseini Qomi, M.J., Ragan, R., 2017. Driving Chemical Reactions in Plasmonic Nanogaps with Electrohydrodynamic Flow. ACS Nano 11, 11317–11329. https://doi.org/10.1021/acsnano.7b05815

Thrift, W.J., Ronaghi, S., Samad, M., Wei, H., Nguyen, D.G., Cabuslay, A.S., Groome, C.E., Santiago, P.J., Baldi, P., Hochbaum, A.I., Ragan, R., 2020. Deep Learning Analysis of Vibrational Spectra of Bacterial Lysate for Rapid Antimicrobial Susceptibility Testing. ACS Nano 14, 15336–15348. https://doi.org/10.1021/acsnano.0c05693

Toze, S., 1999. PCR and the detection of microbial pathogens in water and wastewater. Water Research 33, 3545–3556. https://doi.org/10.1016/S0043-1354(99)00071-8

Tsao, C.-W., DeVoe, D.L., 2009. Bonding of thermoplastic polymer microfluidics. Microfluid Nanofluid 6, 1–16. https://doi.org/10.1007/s10404-008-0361-x

United States Environmental Protection Agency, 2010. National Pollution Discharge Elimination System (NPDES) Permit Writers' Manual.

Vidal-Dorsch, D.E., Bay, S.M., Maruya, K., Snyder, S.A., Trenholm, R.A., Vanderford, B.J., 2012. Contaminants of emerging concern in municipal wastewater effluents and marine receiving water. Enviro Toxic and Chemistry 31, 2674–2682. https://doi.org/10.1002/etc.2004

Von Wintersdorff, C.J.H., Penders, J., Van Niekerk, J.M., Mills, N.D., Majumder, S., Van Alphen, L.B., Savelkoul, P.H.M., Wolffs, P.F.G., 2016. Dissemination of Antimicrobial Resistance in Microbial Ecosystems through Horizontal Gene Transfer. Front. Microbiol. 7. https://doi.org/10.3389/fmicb.2016.00173

Wang, F., Cao, S., Yan, R., Wang, Z., Wang, D., Yang, H., 2017. Selectivity/Specificity Improvement Strategies in Surface-Enhanced Raman Spectroscopy Analysis. Sensors 17, 2689. https://doi.org/10.3390/s17112689

Wei, H., Huang, Y., Santiago, P.J., Labachyan, K.E., Ronaghi, S., Banda Magana, M.P., Huang, Y.-H., C. Jiang, S., Hochbaum, A.I., Ragan, R., 2023. Decoding the metabolic response of Escherichia coli for sensing trace heavy metals in water. Proc. Natl. Acad. Sci. U.S.A. 120, e2210061120. https://doi.org/10.1073/pnas.2210061120

Wei, H., Cho, S.W., 2021. Label-free Surface-enhanced Raman Spectroscopy for Water Pollutant Analysis, in: Liu, Y., Wang, C.-C., Liu, W. (Eds.), Emerging Nanotechnologies for Water Treatment. The Royal Society of Chemistry, pp. 30–47. https://doi.org/10.1039/9781839165092-00030

Wei, H., Hossein Abtahi, S.M., Vikesland, P.J., 2015. Plasmonic colorimetric and SERS sensors for environmental analysis. Environ. Sci.: Nano 2, 120–135. https://doi.org/10.1039/C4EN00211C

World Health Organization, n.d. Antibiotic Resistance. https://www.who.int/news-room/fact-sheets/detail/antibiotic-resistance (accessed Feb 11, 2022).

Williams, F. P., Stetler, R. E., Safferman, R. S., 2001. USEPA MANUAL OF METHODS FOR VIROLOGY (No. EPA/600/4-84/013 (N16)). Washington, DC: U.S. Environmental Protection Agency.

Wu, F., Xiao, A., Zhang, J., Moniz, K., Endo, N., Armas, F., Bonneau, R., Brown, M.A., Bushman, M., Chai, P.R., Duvallet, C., Erickson, T.B., Foppe, K., Ghaeli, N., Gu, X., Hanage, W.P., Huang, K.H., Lee, W.L., Matus, M., McElroy, K.A., Nagler, J., Rhode, S.F.,

Santillana, M., Tucker, J.A., Wuertz, S., Zhao, S., Thompson, J., Alm, E.J., 2022. SARS-CoV-2 RNA concentrations in wastewater foreshadow dynamics and clinical presentation of new COVID-19 cases. Science of The Total Environment 805, 150121. https://doi.org/10.1016/j.scitotenv.2021.150121

Yamin, D., Uskoković, V., Wakil, A., Goni, M., Shamsuddin, S., Mustafa, F., Alfouzan, W., Alissa, M., Alshengeti, A., Almaghrabi, R., Fares, M., Garout, M., Al Kaabi, N., Alshehri, A., Ali, H., Rabaan, A., Aldubisi, F., Yean, C., Yusof, N., 2023. Current and Future Technologies for the Detection of Antibiotic-Resistant Bacteria. Diagnostics 13, 3246. https://doi.org/10.3390/diagnostics13203246

Zhuang, M., Achmon, Y., Cao, Y., Liang, X., Chen, L., Wang, H., Siame, B.A., Leung, K.Y., 2021. Distribution of antibiotic resistance genes in the environment. Environmental Pollution 285, 117402. https://doi.org/10.1016/j.envpol.2021.117402

Zymo research, 2022. Quick-DNA/RNA viral MagBead. https://files.zymoresearch.com/protocols/_r2140_r2141_quick-dna-rna_viral_magbead.pdf (accessed 2.12.2024).

Zhang, W., Liu, Q., Guo, Z., Lin, J., 2018. Practical Application of Aptamer-Based Biosensors in Detection of Low Molecular Weight Pollutants in Water Sources. Molecules 23, 344. https://doi.org/10.3390/molecules23020344

APPENDIX A

SENSING ANTIBIOTICS IN WASTEWATER USING SURFACE-ENHANCED RAMAN SCATTERING

Table A.1. Water quality parameters in the secondary effluent used for seeding study.

Parameter	Concentration	Description	Reference
Aluminum (mg/L)	19	Secondary effluent water quality based on 2008 and 2009 annual average data.	Project No. SP-173, Effluent Reuse Study GWRS Final Expansion FINAL Implementation Plan Volume 1 of 3
NH_3-N (mg/L N)	22.6		
Iron (mg/L)	350		
Manganese (mg/L)	45		
TDS (mg/L)	935		
TOC (mg/L)	14		
Turbidity (NTU)	3.2		
TBOD (mg/L)	11.1	Annual average activated sludge effluent biochemical oxygen demand for fiscal year 2004 -2005	FACILITIES OPERATION AND MAINTENANCE
CBOD (mg/L)	6.3		

Table A.2. The assignment of SERS bands of quinoline.

Experiment (cm^{-1})	Literature (cm^{-1})	Vibrational assignment
770	760	ring deformation
1019	1014	ring breathing
1030	1034	ring breathing
1057	-	CH bending
1133	-	CH bending
1264	-	CNC bending
1314	-	CH bending
1376	1372	CCC stretching
1391	1392	CCC stretching
1440	1433	CH rocking
1463	-	CH rocking
1579	1571	CCC stretching

Figure A.1. Comparison of SERS detection of quinoline in DI water with the quantification results by UPLC-MS/MS.

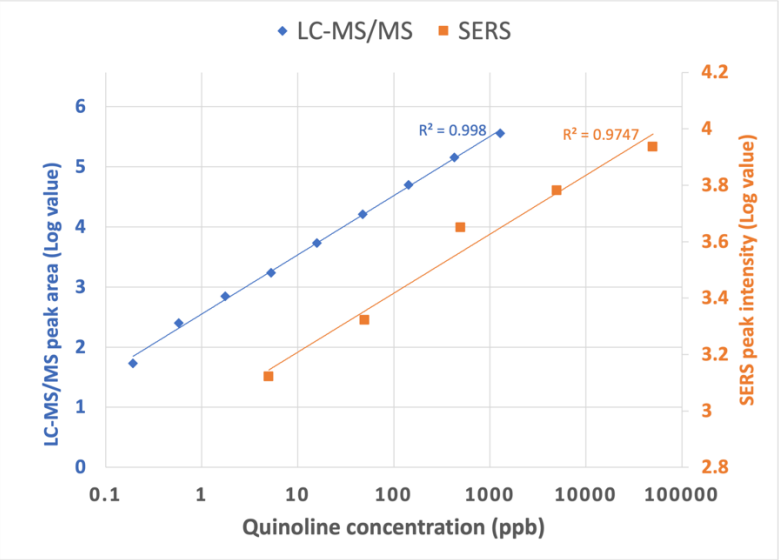

Figure A.2. PCA plot of SERS spectra of DI water, treated wastewater, 50 ppm quinoline spiked in DI water or in treated wastewater. (a) Data collected on Self-Assembled SERS substrate; (b) Data collected on SEStrate.

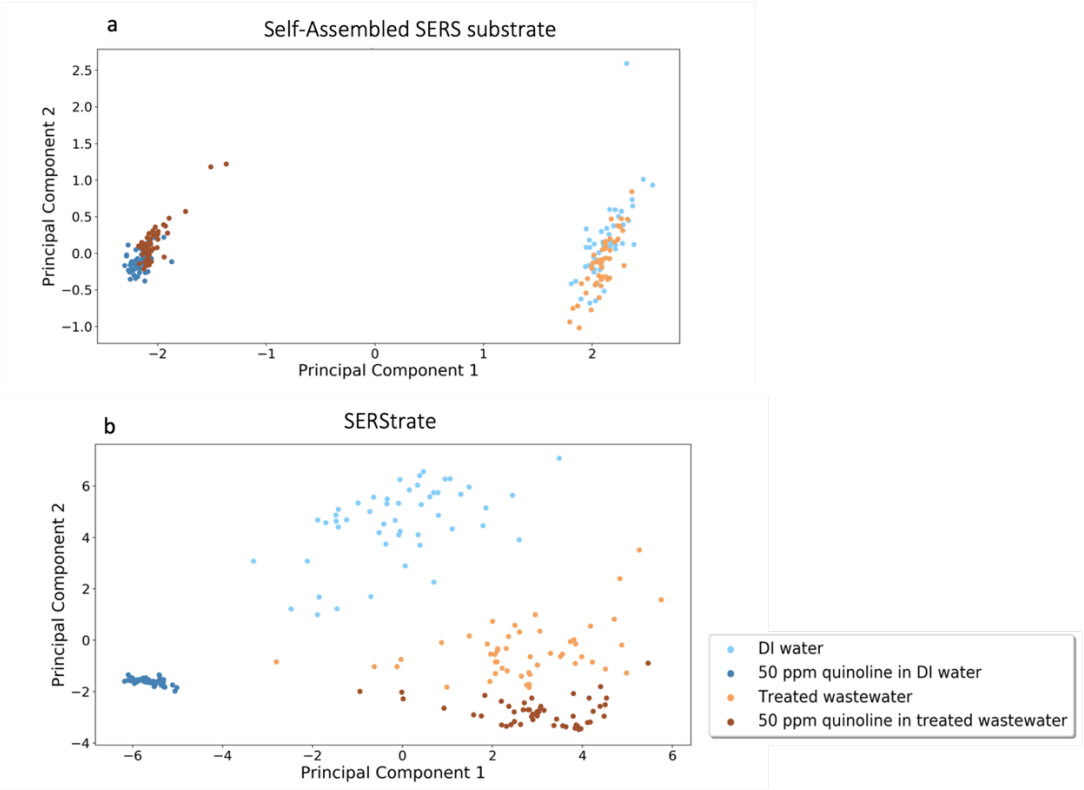

Figure A.3. SERS spectra collected using Self-assembly SERS substrate for erythromycin, humic acid, Microcystin-LR, glycine, L-arginine and quinoline spiked DI water in the concentration of 5 ppm**.**

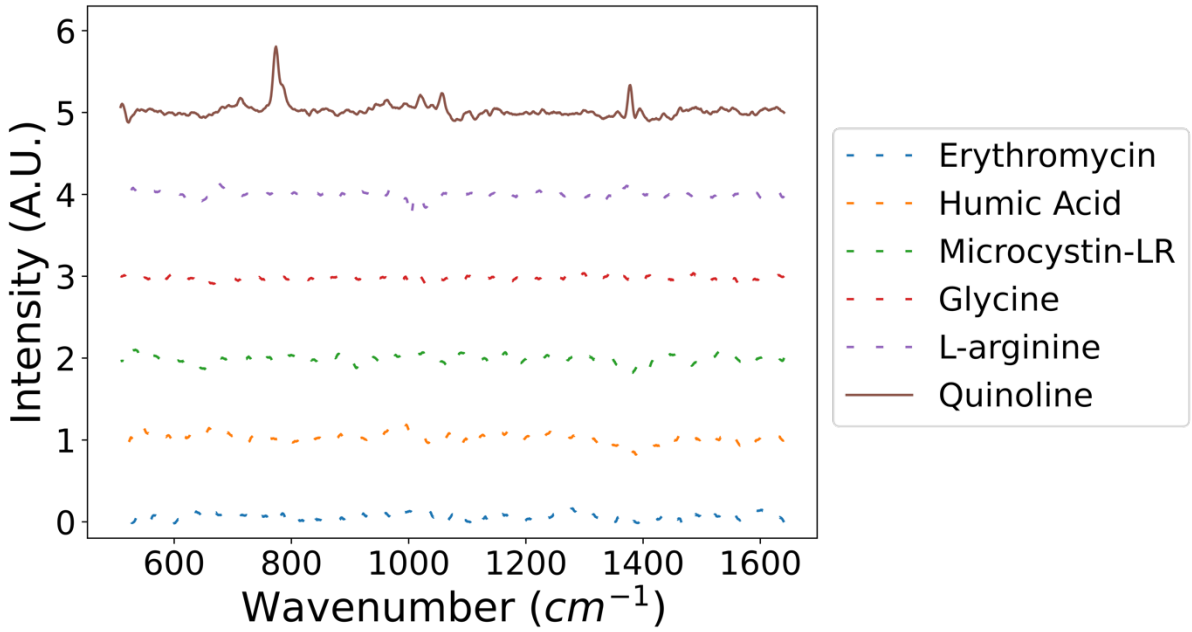

Figure A.4. Microscopy image of (a) fresh Self-Assembly SERS substrate and (b) washed Self-Assembly SERS substrate.

a

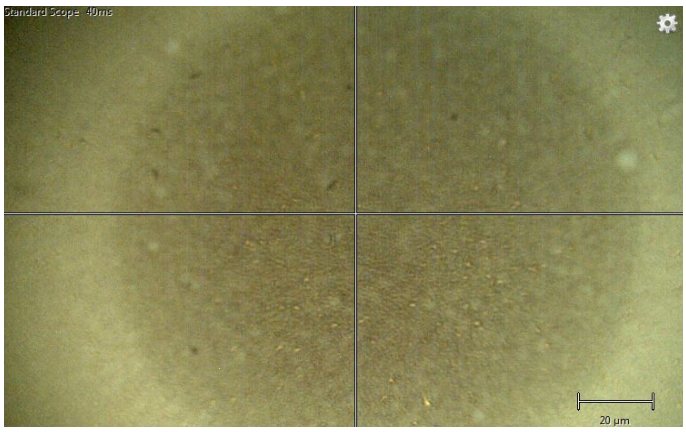

b

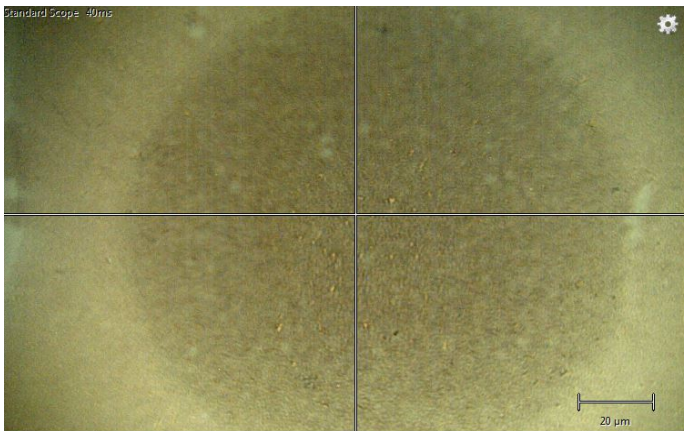

APPENDIX B

QUANTIFICATION OF VIRUSES IN WASTEWATER ON A CENTRIFUGAL MICROFLUIDIC DISC

Table B.1. Components of the RT-LAMP reaction mix.

Reagents	**Volume**
WarmStart LAMP 2X Master Mix	10 µl
Fluorescent dye (50X)	0.4 µl
LAMP Primer Mix (10X)	2 µl
Nuclease-free water	3.6 µl
RNA extracts	4 µl
Total Volume	**20 µl**

Table B.2. LAMP primers for SARS-CoV-2[#] and PMMoV detection.

Primer (concentration)	Sequence
• **SARS-CoV-2 (Ganguli et al., 2020)**	
F3 (0.2 µM)	5'-GTTCCTCATCACGTAGTCG-3'
B3 (0.2 µM)	5'-GTTTGGCCTTGTTGTTGTT-3'
FIP (1.6 µM)	5'-GCCAGCCATTCTAGCAGGAGCAACAGTTAAGAAATTCAACTCC-3'
BIP (1.6 µM)	5'-GATGCTGCTCTTGCTTTGCTACCAGACATTTTGCTCTCAA-3'
LoopB (0.8 µM)	5'-GCTGCTTGACAGATTGAACCAG-3'
• **PMMoV**	
F3 (0.2 µM)	5'-CGCCATATCAAAAGCCATGC-3'
B3 (0.2 µM)	5'-GGCAGCATAGCAGACATGAA-3'
FIP (1.6 µM)	5'-GTGCGAAACGCCTTCGCAGTACGGACGATCCGCAATCA-3'
BIP (1.6 µM)	5'-ATACGCTGTCGCTTTGCACAGTTCAGAAGTGCTGCCCCAA-3'
LoopF (0.8 µM)	5'-GCTGAAAAGGTTTCGAGCACACTAC-3'

Figure B.1. Physical images of the laser-irradiated ferrowax microvalve.

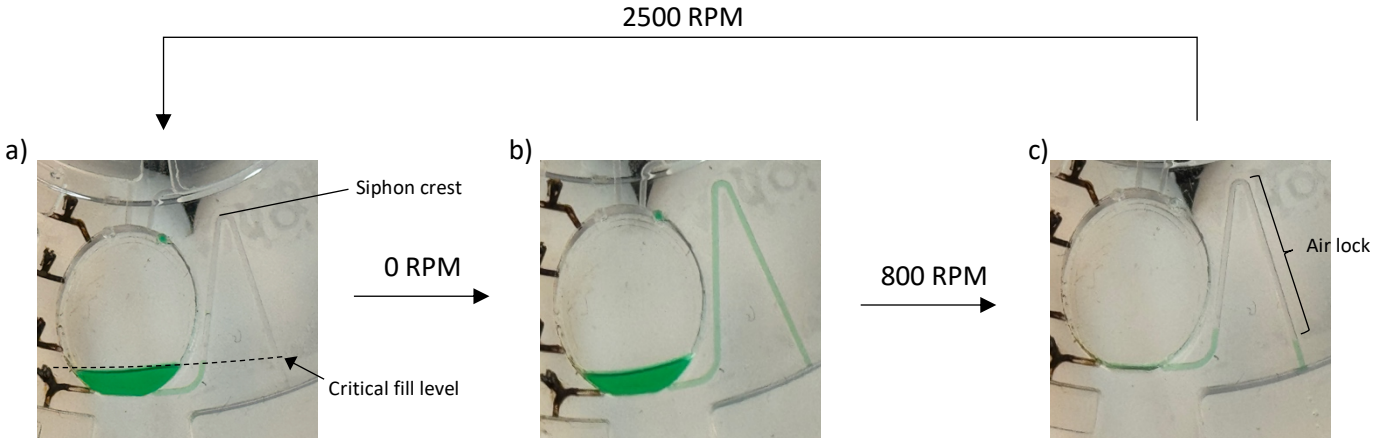

Figure B.2. The operational process of the siphon channel valve. (a) When the CD is rotated in the initial state, the centrifugal force is larger than the capillary force, causing the liquid to be retained in the chamber as the liquid level does not pass the siphon crest. (b) A brief pause is used to prime the siphon channel by capillary forces until the liquid passes the critical fill level, switching the siphon channel to the open state. (c) The CD is rotated at a lower speed to transfer the liquid and turn the siphon channel valve to the closed state by forming an air lock in the siphon. To open the siphon channel valve, a high-speed rotation is applied to remove the air lock, switching the siphon back to the initial state.

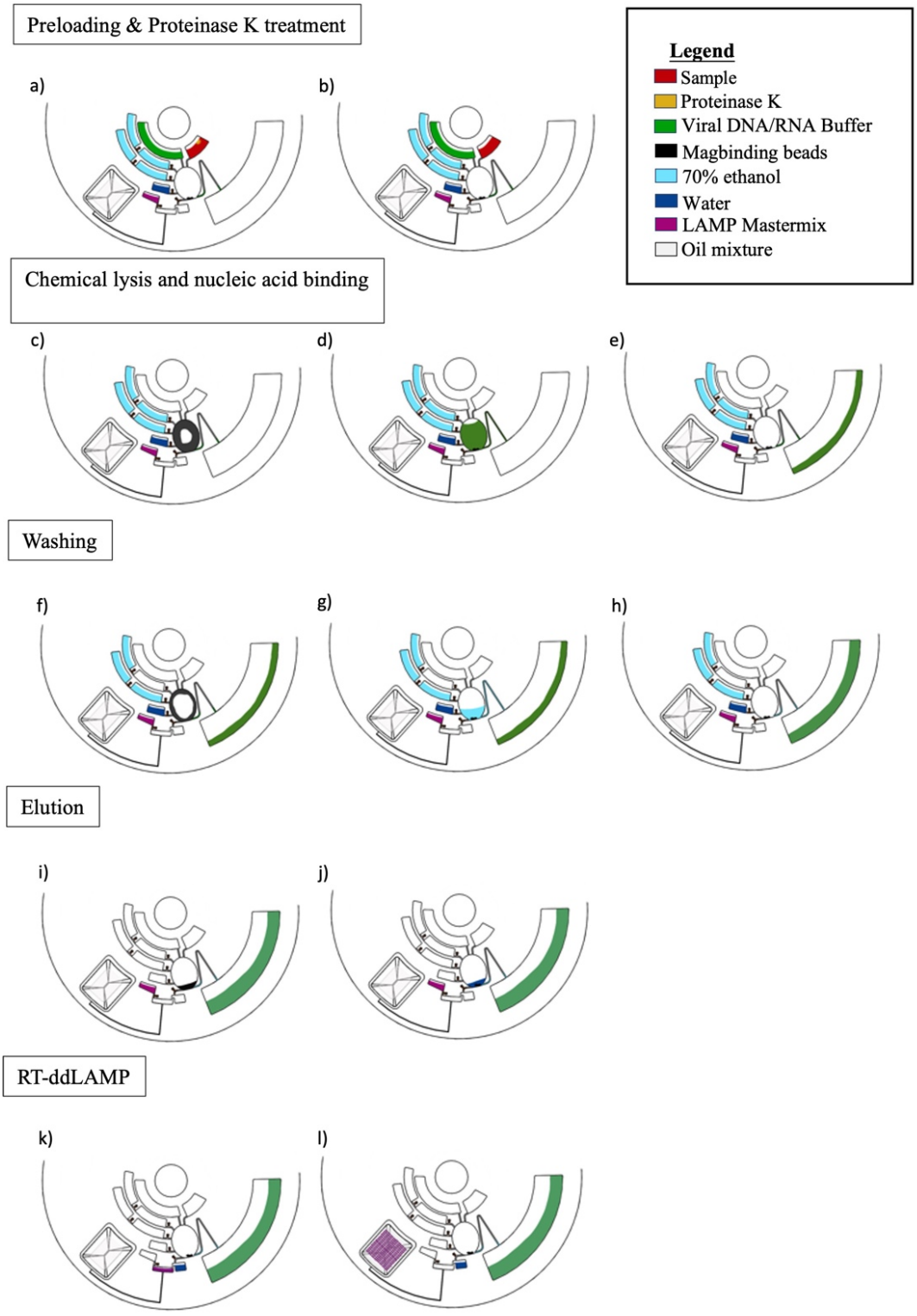

Figure B.3. Schematic illustrations of the fluid handling process.

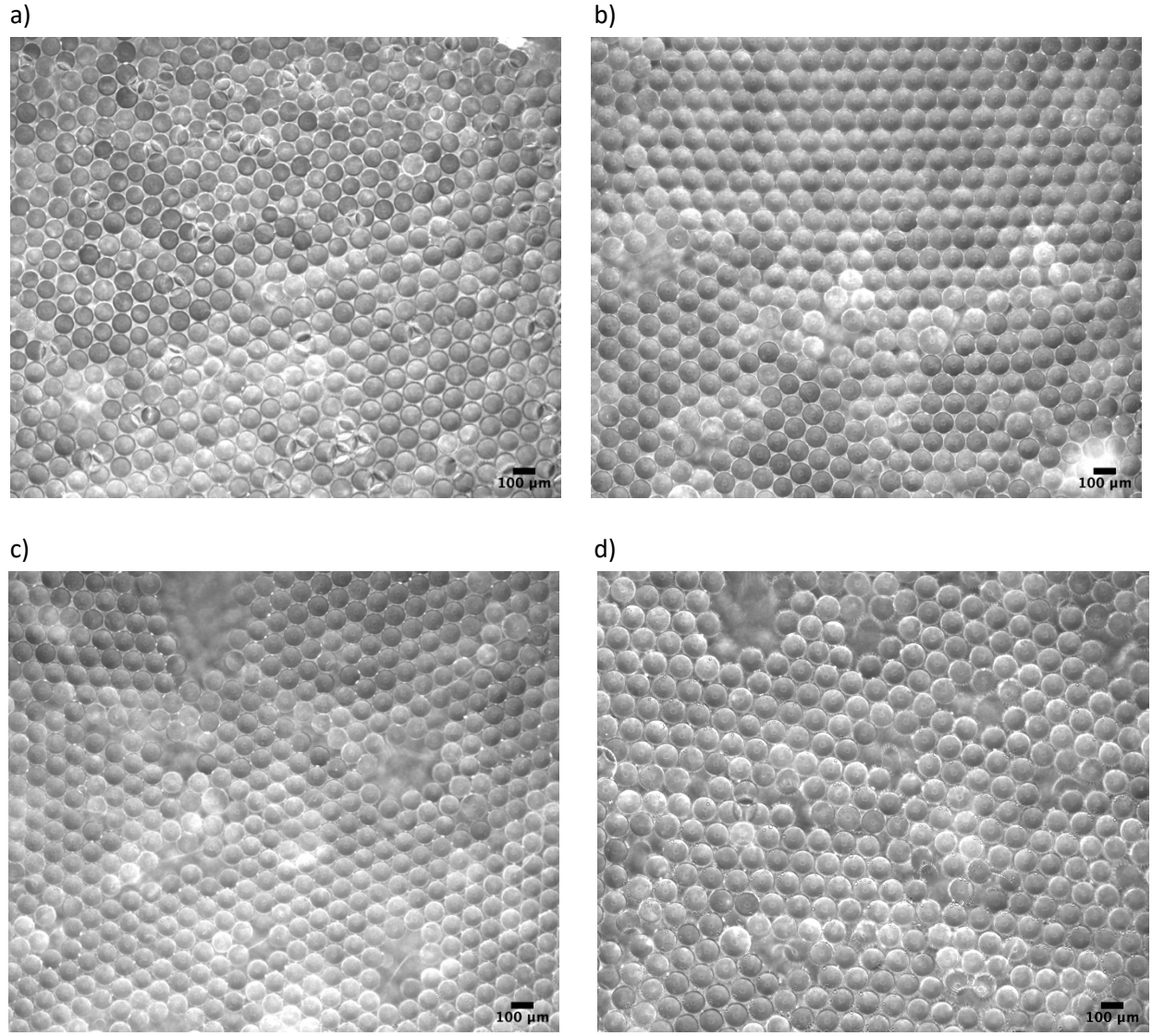

Figure B.4. Microscopy images of reaction-in-oil droplets in 4 different reaction chambers generated on the CDs after heating at 65°C for 30 minutes. The droplets with diameters less than 140 µm remained stable during the heating process, as demonstrated in images (a), (b), (c) and (d). Droplet generation units that produced droplets with diameters larger than 160 µm were considered failed manufactured products and were not used for quantification.

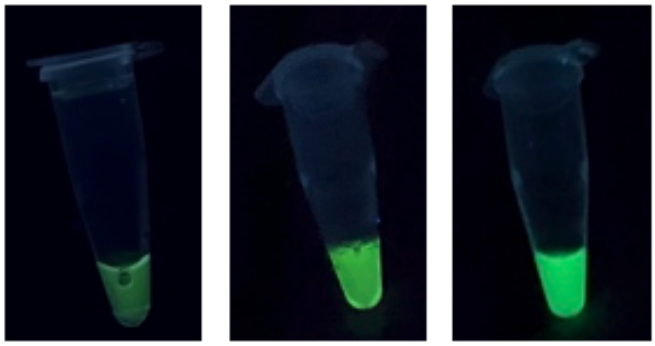

Figure B.5. Images of RT-LAMP results taken by a cell phone camera. (a) negative control, (b) weak positive results, and (c) strong positive results as indicated by relative fluorescence intensity.

Reference

Ganguli, A., Mostafa, A., Berger, J., Aydin, M.Y., Sun, F., Ramirez, S.A.S.D., Valera, E., Cunningham, B.T., King, W.P., Bashir, R., 2020. Rapid isothermal amplification and portable detection system for SARS-CoV-2. Proc. Natl. Acad. Sci. U.S.A. 117, 22727–22735. https://doi.org/10.1073/pnas.2014739117

APPENDIX C

INTEGRATING PHENOTYPIC AND GENOTYPIC METHODS FOR THE RAPID DETECTION OF ANTIBIOTIC-RESISTANT E. COLI ON A CENTRIFUGAL MICROFLUIDIC DISC

Table C.1. LAMP primer.

Primer (concentration)	Sequence
• **E. coli (Hill et al., 2008)**	
F3 (0.2 μM)	5'-GCCATCTCCTGATGACGC -3'
B3 (0.2 μM)	5'- ATTTACCGCAGCCAGACG-3'
FIP (1.6 μM)	5'- CATTTTGCAGCTGTACGCTCGCAGCCCATCATGAATGTTGCT -3'
BIP (1.6 μM)	5'- CTGGGGCGAGGTCGTGGTATTCCGACAAACACCACGAATT -3'
LoopF (0.8 μM)	5'- CTTTGTAACAACCTGTCATCGACA-3'
LoopB (0.8 μM)	5'- ATCAATCTCGATATCCATGAAGGTG -3'

Figure C.1. Photo images of three levels of LAMP positive signals indicated by the turbidity of the reaction mixture.

Reference

Hill, J., Beriwal, S., Chandra, I., Paul, V.K., Kapil, A., Singh, T., Wadowsky, R.M., Singh, V., Goyal, A., Jahnukainen, T., Johnson, J.R., Tarr, P.I., Vats, A., 2008. Loop-Mediated Isothermal Amplification Assay for Rapid Detection of Common Strains of Escherichia coli. J Clin Microbiol 46, 2800–2804. https://doi.org/10.1128/JCM.00152-08